THERAPEUTICALLY TARGETING AUTOPHAGY IN NON-SMALL CELL LUNG CANCER

By

Lisette Pangilinan Yco

A THESIS

Submitted to
Michigan State University
in partial fulfillment of the requirements
for the degree of

Physiology—Master of Science

2019

ABSTRACT

THERAPEUTICALLY TARGETING AUTOPHAGY
IN NON-SMALL CELL LUNG CANCER

By

Lisette Pangilinan Yco

Autophagy is a conserved catabolic pathway which sequesters intracellular components in lysosomes to recycle macromolecules for cell maintenance. The role of autophagy in tumor cells is dynamic and depends on many factors including tumor types, tumor stages, and activity of several tumor suppressors and oncogenes. In this thesis, I wanted to improve our understanding of the unique relationship of autophagy with tumor suppressor p53 and oncogenic KRAS in cancer cells, particularly in NSCLC. First, I demonstrated that stabilized nuclear wild-type p53 through HDM2 inhibition with MK-8242 or nutlin-3a could induce autophagy in tumor cells through transactivation of several autophagy-related genes (*DRAM*, *FOXO3A*, *SESN2*, and *MRCKα*) and autophagy core genes (*ATG4A*, and *ULK1*). In addition, I found that inhibiting of $KRAS^{G12C}$ signaling and suppressing mTORC1 activity by selective $KRAS^{G12C}$ inhibitor, ARS-853, could drive autophagy response in $KRAS^{G12C}$ NSCLC cell lines. Since autophagy could also promote survival under stress induced by several anticancer agents, I designed a combination study using newly reported selective ULK1 inhibitor, ULK-101, with ARS-853 in KRAS mutant NSCLC. Autophagy inhibition with ULK-101 dramatically enhanced the ability of selective $KRAS^{G12C}$ inhibitor to impair the viability of $KRAS^{G12C}$ NSCLC. Together, my study provided evidence that autophagy serves as a survival pathway in tumor cells and that future assessment of small molecule that target autophagy core proteins may be potential cancer therapeutic option in p53 wild-type and $KRAS^{G12C}$ NSCLC.

ACKNOWLEDGEMENTS

First and foremost, I would like to thank Dr. Jeff MacKeigan for his guidance, support, and patience. Thank you for your unwavering encouragement especially during challenging times when I was ready to give up. Thank you for giving me the freedom to improve my scientific skills but also prepared to be by my side when I needed direction. I also want to express my gratitude to my Physiology Graduate director, Dr. Andrea Doseff. Your undying persuasion gave me the strength to finish what I have started. I thank Dr. Kathleen Gallo, Dr. Eran Andrechek, and Dr. Sophia Lunt for their role as members of my guidance committee. I value every advice you shared with me throughout this journey.

To the members of the MacKeigan lab who have I crossed paths with, I will forever treasure the friendship you have given me. Thank you for allowing me to be part of your family. Thank you for your patience and understanding during times when I was demanding. I am greatly indebted to all of you. To the Physiology Graduate Student Council and the Van Andel Institute Graduate Student Association, thank you for all the support and friendship. To the people of Department of Physiology and Department of Obstetrics, Gynecology and Reproductive Biology, I am grateful for providing me the assistance I need while I split my time studying at Michigan State University and conducting research at Grand Rapids Research Center.

Finally, I want to thank my friends, Emmy, Luke, and Ken. All of you had given me strength when I needed it. Thank you, Ken, for being my cheerleader during challenging times. Most importantly, to my family who has given me unconditional love and support along the way. To my parents who welcomed my stubbornness and independence but also allowed let me be vulnerable during difficult times. I will be eternally grateful to all the love, patience, and

understanding. To my sisters, thank you for taking care of mom and dad while I am away. I will forever treasure our Sunday's phone conversion. They're my weekly recharge. To my dearest nephew, Jaron, thank you for being the most thoughtful affectionate boy I know. I miss you every day and cry when I don't hear your voice. You are my joy and strength. To everyone who is by my side the entire time encouraging me to finish. Thank you. Mahalo. Si Yu'os Ma'åse'.

TABLE OF CONTENTS

LIST OF TABLES

LIST OF FIGURES

KEY TO ABBREVIATIONS

AMPK	AMP-activated protein kinase
ATG	Autophagy-related protein
BafA1	Bafilomycin A1
CQ	Chloroquine
CytD	Cytochalasin D
DFCP1	Zinc- finger FYVE domain-containing protein 1
HCQ	Hydroxychloroquine
JMY	Junction-mediating and regulatory
LatB	Latrunculin B
MAP1LC3B/LC3B	Microtubule-associated protein 1 light chain 3
MDM2	Murine double minute 2
MLC2	Regulatory light chain of MYO2
MRCKα	Myotonic dystrophy kinase-related Cdc42-binding kinase alpha
mTORC1	Mechanistic target rapamycin complex 1
MYO2	Non-muscle myosin II
MYPT1	Myosin phosphates target subunit
NPF	Nuclear promoting factor

PI	Phosphatidylinositol
PI3P	Phosphatidylinositol-3-phosphate
PIK3C3	Class III phosphatidylinositol 3-kinase complex
ULK1	Unc-51-like autophagy initiating kinase 1
WASH	WASP-SCAR homolog
WASP	Wiskott–Aldrich syndrome protein
WHAMM	WASP homolog associated with actin, membranes, and microtubules
WIPI	WD-repeat domain phosphoinositide-interacting protein

CHAPTER 1.

INTRODUCTION

From Lysosome to Yeast

The first significant break-through in autophagy research involved the discovery of the lysosome by Christian de Duve. Interestingly, de Duve described his discovery of lysosome as a "serendipitous observation" (de Duve, 2005). His attempt to characterize hepatic glucose 6-phosphatase using what was at the time a newly developed centrifugal cellular fractionation led him to discover the lytic properties of lysosomes (De Duve et al., 1955). With further analyses and collaboration with Alex Novikoff, de Duve used electron microscopy to characterize lysosome as a new and unique cellular compartment containing bodies surrounded by a membrane (Novikoff et al., 1956). In 1963, the Ciba Foundation celebrated De Duve's discovery of the lysosome by organizing the first international symposium of lysosomes. During the symposium, Ciba branded lysosome as an organelle that digests extracellular and intracellular materials delivered by endocytosis and autophagy, respectively (Arstila and Trump, 1968; De Duve, 1963; Deter et al., 1967). Notably, in 1974 Christian de Duve's discovery was awarded by a Nobel Prize in Physiology or Medicine.

The second major break-through occurred almost four decades later when Yoshinori Ohsumi discovered autophagy in *Saccharomyces cerevisiae*. Ohsumi reasoned that yeast with deficient mutant proteinase, essential in protein turnover, induce autophagic bodies when challenged by nitrogen-depleted condition (Takeshige et al., 1992). Furthermore, Ohsumi used his yeast model to identify and characterize fifteen essential autophagy-related proteins (ATGs) required for the autophagic process (Tsukada and Ohsumi, 1993). Consequently, these fifteen genes were found to be conserved and essential in human cells. From that point onward, autophagy has been investigated in many other organisms and recognized as a significant physiological function in human health and disease (Choi et al., 2013; Jiang and Mizushima, 2014). In 2016,

Yoshinori Ohsumi was awarded the Nobel Prize in Physiology or Medicine "for his discoveries of mechanisms for autophagy."

Autophagy and Actin Cytoskeleton Dynamics

Actin cytoskeleton dynamics play a vital role in a wide range of cellular processes including cell motility, cytokinesis, exocytosis, and endocytosis. Actin-binding proteins that control the actin filament assembly and disassembly have also been linked to macroautophagy, hereafter referred to as autophagy. As shown in **Figure 1.1A**, autophagy can be divided into distinct stages. Autophagy induction results in recruitment of ATGs and nucleation of isolation membrane forming cup-shaped phagophore. The phagophore elongates into a double-membraned autophagosome sequestering intracellular materials. The matured autophagosome fuses with the lysosome, and the process completes after the lysosome engulfs the autophagosome. This last step allows autophagosome cargo to be degraded by the acidic hydrolases into biochemical building blocks for cells to reuse (Dikic and Elazar, 2018).

Several cytoskeleton assembly factors were characterized to have essential roles in different stages of autophagy (**Figure 1.1B**) (Kast and Dominguez, 2017; Kruppa et al., 2016). Actin nucleator Arp2/3 complex and nuclear promoting factors (NPFs) junction-mediating and regulatory protein (JMY) (Coutts and La Thangue, 2015; Moreau et al., 2015), Wiskott–Aldrich syndrome protein (WASP) homolog associated with actin, membranes, and microtubules (WHAMM) (Kast and Dominguez, 2015; Kast et al., 2015), and WASP-SCAR homolog (WASH) (Xia et al., 2013; Zavodszky et al., 2014) have been shown to colocalized during autophagy initiation, phagophore expansion, and autophagosome maturation. In fact, deregulation of NPFs resulted in elongation of tubular structures instead of membrane curvature formation during

phagophore expansion (Holland and Simonsen, 2015). As the motor protein myosin is important in transporting and sorting protein complexes along with cell membranes, the non-muscle myosin II (MYO2) is also linked to phagophore expansion, in delivering ATG9-containing vesicles from Golgi complex (Tang et al., 2011). These series of studies provide evidence that actin cytoskeleton is necessary to orchestrate the multi-step process of autophagy.

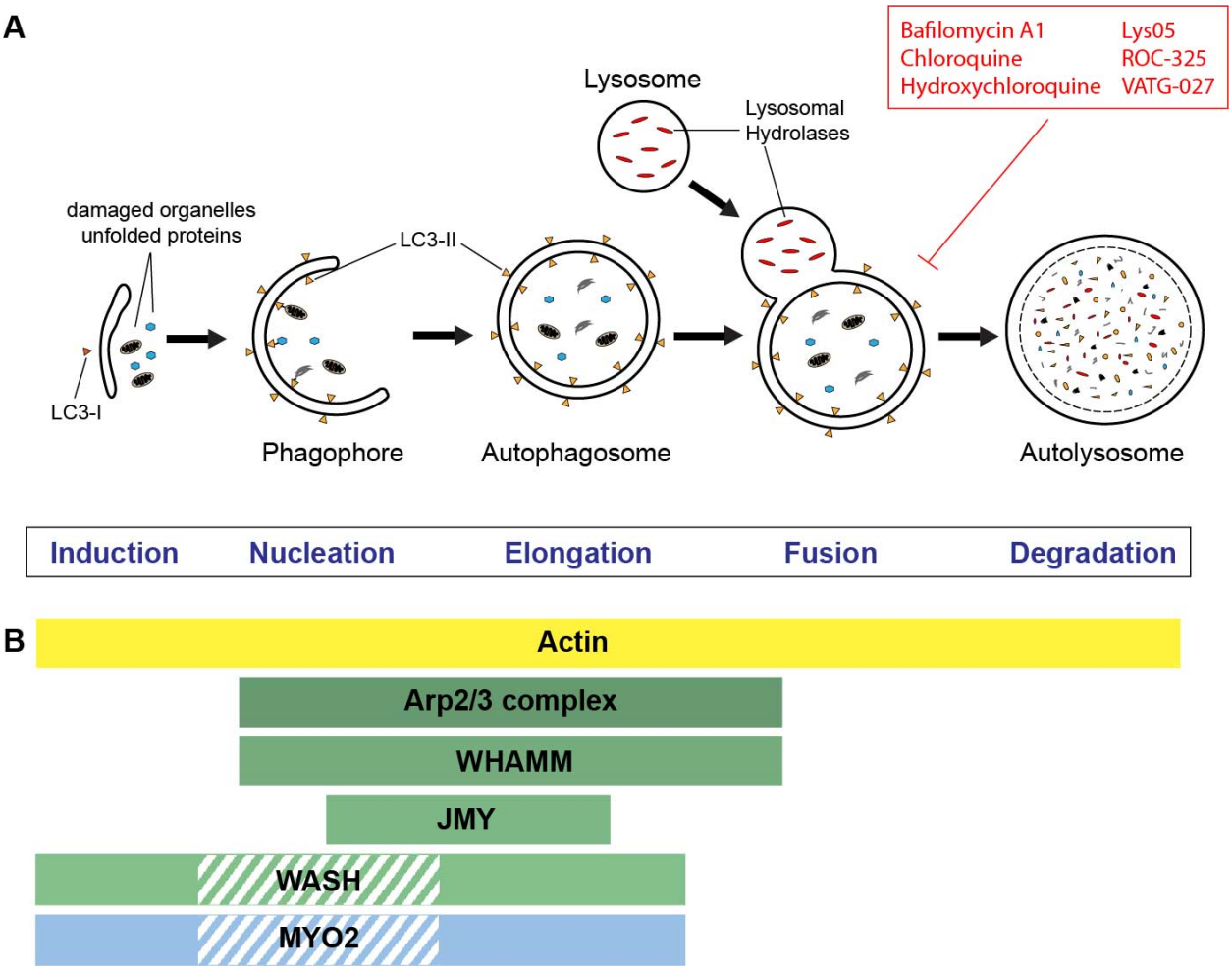

Figure 1.1. Autophagy and cytoskeleton regulatory proteins.

(A) Basal autophagy is a low-level constitutive process in cells, while induced autophagy is a result of metabolic and nutrient stress. The autophagic process begins with the nucleation of isolation membranes and phagophores. The phagophore will continue to elongate to form into a double-membraned autophagosome that sequesters intracellular cargo. Matured autophagosome will then fuse to the lysosome where acidic hydrolases degrade autophagosomes and its cargo. Inhibitors designed to disrupt lysosomal function (Bafilomycin A1, Chloroquine, Hydroxychloroquine, Lys05, ROC-325, and VATG-027) target the later stages of autophagy (lysosome fusion and degradation). **(B)** The bars indicate the arrival and departure of cytoskeletal regulatory proteins

Figure 1.1. (cont'd)

associated in various stages of autophagy. Solid bars represent the timing of cytoskeletal proteins based on published evidence. The striped bar for WASH and myosin 2 (MYO2) represents the predicted time each protein's arrival based on known function in the actin cytoskeleton dynamics.

Molecular Regulation of Autophagy

Autophagy is a highly conserved catabolic process that responds to both basal and induced signaling events. Basal autophagy serves as a homeostatic function to maintain and eliminate proteins or organelles for turnover, and if left unattended could become toxic to the cells (Liu and Debnath, 2016; Murrow and Debnath, 2013; Rabinowitz and White, 2010). Induced autophagy is believed to be a response to a wide variety of cellular stresses, including nutrient deprivation, growth factor depletion, oxidative stress, infection, and hypoxic conditions (Kroemer et al., 2010; Murrow and Debnath, 2013; Rabinowitz and White, 2010). Mechanistically, a series of complexes made up by the core autophagy proteins coordinate to form the autophagosome (**Figure1.2A and 1.2B**). Initiation of autophagy is governed primarily by serine/threonine kinase, unc-51-like autophagy initiating kinase 1 (ULK1), a mammalian ortholog of yeast Atg1.

The nutrient-sensing mechanistic target rapamycin complex 1 (mTORC1) and the energy-sensing AMP-activated protein kinase (AMPK) both regulate ULK1 activation (Alers et al., 2012; Kim et al., 2011) (**Figure 1.2A**). Under high-nutrient conditions, mTORC1 prevents autophagy induction by phosphorylating ULK1 at serine 757 (Ser 757) leading to kinase inactivation. Upon nutrient starvation, such as amino acids depletion, mTORC1-dependent phosphorylation site in ULK1 is dephosphorylated relieving ULK1 and allowing autophagy to proceed (Jung et al., 2009; Saxton and Sabatini, 2017). In contrast, when cellular energy levels decline, sensed through ATP: AMP ratio, and through phosphorylation by liver kinase B1 (LKB1), AMPK is activated and promotes autophagy induction by inhibiting mTORC1 activity (Gurumurthy et al., 2010; Roach, 2011). AMPK can also bind and phosphorylate ULK1 at serine 317 and 777, along with other reported phosphorylation sites (Alers et al., 2012; Egan et al., 2011; Kim et al., 2011) leading to

autophagy initiation. As mTORC1 and AMPK regulate ULK1, ULK1 can also inhibit its upstream regulators (Ganley et al., 2009; Jung et al., 2009).

The ULK complex induces nucleation of phagophores by phosphorylating the components of yet another protein complex referred to the class III phosphatidylinositol 3-kinase complex (PIK3C3). PIK3C3 consists of lipid kinase PI3K, Beclin-1, ATG14, activating molecule in Beclin 1-regulated autophagy protein 1 (AMBRA1), and general vesicular transport factor (p115). Activation of PIK3C3, specifically VPS34, converts phosphatidylinositol (PI) to phosphatidylinositol-3-phosphate (PI3P) and recruits PI3P effectors, such as zinc- finger FYVE domain-containing protein 1 (DFCP1) and WD-repeat domain phosphoinositide-interacting (WIPI) proteins (Russell et al., 2013).

As phagophore expands and matures to the autophagosome, ATG9 recruits other membrane sources from other organelles, including ER, Golgi, plasma membrane, and endosomes (Papinski et al., 2014; Shirahama-Noda et al., 2013). Phagophore expansion also requires two ubiquitin-like conjugation systems, ATG5-ATG12, and ATG8/LC3-phosphatidylethanolamine (PE). For AT5-ATG12 conjugation, the E1-like protein ATG7 activates the ATG12 protein and transfers ATG12 to the E2-like protein ATG10, linking ATG12 to ATG5 (Romanov et al., 2012; Walczak and Martens, 2013). The ATG5-ATG12 conjugated proteins associate to expanding phagophore by forming a complex with ATG16L1 recently reported interacting with WIPI2 (Dooley et al., 2014). As for the second conjugation system, pro-LC3 is first cleaved by the ATG4 protease to generate LC3-I. Then, ATG7 and ATG3 (E2-like enzyme) mediate the conjugation of LC3-I to membrane lipid phosphatidylethanolamine (PE) forming a membrane-bound LC3-II. A common autophagy vesicle membrane marker is LC3-II (Kabeya et al., 2000)

The detailed mechanism of autophagosome and lysosome fusion remained poorly understood. However, many mediators of the process are identified already, including Rab7 GTPase (Gutierrez et al., 2004; Jager et al., 2004), soluble N-ethylmaleimide-sensitive factor attachment protein receptors (SNAREs) (Diao et al., 2015; Itakura et al., 2012), and tethering factors such as homotypic fusion and protein sorting (HOPS) complex (Jiang et al., 2014; McEwan et al., 2015). These mediator proteins form complexes to tether and fuse autophagosome to the lysosome. Ultimately, autophagosome-lysosome fusion transformed to autolysosome where acidic hydrolases degraded contents of autophagosome including its cargo into macromolecules for cells to reuse (Nakamura and Yoshimori, 2017).

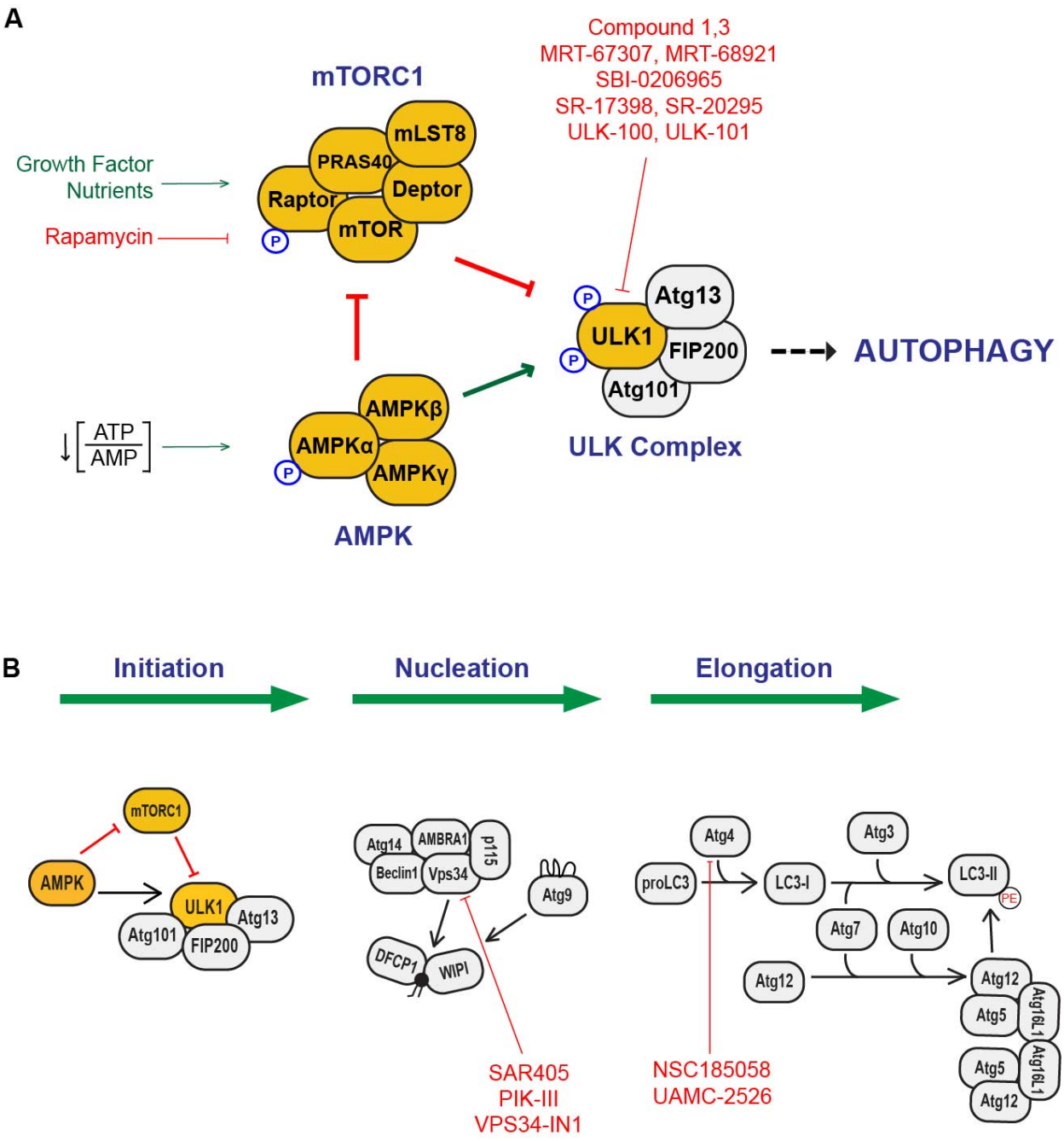

Figure 1.2. Key autophagy proteins and their regulators.

(A) mTORC1 and AMPK regulate the ULK1 complex. Under the nutrient-rich conditions, active mTORC1 directly phosphorylates and inhibits ULK1. mTORC1 inhibition by either nutrient starvation or rapamycin treatment leads to ULK1 complex activation and autophagy. As cellular energy declines, AMPK induces autophagy by inhibiting mTORC1 activity. AMPK can also

Figure 1.2. (cont'd)

promote autophagy by directly phosphorylating ULK1. ULK1 kinase is a promising target for autophagy inhibition, and nine ULK1-targeted compounds (Compound 1 and 3, MRT-67307, MRT-68921, SBI-0206965, SR-17398, SR-20295, ULK-100, and ULK-101) have been reported. **(B)** The ULK1 complex nucleates phagophores by activating components PI3P by the class III PI3K complex (Beclin1, ATG14, AMBRA1, p115, and VSP34) which converts phosphatidylinositol (PI) to PI3P and recruits PI3P effectors (DFCP1 and WIPI proteins). VSP34 is another core autophagy protein identified as a promising candidate for targeted therapy (SAR405, PIK-III, and VPS34-IN1). As the phagophore elongates and matures to the autophagosome, ATG9-containing vesicles recruit other membrane sources. ATG5-ATG12-ATG16L1 and ATG8/LC3-PE conjugation systems are important in autophagosome formation and maturation. The cysteine protease ATG4, specifically ATG4B, is another known viable target to inhibit autophagy. There are currently two reported ATG4B target inhibitors, NSC185058, and UAMC-2526.

Table 1.1. Current Autophagy Inhibitors.

Target	Compound	References
Lysosome	Bafilomycin A1	(Yamamoto et al., 1998; Yoshimori et al., 1991)
	Chloroquine	(Glaumann and Ahlberg, 1987)
	Hydroxychloroquine	(Amaravadi et al., 2011)
	Lys05	(Amaravadi and Winkler, 2012; McAfee et al., 2012)
	ROC-325	(Carew et al., 2017; Carew and Nawrocki, 2017)
	VATG-027	(Goodall et al., 2014)
ULK1	Compound 1	(Lazarus et al., 2015)
	Compound 3	(Lazarus and Shokat, 2015)
	MRT-67307	(Petherick et al., 2015)
	MRT-68921	(Petherick et al., 2015)
	SBI-0206965	(Egan et al., 2015)
	SR-17398	(Wood et al., 2017)
	SR-20295	(Wood et al., 2017)
	ULK-100	(Martin et al., 2018)
	ULK-101	(Martin et al., 2018)
VPS34	SAR405	(Peppard et al., 2014; Ronan et al., 2014)
	PIK-III	(Dowdle et al., 2014)
	VPS34-IN1	(Bago et al., 2014)
ATG4B	NSC185058	(Akin et al., 2014)
	UAMC-2526	(Kurdi et al., 2017)

Role of Autophagy in Cancer

Initial reports showing deletion of the essential autophagy gene Beclin 1 (*BECN1*) on chromosome 17q21 highlighted that autophagy could also be a tumor suppressive pathway. Allelic deletions of 17q21 are frequently observed in sporadic ovarian (Cliby et al., 1993), breast (Saito et al., 1993), and prostate (Gao et al., 1995) cancer. Early reports showed up to 40% to 75% BECN1 monoallelic loss in these cancer types (Aita et al., 1999; Gao et al., 1995; Liang et al., 1999; White, 2015). Furthermore, Liang et al. demonstrated that human breast carcinoma cell line MCF7 with exogenous expression of BECN1 could function as a negative regulator of tumorigenesis (Liang et al., 1999).

The role of BECN1 as a tumor suppressor is now considered controversial. The proximity of BECN1 to a known tumor suppressor gene, BRCA1, on chromosome 17q21 provide strong evidence that BECN1 is not a tumor suppressor gene. Based on the further interrogation of The Cancer Genome Atlas (TCGA) data and other databases, BECN1 loss, in fact, a rare event in breast, ovarian, and prostate cancers (Laddha et al., 2014; Tang et al., 2015). Also, Laddha et al. only identified significant enrichment of truncated mutation and deleted BRCA1, and deleted BRCA1 and BECN1, but failed to observe truncated mutation or deleted BECN1 alone. Thus, indicating that BECN1 is likely not a tumor-suppressor gene, but instead should be considered passenger mutation (Laddha et al., 2014). Despite BECN1 not being a tumor suppressor, some in the autophagy field still recognize autophagy as a tumor suppressive mechanism found on the observation that autophagy inhibition causes oxidative stress and DNA damage which are known to trigger tumor initiation (Karantza-Wadsworth et al., 2007; Mathew et al., 2009).

Aside from tumor suppression, other investigators recognized autophagy to possess a pro-tumorigenic role in multiple cancer types. Early on, elevated levels of autophagosomes were found

in the hypoxic core of solid tumors that further diffused as the tumor established became vascularized and less hypoxic (Degenhardt et al., 2006). Previous studies also showed that established tumors rely on autophagy for the proper functioning of organelles and metabolic support to survive in response to nutrient starvation (Guo et al., 2011; Lock et al., 2011; Yang et al., 2011). Highly proliferating tumor cells have high demands for metabolic intermediates (lipids, carbohydrates, and amino acids); and autophagy could generate and supply these metabolic intermediates to proliferating tumor cells.

Subsequent research has shown that autophagy inhibition could impair tumor growth in both *in vitro* and *in vivo* models. For instance, in pancreatic ductal adenocarcinoma (PDAC) model, Alec Kimmelman and colleagues demonstrated elevated basal autophagy in oncogenic KRAS PDAC cell lines and primary tumors (Yang et al., 2011). Thus, indicating the importance of autophagy for KRAS transformed cells. In agreement with this idea, KRAS-driven PDAC cell lines showed susceptibility to autophagy inhibitions by chloroquine (CQ; inhibitor that blocks the function of lysosome) treatment and genetic means (*ATG5* siRNA). Autophagy inhibition in these cells also revealed impaired mitochondrial function and defected energy homeostasis. A similar effect was found in which genetically engineered mouse model (GEMM) $Kras^{G12D}$-driven PDAC showed reduced progression of premalignant intraepithelial neoplasia (PanIN) to invasive malignant PDAC after deletion of the autophagy gene *Atg5* (Rosenfeldt et al., 2013; Yang et al., 2014). Consistent with earlier findings, Eileen White and colleagues observed that cancer cells with RAS mutations showed a high level of basal autophagy (Yang et al., 2014), and this allowed for maintenance of functional mitochondria required for tumor cells survival (Guo et al., 2011). Moreover, deletion of *Atg7* in the lungs of $Kras^{G12D}$-driven GEMMs prevented the formation of adenomas to adenocarcinomas, instead transformed into a benign form of oncocytoma. *Atg7*-

deficient tumors also showed defective mitochondria and fatty acid oxidation, consistent with the *in vitro* data (Guo et al., 2013a).

Aside from Kimmelman and White labs, other investigators used GEMMs to evaluate the function of autophagy in multiple tumor types, including breast cancer (Wei et al., 2011), melanoma (Xie et al., 2015), and lung cancer (Rao et al., 2014). Each of these studies helped unveil the contextual role of autophagy in cancer. One best example is the unique difference between $Kras^{G12D}$- (Guo et al., 2013a) and $Braf^{V600E}$-driven lung cancers (Strohecker et al., 2013). In the presence of wild-type p53 ($p53^{+/+}$), autophagy deficiency ($Atg7^{-/-}$) in both *in vivo* models showed decreased lung tumor burden. However, only the $Braf^{V600E}$ mutant *Atg7*-deficient ($Braf^{V600E/+}$; $Atg7^{-/-}$) mice showed increased overall survival as the $Kras^{G12D}$ mutant *Atg7*-deficient ($Kras^{G12D/+}$; $Atg7^{-/-}$) mice died from pneumonia that confounded the overall survival data. Furthermore, $Kras^{G12D}$ mutant, *Atg7* deleted, *Trp53*-deficient ($Kras^{G12D/+}$; $Atg7^{-/-}$; $p53^{-/-}$) tumors revealed defective fatty acid oxidation and lipid accumulation. Thus, suggesting differential regulation of mitochondrial metabolism based on the oncogenic driver.

As mentioned above, autophagy could mediate the suppression of p53 in both KRAS- and BRAF-driven lung cancers. The tumor suppressor p53 is a critical regulator in response to stress stimuli including DNA damage, oncogene activation, and oxidative stress. Since autophagy is also an adaptive response to many cellular stresses, the two signaling pathways were believed to functionally intertwined in tumor cells (Guo et al., 2013b; White, 2016)). Indeed, the role of p53 in autophagy may depend on its subcellular localization. Guido Kroemer and colleagues reported that cytosolic mutant p53, by deletion of the nuclear export signaling ($p53^{\Delta NES}$), suppressed autophagy (Morselli et al., 2008). Conversely, Tasdemir et al. showed that inhibition of p53 by cyclic pifithrin-α (PFT-α; a pharmacological antagonist of p53) treatment and genetic means

(*TP53* siRNA) induced autophagy (Tasdemir et al., 2008). In contrast, stabilized nuclear wild-type p53 transactivates autophagy-related target genes, including *AMPK*, *TSC2* (Feng et al., 2005) and sestrins (*SESN1* and *SESN2*) (Budanov and Karin, 2008), which could lead to mTOR inhibition and autophagy induction. Moreover, Kevin Ryan and colleagues showed that nuclear p53 regulates damage-regulated autophagy modulator (*DRAM*) that encodes a lysosomal protein leading to autophagy induction (Crighton et al., 2006). Finally, by using chromatin immune-precipitation (ChIP) and sequencing (ChIP-seq) with RNA sequencing (RNA-Seq) the Attardi group identified direct p53 target autophagy core genes such as *Atg4A*, *Atg4C*, *Atg7*, *Ulk1*, and *Ulk2* in response to DNA damage and p53 activation by HDM2 inhibitor nutlin-3a (Kenzelmann Broz et al., 2013). I reasoned that the relationship between p53 and autophagy remained unclear and required further investigation.

Targeting Autophagy in Cancer

In addition to autophagy's established role in tumor maintenance and metabolic adaptation. Previous works showed that autophagy could also support tumor growth by promoting resistance to a variety of therapies (Carew et al., 2007; Degtyarev et al., 2008; Zhang et al., 2012). One notable study by Craig Thompson and colleagues demonstrated that tumor cells use autophagy to survive cytotoxic chemotherapy (Amaravadi et al., 2007). This *in vivo* study showed that autophagy inhibition with either CQ or *ATG5* short hairpin RNA (shRNA) enhanced the ability of tamoxifen-induced p53 apoptotic cell death or alkylating drug therapy (cyclophosphamide).

Since then, efforts from academia, biotech, and the pharmaceutical industry focused on developing small molecule inhibitors targeting the machinery of the autophagy pathway. To date, there are numerous ongoing clinical trials (ClinicalTrials.gov) targeting multiple cancer types to

assess the effect of autophagy inhibitors alone or in combination with chemotherapy, radiotherapy, and target agents. All reported trials use CQ or its derivative, hydroxychloroquine (HCQ). CQ and HCQ are FDA approved for the treatment of malaria, and known to block the function of the lysosome, the ultimate destination for autophagic cargo. Unfortunately, results from recent Phase I and II clinical trials resulted in varying levels of efficacy due to the level of autophagy inhibition and unfavorable pharmacokinetics (Rebecca and Amaravadi, 2016; Wang et al., 2016). Therefore, there is an intensive effort to develop better-improved lysosome inhibitors, including Lys05, ROC-325, and VATG-027 (**Figure 1.1, Table 1.1**).

As the field continued to uncover more intricate details about the molecular mechanisms of autophagy and its importance in cancer, new promising small molecules that target the autophagy core proteins have emerged (Limpert et al., 2018). Currently, there are ongoing studies that evaluate the efficacy of small molecule inhibitors directed against VPS34 and ULK1/2 (**Figure 1.2, Table 1.1**). Since ULK1 is an integral player of autophagy initiation machinery, ULK1 is a highly sought-after target for autophagy inhibition. To date, many groups focus on evaluating the structure and activity of ULK1 to develop potent and selective small molecule inhibitors that suppress the kinase activity and blocks the autophagy process.

Study Overview

The function of autophagy in cancer is complex. GEMM studies illustrated the role of autophagy in cancer highly dependent on the tumor stage, the tissue of origin, and cellular context. Thus, creating uncertainties regarding the use of autophagy inhibitor as cancer therapy. Interestingly, *in vivo* studies described above helped identified potential candidate biomarkers that

may benefit to autophagy inhibitions, including p53 wild-type status and KRAS mutation in non-small cell lung cancer (NSCLC).

Therefore, in this current study, I hypothesized that NSCLC which harbor p52 wild-type and KRAS mutation, particularly $KRAS^{G12C}$, would have a susceptible response to autophagy inhibition. In order to test my hypothesis, I used small molecules inhibitors either stabilized wild-type p53 or inhibited $KRAS^{G12C}$ and examined the mechanism underlying the autophagy response in tumor cells, particularly NSCLC. I used HDM2 inhibitors MK-8242 and nutin-3a to induce wild-type p53, and the $KRAS^{G12C}$ inhibitor ARS-853 to inhibit oncogenic $KRAS^{G12C}$ signaling.

Based on *in vivo* studies described above, tumor suppressor p53 and oncogenic KRAS showed a unique relationship with autophagy in lung cancer. Mechanistically, p53 and KRAS signaling pathways both regulate the activity of mTORC1, a key inhibitor of autophagy. In this study, I first elucidated the role of wild-type p53 on autophagy in osteosarcoma and NSCLC lines. Next, I further examined the relationship between $KRAS^{G12C}$ and autophagy in $KRAS^{G12C}$ mutant NSCLC lines. Finally, I evaluated the therapeutic potential of autophagy inhibition in $KRAS^{G12C}$ NSCLC as single-agent and combination with selective $KRAS^{G12C}$ inhibitor. In the end, my collected data would provide additional insight into the role of autophagy in tumor cell survival and cancer therapeutics.

CHAPTER 2.

IDENTIFICATION OF MYOTONIC DYSTROPHY KINASE-RELATED CDC42-BINDING KINASE (MRCKα) IN p53-DEPENDENT AUTOPHAGY

Modified from

Stephanie L. Celano, Lisette P. Yco, Matthew G. Kortus, Abigail R. Solitro, Hakan Gunaydin, Mark Scott, Edward Spooner, Ronan C O'Hagan, Peter Fuller, Katie R. Martin, Stuart D. Shumway, and Jeffrey P. MacKeigan. Identification of kinases responsible for p53-dependent autophagy (2019). Identification of kinases responsible for p53-dependent autophagy. *In press*.

ABSTRACT

Autophagy is a dynamic intracellular trafficking pathway which transports intracellular organelles and protein to the lysosome. A series of previous studies suggest that actin cytoskeleton and cytoskeletal regulatory proteins play a critical role in autophagy. In this study, we provided additional findings that demonstrate the association of cytoskeletal proteins in p53-dependent autophagy. The tumor suppressor p53 has been shown to have a dual function in the autophagy which dependent on its subcellular localization. Cytosolic p53 is recognized as an inhibitor of autophagy. On the other hand, nuclear p53 transactivate autophagy-related genes in response to cellular stress, such as nutrient deprivation. Using HDM2 inhibitor which blocks HDM2-p53 interaction and stabilizes nuclear p53, we observed autophagy induction in wild-type p53 U2OS cells. We also identified kinases, including ULK1 and MRCKα, required in p53-dependent autophagy by performing fluorescence microscopy siRNA screen. CDC42 effector protein kinase MRCKα is known to regulate actin-myosin contractility through MLC2 phosphorylation. However, no current published reports associate MRCKα to autophagy. Based on our results, we found that knockdown MRCKα treated with HDM2 inhibitor decreased EGFP-LC3B positive autophagic vesicle. Thus, suggesting that MRCKα plays a role in autophagosome maturation. Our study provided evidence linking MRCKα to autophagy.

INTRODUCTION

Autophagy is a cellular recycling process that degrades intracellular proteins and organelles. It is a highly conserved catabolic process involving recruitment of autophagy core proteins and nucleation of membrane leading to the formation of a double-membrane autophagosome which transports intracellular components for lysosomal degradation. As our understanding of autophagy continues to expand, we rarely consider autophagy as a cytoskeleton directed membrane trafficking pathway. In fact, cells depend on the actin cytoskeleton assembly to orchestrate the biogenesis and trafficking of autophagosome to lysosome within a three-dimensional space (Chan and Olson, 2016; Kast and Dominguez, 2017; Zientara-Rytter and Subramani, 2016).

William Dunn Jr. and colleague's first recognized the role of actin in autophagy using actin depolymerizing agents (Aplin et al., 1992). The Dunn group demonstrated the importance of actin polymerization by treating normal rat kidney (NRK) cells with cytochalasin B (cytB) or D (cytD). Using electron microscopy and micrograph, they found decreased autophagic vacuoles in cytB or cytD treated NRK cells cultured in amino acid-deprived media. Then in 2008, another independent study showed that actin cytoskeleton dynamics is critical during autophagosome formation. Maria Isabel Colombo and colleagues revisited the effect actin depolymerizing agents on autophagosome formation using more advanced molecular techniques (Aguilera et al., 2012). In this study, they treated Chinese hamster ovary (CHO) and HeLa cells expressing GFP-microtubule-associated protein 1 light chain 3 (MAP1LC3) with another actin depolymerizing agent latrunculin B (latB). Using immunofluorescent microscopy, they observed that latB also reduced the number of starvation- and rapamycin-induced GFP-MAP1LC3 positive puncta, without affecting basal

autophagy. Together, the Dunn group and Colombo group highlighted the importance of actin polymerization in induced autophagy.

Actin cytoskeleton nucleation is thermodynamically unfavorable such that cells use nucleation regulatory factors including Arp2/3 complex and nucleation promoting factors (NPFs) WHAMM, JMY, and WASH to promote actin polymerization (Blanchoin et al., 2014). Today, a series of studies connected Arp2/3 complex and NPFs to autophagy. Zusen Fan and colleagues found that WASH knockout mouse model showed elevated autophagy which leads to embryonic lethality (Xia et al., 2013). Furthermore, two independent studies linked JMY (Coutts and La Thangue, 2015) and WHAMM (Kast and Dominguez, 2015) in autophagosome biogenesis and formation. Thus, these recent results provided additional evidence linking actin polymerization to autophagy.

Another way actin cytoskeleton could mediate autophagy is by providing tracks to motor proteins myosin. These motor proteins play an essential role in many cellular processes required for transport (Vicente-Manzanares et al., 2009). A previous report showed that ULK1 regulates the activation of non-muscle myosin II (MYO2) during ATG9 trafficking in the formation of the autophagosome (Tang et al., 2011). The Chen group demonstrated, both in *Drosophila* and mammalian cells, that ULK1 phosphorylates myosin light chain-like kinase (Spaghetti squash (Sqh) in Drosophila and zipper-interacting protein kinase, ZIPK, in mammalian cells) leading to phosphorylation of regulatory light chain of MYO2 (MLC2). Activated MYO2 then interacts with actin forming actomyosin filament that provides force or tract for ATG9 trafficking from Golgi to the site of expanding phagophores (Kruppa et al., 2016; Tang et al., 2011). Despite the findings that actin- and myosin-based transport is important in autophagy, a detailed association of these cellular processes is still unclear.

In this study, we provided new and promising data illustrating how actin filaments and cytoskeletal proteins could regulate p53-dependent autophagy. p53 responds to a wide range of stimuli, including DNA damage and metabolic stress (Joerger and Fersht, 2016; Kastenhuber and Lowe, 2017; Kruiswijk et al., 2015). In turn, once p53 is stabilized and activated this allows p53 to bind to sequence-specific response elements in specific target genes. Once bound to DNA, p53 transcriptionally activates genes involved in distinct biological processes, including cell cycle, apoptosis, and senescence (Bieging et al., 2014; Junttila and Evan, 2009). Previous works also suggested that p53 could regulate "non-canonical" programs, including autophagy (Kastenhuber and Lowe, 2017). In fact, p53 demonstrated both negative (Morselli et al., 2008; Tasdemir et al., 2008) and positive (Budanov and Karin, 2008; Kenzelmann Broz et al., 2013) function in autophagy which dependents on its cellular localization.

Using human osteosarcoma U2OS cells, we completed fluorescence microscopy-based kinome siRNA screening to identify kinases involved in HDM2 inhibitor-induced p53-dependent autophagy. We treated wild-type p53 cells with HDM2 inhibitor MK-8242 leading to stabilization and activation of p53. We found that ULK1 and myotonic dystrophy kinase-related Cdc42-binding kinase alpha (MRCKα, encoded by CDC42BPA) are required for p53-induced autophagy. ULK1 is a well-known autophagy kinase. On the other hand, no published reports link the CDC42 effector protein kinase MRCKα to autophagy. Interestingly, MRCKα regulates actin-myosin contractility through phosphorylation of MLC2 and myosin phosphates target subunit 1 (MYPT1) (Leung et al., 1998; Unbekandt and Olson, 2014). Based on our results, we proposed that MRCKα is necessary during autophagosome maturation of p53-dependent autophagy. Furthermore, MRCKα could be a promising marker that could improve our understanding of the relationship between actin cytoskeleton and autophagy.

RESULTS

HDM2 inhibitor promotes p53-dependent autophagy

E3 ubiquitin-protein ligase murine double minute 2 (MDM2; HDM2 in humans) tightly regulates the protein level of wild-type p53. HDM2 directly binds to p53 and promotes its ubiquitination which drives to proteasome degradation of p53 protein (Wu et al., 1993). Since many human cancers showed amplified HDM2 gene (Fakharzadeh et al., 1993; Fakharzadeh et al., 1991) one of the efforts to gain insight into the function of wild-type p53 in cancer is the development of HDM2 inhibitors. Here, we first tested whether MK-8242-induced p53 stabilization activates autophagy.

To confirm the inhibitory effect of MK-8242 on HDM2, we treated U2OS cells with a concentration gradient of MK-8242 (0.1-20 μM) and measured the protein level of p53 and its target $p21^{Waf1}$ (CDKN1A, CIP1, WAF1, p21) (el-Deiry et al., 1993; el-Deiry et al., 1995; Levine, 1997) by immunoblotting. After 24 hours of treatment, 1.0 μM MK-8242 showed a pronounced effect on the protein level of p53 and p21 (**Figure 2.1A**). By using p53 DNA binding assay, the observed increased protein level of p53 and p21 was due to MK-8242-induced nuclear p53 stabilization (**Figure 2.1B**).

Next, we wanted to test whether HDM2 inhibition induces autophagy, we measured BafA1-induced LC3B accumulation in MK-8242 treated cells. Adding BafA1 on the last 1.5 hours of treatment disrupts the lysosomal function and inhibits degradation stage of autophagy. This step is critical as it allows autophagy investigators to measure the LC3B-II protein level associated with the overall rate of autophagy (Klionsky et al., 2016). As shown in **Figure 2.1C**, BafA1-induced MK-8242 treated U2OS cells showed higher accumulation of LC3B-II protein level compared to

control and BafA1 treated cells. To further validate the observed phenotype, EGFP-LC3B expressing U2OS cells were treated with MK-8242 and quantified autophagic puncta. As predicted, cells treated with MK-8242 showed a higher number of EGFP-LC3B-labeled positive puncta representing autophagic vesicles compared to control (**Figure 2.1D and 2.1E**). These data suggest that MK-8242 effectively induce autophagy in wild-type p53 cells.

Since various cellular stressors activate autophagy, it is important to determine whether the observed autophagy induction is precisely due to HDM2 inhibition. Thus, we transfected U2OS cells with *TP53* or control siRNA construct and treated with MK-8242 (1.0 μM) for 24 hours adding BafA1 for the last 1.5 hours. As shown in **Figure 2.1F**, *TP53* siRNA U2OS cells failed to show stabilization of p53 and expression of p21 protein when treated with MK-8242 compared to MK-8242 treated control siRNA cells. Also, TP53 knockdown prevented the accumulation of BafA1-induced LC3B-II after treated with MK-8242 (**Figure 2.1F**). Together, the above findings strongly indicate that MK-8242-induced autophagy is specifically due to stabilization of p53 and activation of p53 signaling.

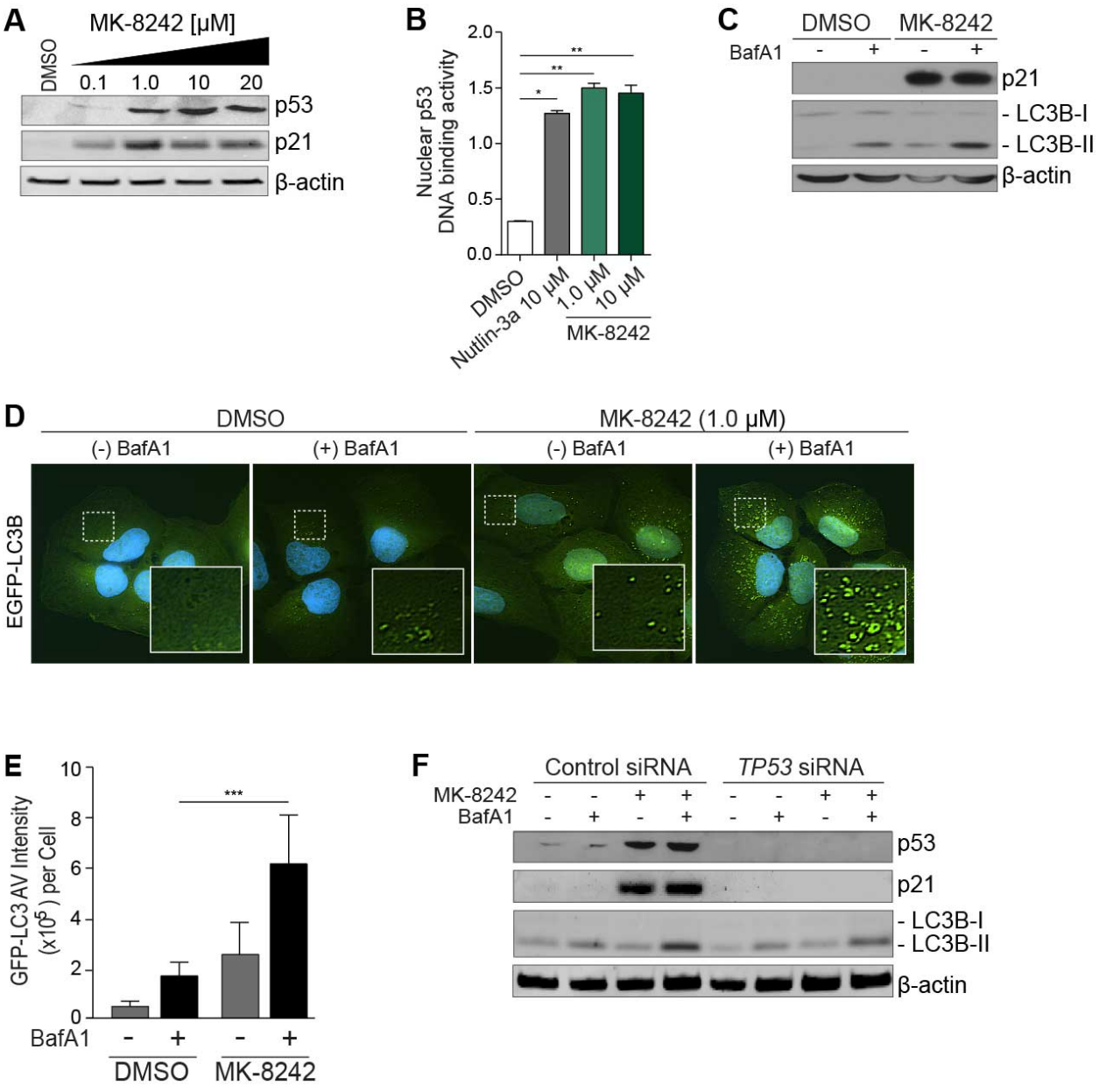

Figure 2.1. HDM2 inhibitor stabilizes nuclear p53 leading to autophagy induction.

(A) U2OS cells treated with increasing concentration of MK-8242 for 24 hours (n=2 biological replicate). **(B)** Nuclear fraction lysates of U2OS cells treated with Nutlin-3a (10 μM) or MK-8242 (1.0 or 10 μM) for 24 hours collected and assessed for p53 DNA binding activity (n=3 biological replicates; SEM). **(C)** Whole-cell lysates of U2OS treated with 1.0 μM of MK-8242 for 24 hours with (+) or without (-) 100 nM BafA1 for the final 1.5 hours of treatment. Insets 2x magnification

Figure 2.1. (cont'd)

(n=3 biological replicate). **(D)** Fluorescence microscopy images of U2OS-EGFP-LC3B cells treated with 1.0 μM of MK-8242 for 24 hours with (+) or without (-) 100 nM BafA1 for the final 1.5 hours of treatment. Insets 2x magnification. **(E)** Single cell EGFP-LC3B positive puncta (green) captured and intensity quantified. Bar graphs represent the mean intensity of all cells and SEM). EGFP-LC3B positive puncta (green). Nuclei counterstained (blue). **(F)** Control siRNA and *TP53* siRNAs U2OS treated with 1.0 μM MK-8242 for 24 hours with (+) or without (-) 100 nM BafA1 for the final 1.5 hours of treatment (n=2 biological replicate). *$p < 0.05$, **$p < 0.01$, ***$p < 0.001$.

p53 induces autophagy genes in response to HDM2 inhibition

At the molecular level, p53 functions as a transcription factor that induces a variety of gene networks involved in distinct biological processes, such as cell cycle and apoptosis. Previously, Laura Attardi and colleagues used primary mouse embryo fibroblasts (MEFs) and identified numerous genes that contribute to autophagy after DNA damage (Kenzelmann Broz et al., 2013). Here, our laboratory predicted that activating p53 by inhibiting HDM2 will also transcriptionally activate genes involved in the autophagy process. In order to test this, wild-type p53 osteosarcoma cell line, U2OS, was treated with nutlin-3a and measured the expression of well-known p53-target genes involved in autophagy, including *DRAM1* (Crighton et al., 2006), *SESN2* (Budanov and Karin, 2008), *FOXO3A*, *ATG4A* (Fitzwalter et al., 2018; Kenzelmann Broz et al., 2013; Mrakovcic and Frohlich, 2018; van der Vos et al., 2012), and *ULK1* (Kenzelmann Broz et al., 2013), using quantitative real-time PCR. As shown in **Figure 2.2A and 2.2B**, nutlin-3a (10 μM) treated U2OS cells showed increased expression of p53-target autophagy genes and known p53-target gene *CDKN1A* (p21).

To further evaluate if the induction of observed autophagy-related genes is dependent on p53 activation in response to HDM2 inhibition, U2OS cells were transfected with either siRNA control or siRNA directed against p53 (*TP53*). After 48 hours incubation, the siRNA control and siRNA p53 U2OS cells were treated with nutlin-3a for 24 hours. Indeed, the p53 knockdown decreased the expression of all five autophagy-related genes (*DRAM1*, *SESN2*, *FOXO3A*, *ATG4A*, and *ULK1*) (**Figure 2.2A**), including p53-target gene *CDKN1A* (p21) (**Figure 2.2B**), which clearly show p53-dependent induction in response to nutlin-3a treatment. Together, these findings suggest that HDM2 inhibition is capable of inducing p53-target autophagy-related genes.

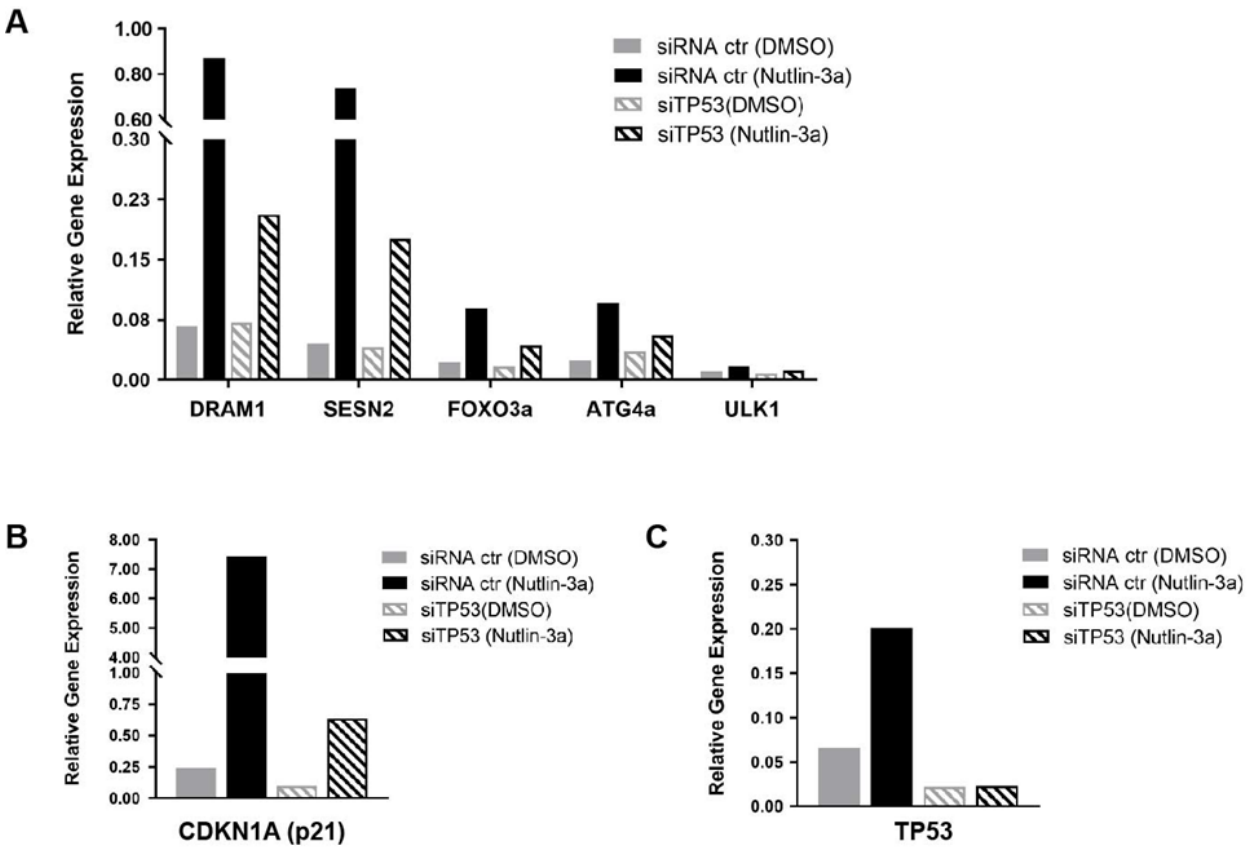

Figure 2.2. Active p53 regulates autophagy-related genes in response to nutlin-3a.

Quantitative RT-PCR analysis of U2OS transduced with control or *TP53* siRNA treated with nutlin-3a for 24 hours. Relative expression gene of **(A)** autophagy-related genes, **(B)** *CDKN1A* (p21), and **(C)** *TP53*.

ULK1 and MRCKα kinases necessary in p53-dependent autophagy

In order to elucidate the p53-dependent autophagy, our laboratory completed fluorescence microscopy-based siRNA screen to identify human kinases involved in MK-8242-induced autophagy. U2OS-ptfLC3B cells were transfected with libraries of siRNAs (pool of four independent sequences per target gene per well) for 24 hours before MK-8242 treatment. These siRNA knockdown cells were then treated with MK-8242 for an additional 24 hours adding BafA1 for the last hour. Cells were fixed and quantified EGFP-LC3B positive puncta. Knocking down well-known autophagy genes *ATG5/12* and *ATG9A/B* using siRNAs were added as a positive control. After screening a total of 755 gene targets and reevaluating the observed top 50 siRNAs, ULK1 and MRCKα siRNA cells showed the significant reduced autophagic vesicles (**Figure 2.3A**). As expected, TP53 knockdown reduced EGFP-LC3B autophagic vesicles (**Figure 2.3A**), consistent from the above assay (**Figure 2.1F**).

Serine/threonine ULK1 kinase is well-known for its integral role in autophagy induction. Therefore, ULK1 as one of the top hits from the screening was an intuitive finding. On the other hand, the identification of MRCKα was very intriguing. MRCKα is a CDC42 effector protein which regulates cellular actin-myosin cytoskeleton organization (Unbekandt and Olson, 2014). In addition, there is currently no defined relationship between MRCKα and autophagy. In order to verify the autophagy suppression phenotype observed from the screen, we transfected U2OS-ptfLC3B cells with individual ULK1 siRNA or MRCKα siRNA and again measured MK-8242-induced EGFP-LC3B-II autophagic vesicles. Indeed, ULK1 and MRCKα knockdown suppressed MK-8242-induced autophagy (**Figure 2.3B and 2.3C**). Thus, the validation experiments strengthen the screen data that ULK1 and MRCKα are key kinase players in p53-dependent autophagy.

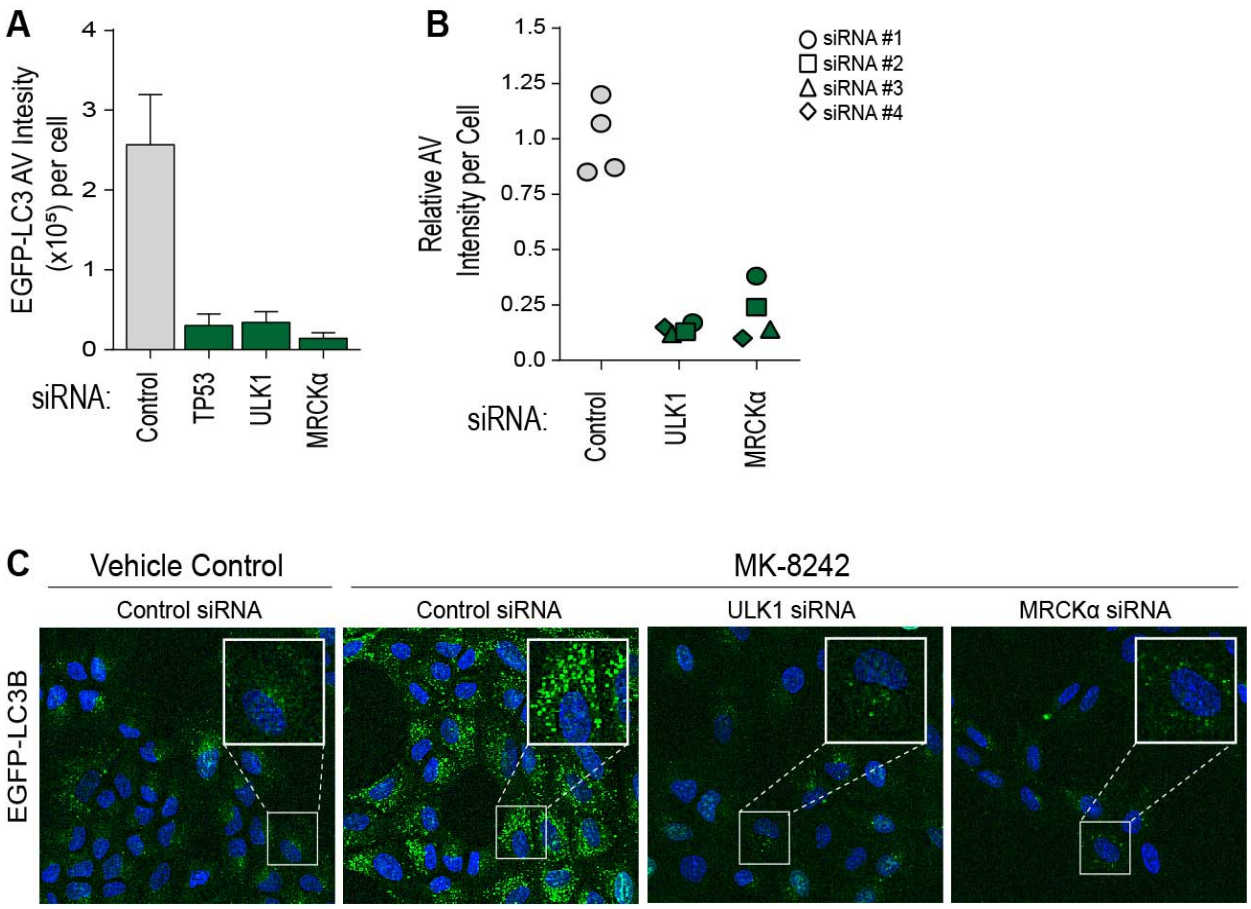

Figure 2.3. Kinase ULK1 and MRCKα are necessary for p53-dependent autophagy.

(A) MK-8242 treated siRNAs (TP53, ULK1, and MRCKα) that showed pronounced decreased EGFP-LC3B autophagic vesicles (AVs) in siRNA rescreen assay. Bars represent the mean intensity per siRNA cells and SEM. **(B)** All four siRNA constructs (each siRNA construct represent a shape) used in the pool tested independently for control, ULK1, and MRCKα. Relative EGFP-LC3B intensity (AV) per cell for each independent siRNA construct reported. **(C)** U2OS-EGFP-LC3B cells treated with MK-8242, and ULK1 siRNA and MRCKα siRNA. Nuclei counterstained (blue). Insets at 2x magnification.

MRCKα important for autophagosome maturation

Rho-family GTPases (Rho, Rac, and Cdc42) control actin cytoskeleton by regulating actin filament nucleation factor Arp2/3. As a series of reports started to reinforce the link of Arp2/3 complex and its NPFs with autophagy (Kast and Dominguez, 2017; Kruppa et al., 2016) , Rho GTPases connection in autophagy became an interest. In fact, recent studies suggested a multifactorial role of RhoA-associated protein kinase, ROCK1/2 in autophagy (Aguilera et al., 2012; Gurkar et al., 2013; Mleczak et al., 2013). Since MRCKα is a CDC42 effector kinase and shares substrates with ROCK1/2, we wanted to assess the role of MRCKα in p53-dependent autophagy further.

ROCK kinases were indicated to modulate the early stage of autophagosome formation. Also, ROCK shared many functions in actin-myosin dynamics with MRCK (Kale et al., 2015; Unbekandt and Olson, 2014). Both ROCK and MRCK regulate actin-myosin contraction by MLC2 (Ser19) phosphorylation and MYPT1 inactivation. Thus, we predicted that the requirement of MRCKα is necessary during the early stage of autophagosome formation. To test this, we first examined the effect MK-8242 in the nucleation stage of autophagy. We treated EGFP-DFCP1 (a marker for nucleation) expressing U2OS with MK-8242 and found MK-8242 significantly increased EGFP-DFCP1 positive puncta (**Figure 2.4A**). However, MRCKα knockdown using siRNA failed to reveal suppression of DFCP1 phenotype when knockdown cells were treated with MK-8242 (**Figure 2.4B**).

Interestingly, we again observed that MRCKα knockdown reduced EGFP-LC3B autophagic vesicle in response to HDM2 inhibitor MK-8242 (**Figure 2.4C and 2.4D**). Thus, strongly support the above findings that MRCKα has a critical role in p53-dependent autophagy. In summary, our data suggest that MRCKα does not play a role during DFCP1 recruitment to the

phagophore membrane. Instead, MRCKα may involve during phagophore expansion and autophagosome maturation.

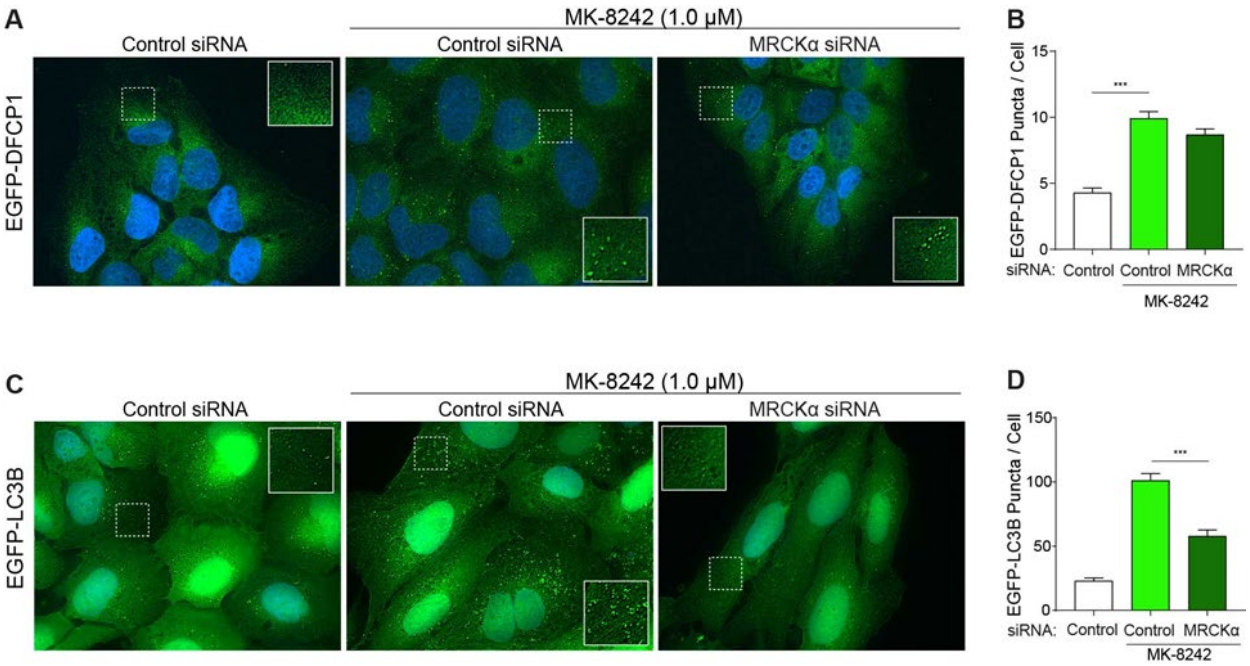

Figure 2.4. MRCKα plays a role in autophagosome maturation.

(A) EGFP-DFCP1 and **(C)** EGFP-LC3B expressing U2OS cells treated with the control and MRCKα siRNAs for 24 hours and treated with MK-8242 (1.0 μM) for another 24 hours. Nuclei were counterstained (blue). Insets are a 2x magnification. **(B)** The number of EGFP-DFCP1-positive puncta quantified from the images in (A). **(D)** The number of EGFP-LC3B-positive puncta quantified from the images in (C). Bars represent means of all cells and SEM. ***$p < 0.001$.

Depolymerization of actin filament mediates autophagy in response to starvation

The identification of MRCKα in our siRNA kinome screening inspired me to examine actin cytoskeleton in starvation-induced autophagy using our monoclonal U2OS-ptfLC3B cells. As mentioned above, Aguilera et al. reported the involvement of actin polymerization during autophagosome formation. They demonstrated that actin depolymerizing agent latrunculin B (latB) treated cells prevented BafA1-induced MAP1LC3-positive puncta accumulation in response to starvation (Aguilera et al., 2012). Here, in order to confirm the association of actin assembly during autophagosome formation, EGFP-LC3B expressing U2OS cells was treated with latB and another actin depolymerizing drug, cytochalasin D (cytD). LatB forms a 1:1 complex with globular-actin (G-actin) preventing the addition of actin subunits to the filament ends (Spector et al., 1989). On the other hand, the cytD agent reported to strongly disrupt actin polymerization by binding at the barbed-end of filamentous-actin (F-actin) (Carlier et al., 1986).

In order to investigate the effect of latB and cytD in autophagy, I measured microtubule-associated protein 1 light chain 3 (MAP1LC3B/LC3B), a known biomarker to measure autophagy, using fluorescence microscopy (Klionsky et al., 2016). Since autophagic flux is often interpreted based on LC3B-II turnover by the lysosome, we added vacuole H+-ATPase inhibitor Bafilomycin A1 (BafA1) toward the end of treatments. BafA1 interferes with the autophagosome-lysosome fusion and degradation stage of autophagy giving an adequate measurement of the rate of autophagosome synthesis or degradation over a given time frame.

In agreement with previous studies, latB and cytD treated cells showed depolymerization of actin microfilaments. Control treated cells revealed phalloidin-labeled stress fibers (**Figure 2.5A**) cultured in full growth or starve (1X HBSS with 2g/L glucose). While the 2-hour latB (5.0μM) and cytD (2.0μM) treated cells showed abolished phalloidin-labeled stress fibers in

response to starvation (**Figure 2.5B**). Also, it is important to note that adding BafA1 (100 nM) on the last hour of treatment showed no effect on actin stress fibers (**Figure 2.5A**).

Next, I measured EGFP-LC3B autophagic vesicle in latB and cytD treated cells. As shown in **Figure 2.5B and 2.5C**, I observed a decrease in EGFP-LC3B autophagic vesicle in latB treated cells cultured in HBSS starvation media. In contrast, cytD did not decrease the number of EGFP-LC3B positive autophagic vesicles (**Figure 2.5B and 2.5C**). Interestingly, my cytD findings did not agree with Aguilera et al. published report (Aguilera et al., 2012), thus suggesting that each actin depolymerizing agent could cause a different effect on autophagy process.

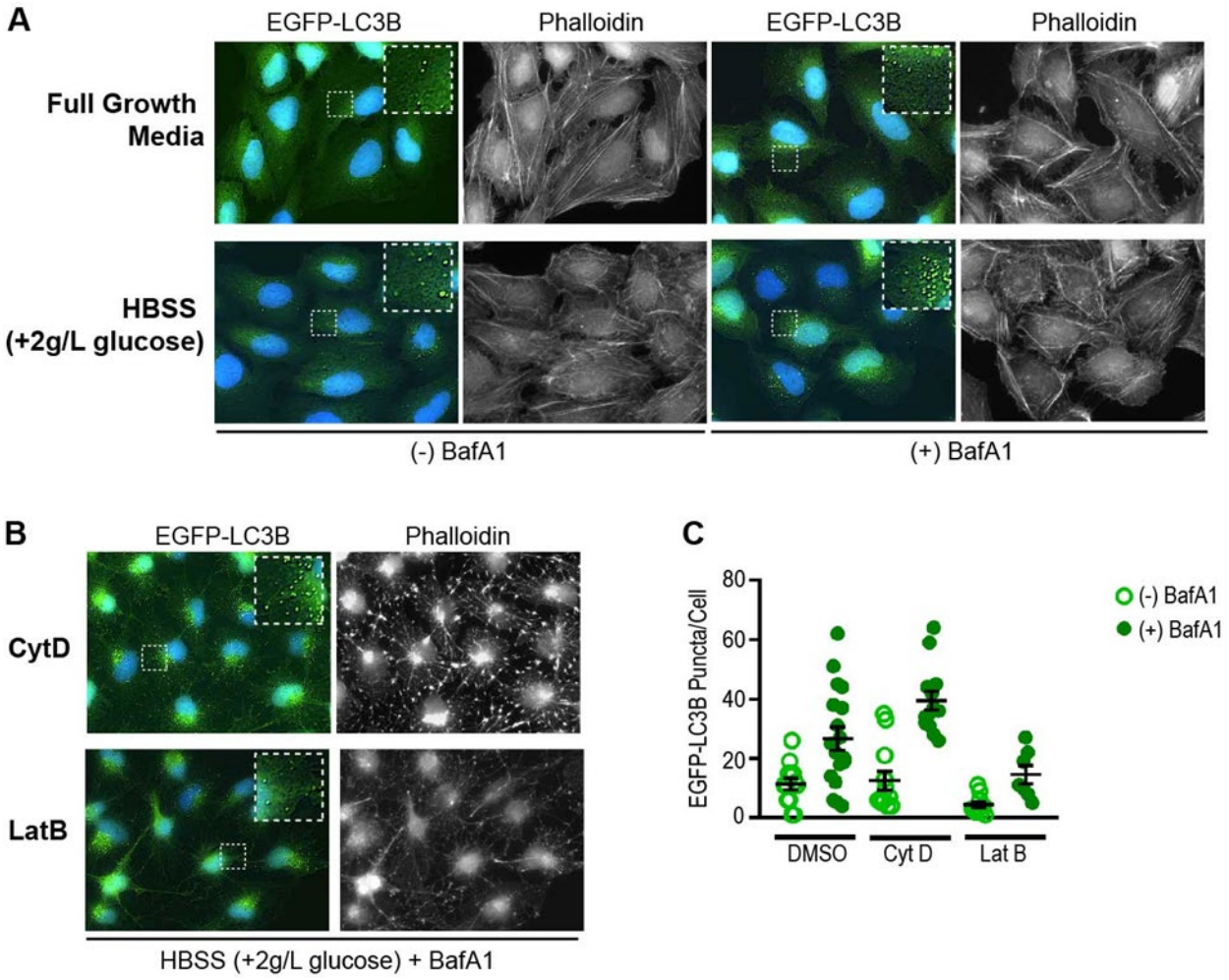

Figure 2.5. Actin depolymerizing agents affect starvation induced-autophagy.

(A) U2OS-EGFP-LC3B cells cultured in full growth or HBSS starvation media for 2 hours with (+) or without (-) 100 nM BafA1 for the final hour of treatment. **(B)** U2OS-EGFP-LC3B cells treated with cytD (2.0 μM) or latB (5.0 μM) in HBSS starvation media for 2 hours with (+) 100 nM BafA1 for the final hour of treatment. **(C)** Dot plots represent the number of EGFP-LC3B positive puncta (green) per cell captured in (B). F-actin phalloidin-stained (grayscale). Nuclei counterstained (blue). Insets 2x magnification.

DISCUSSION

The tumor suppressor p53 is activated by various stressors including DNA damage and metabolic stress. In turn, p53 transcriptionally regulates its target genes involved in the distinct biological process such as cell cycle, apoptosis, and autophagy. In order to better understand the relationship between wild-type p53 and autophagy, we treated wild-type p53 U2OS cells with the p53-HDM2 inhibitor MK-8242 (Ravandi et al., 2016; Tisato et al., 2017; Wagner et al., 2017). We first showed that MK-8242 inhibits HDM2 and induces p53 stabilization starting at 1.0μM concentration, a better potency when compared to first HDM2 inhibitor nutlin-3a (Vassilev et al., 2004). By measuring the accumulation of LC3B using immunoblotting and fluorescent microscopy, we found that stabilization of nuclear p53 due to HDM2 inhibition induces autophagy.

Also, our laboratory completed a kinome siRNA screen to identify critical molecular players required in p53-dependent autophagy in response to HDM2 inhibitor MK-8242. Assessment of kinome siRNA screen with validation experiments, we identified two kinases. The serine/threonine kinase ULK1 which known to play a critical role in the initiation of canonical autophagy. Notably, we also identified MRCKα which showed no present published association to autophagy. MRCKα is CDC42 effector protein kinase associated in regulating cellular actin-myosin dynamics through phosphorylation of MLC2 (Leung et al., 1998; Tan et al., 2008), MYPT1(Tan et al., 2001; Wilkinson et al., 2005), and LIM domain kinase 1 and 2 (LIMK1 and LIMK2) (Scott and Olson, 2007; Sumi et al., 2001). Furthermore, Leung group reported that MRCKα forms a complex with leucine-rich adaptor protein LRAP35a, and myosin 18A (MYO18A) to activate MYO2A-dependent lamellar actomyosin assembly (Tan et al., 2008).

Together, these data suggest that MRCKα is important in cellular activities including protrusion and migration.

MRCKα and ROCK share regulatory function in the actin-myosin contractile. ROCK1/2, like MRCKα/β, directly phosphorylate MLC2 (Ser19) and inactivate MYPT1 leading to actin-myosin contraction (Unbekandt and Olson, 2014). Moreover, independent studies suggested that ROCK have multiple mechanisms in autophagy initiation and autophagosome formation (Aguilera et al., 2012; Gurkar et al., 2013; Mleczak et al., 2013). As a study in *Drosophila* demonstrated that myosin II is essential during autophagosome biogenesis (Tang et al., 2011), I hypothesized that MRCKα could also mediate the early stage of autophagosome formation. To test this, we examined the importance of MRCKα during the nucleation stage of autophagy by measuring DFCP1. However, we failed to observe a reduction in MK-8242 induced EGFP-DFCP1 positive puncta in MRCKα knockdown. Since we observed decreased EGFP-LC3B positive autophagic vesicle in MRCKα knockdown treated with MK-8242, additional experiments are necessary with other autophagy core proteins involved during autophagosome biogenesis, including ATG9, ATG12-ATG5 conjugation or ATG16L1 complex. ATG9 recruit membrane sources to expanding phagophores from other organelles, including ER, Golgi, plasma membrane, and endosomes (Papinski et al., 2014; Shirahama-Noda et al., 2013). A study showed ULK1 regulate the actomyosin activation and ATG9 trafficking in starvation-induced autophagy, and it would be interesting to examine if MRCKα would have a similar role in p53-dependent autophagy. Another point of interest is the ATG12-ATG5 conjugation system or ATG16L1 complex which involves autophagosome formation (Romanov et al., 2012).

Identifying MRCKα as an essential kinase in p53-dependent autophagy led me to re-assess the role actin cytoskeleton in autophagy. In this current study, I first wanted to examine the

reported inhibitory effect of latB and cytD (Aguilera et al., 2012; Aplin et al., 1992) actin depolymerizing agents in starvation-induced autophagy using U2OS-ptfLC3B cells as my model. Agreeing to the previous report, I found a decreased accumulation of EGFP-LC3B autophagic vesicles in latB treated cells cultured in HBSS starvation media. However, I failed to observe autophagy suppression in cytD treated cells. The distinct effect of each drug could be because latB and cytD use different mechanism to alter the state actin polymerization. LatB directly binds to monomeric G-actin (Spector et al., 1989) while cytD binds and caps the barbed-end of F-actin (Carlier et al., 1986). Also, the two agents illustrated different efficacy to cultured cells; cytD is more stable compared to latB (Wakatsuki et al., 2001). Finally, the experimental design used in this study is also very different from Colombo's published investigation. The Colombo group failed to add BafA1 in their cytD treatment which could lead to misinterpretation when measuring MAP1LC3-positive puncta.

Finally, one encouraging discovery presented in this study is the association of MRCKα in p53-dependent autophagy. As stated above, MRCKα catalyzed the phosphorylation of substrates involved in actin-myosin cytoskeleton and dynamics. Accumulating evidence links actin-myosin cytoskeleton regulators in cancer cell metastasis and invasion (Kale et al., 2015; Olson and Sahai, 2009). Indeed, Michael Olson and colleagues developed MRCK kinases inhibitors which reveal the importance of MRCK in cancer cell viability and motility, particularly in squamous cell carcinoma cells (Unbekandt et al., 2018; Unbekandt and Olson, 2014). Although it is too early to predict that MRCKα as a potential candidate biomarker that may benefit to autophagy inhibitions, a future study needs to focus on uncovering the underlying mechanism of MRCKα in p53-dependent autophagy.

MATERIALS AND METHODS

Mammalian cell cultures, reagents, and antibodies

The human osteosarcoma cell line U2OS (ATCC, HTB-96) was cultured in McCoy's 5A medium (Gibco, 16600-082) supplemented with 10% FBS and maintained in a humidified atmosphere containing 5% CO2 at 37°C. Cells were seeded 18-24 hours before the start of assays. Selective HDM2 inhibitors nutlin-3a (Selleck Chemicals, S1061) and MK-8242 (Merck & Co., Inc.) were used to block the HDM2-p53 interaction in cells. The mTOR inhibitor rapamycin (553210), also called as sirolimus, was obtained from Millipore-Sigma. Actin depolymerizing agents cytochalasin D and latrunculin B were used to assess actin assembly. Vacuole H+-ATPase inhibitor Bafilomycin A1 (BafA1; AG Scientific, B1183) was added on the final 1.5 or 1 hour of treatment to block lysosomal function. All inhibitor stock solutions were prepared in Dimethyl Sulfoxide (DMSO) (Sigma-Aldrich, D2650), aliquoted, and stored at -80°C freezer. Equal concentration of DMSO was used for control treatments. Actin filaments were stained using CF647 Dye Phalloidin Conjugates (Biotium, 00041). LC3B (1:1000; Sigma-Aldrich, L7543), p21Waf1/Cip1 (1:1000; Cell Signaling Technology, 2947), and p53 (1:1000; Cell Signaling Technology, 2527) antibodies were used for Western blot analysis. Mouse monoclonal antibody β-actin (1:5000; CST, 3700) was used as a loading control. Horseradish peroxide (HRP)-conjugated secondary anti-mouse (NA931V), and anti-rabbit (NAV934V) were purchased from GE Healthcare Life Sciences. IRDye infrared fluorescent 800CW secondary goat anti-rabbit (926-32211) and anti-mouse (926-32210), and 680RD secondary goat anti-rabbit (926-68071) and anti-mouse (926-68070) were obtained from LI-COR.

Western blot analysis

Cell lysate buffer was prepared in ice-cold lysis buffer [10mM potassium phosphate, 1 mM ethylenediaminetetraaceticacid (EDTA), 10 mM magnesium chloride, 5 mM ethylene-bis(oxyethylenenitrilo)tetraacetic acid (EGTA), 50 mM bis-glycerophosphate, 0.5% Nonidet P-40 (NP-40), 0.1% Brij35, 0.1% sodium deoxycholate, 2 mM dithiothreitol, 1 mM sodium orthovanadate, 5 mM sodium fluoride, and protease inhibitor cocktail (Sigma-Aldrich, P8340)]. Whole cell lysates were then prepared using the freshly prepared ice-cold lysis buffer. Lysate samples were incubated in the ice bath for 10 min and clarified by centrifugation for 10 min at 13,000 rpm and 4°C. Total protein concentration was determined using Protein Assay Dye Reagent Concentrate (Bio-Rad, 5000006). The supernatant was collected and stored in -80°C freezer until further use. Sample buffer [25mM Tris-HCl, 10% SDS, 38% glycerol, and bromophenol blue] containing fresh 10% beta-mercaptoethanol (Sigma-Aldrich, M6250) solution was added to lysates and boiled for 5 min. Proteins were resolved by Sodium Dodecyl Sulfate (SDS)-polyacrylamide gel or pre-cast 4-12% BOLT Bis-Tris Plus gel (Invitrogen, NW04125BOX) and electrotransferred onto either nitrocellulose or polyvinylidene difluoride membranes. Membranes were blocked with 5% nonfat dry milk in 1X Tris-buffered solution and 0.1% Tween-20 (0.1% T-TBS) or StartingBlock (TBS) Blocking Buffer (Thermo Scientific, 37542) followed by overnight incubation of primary antibodies diluted in 5% Bovine Serum Albumin (BSA) (Millipore-Sigma, A7906), 0.1% T-TBS solution or StartingBlock T20 (TBS) Blocking Buffer (Thermo, 37543) at 4°C. After three 5-minute 0.1% T-TBS washes, membranes were incubated in secondary antibodies diluted in 5% milk/BSA, 0.1% T-TBS buffer or StartingBlock T20 (TBS) Blocking Buffer for 1 hour at room temperature. Protein bands were detected by enhanced chemiluminescence, West Femto Maximum Sensitivity Substrate (Thermo, 34095), or imaged

using LI-COR Odyssey Infrared Imaging System and quantified with LI-COR Image Studio Software.

Purification of nuclear extracts

Purification of nuclear extracts from U2OS cells treated with nutlin-3a (10 μM) or MK-8242 (1 μM, 10 μM) was carried out with Cayman's Nuclear Extraction Kit (10009277), following the manufacturer's protocol. Briefly, treated cells were collected and washed using ice-cold 1X PBS/phosphatase inhibitor solution. Cells were pelleted by centrifugation (300 x g) for five minutes at 4°C. Next, pellets were resuspended in ice-cold complete hypotonic buffer and allowed to swell for 15 minutes. NP-40 assay reagent was added and mixed into the samples, and centrifuged (14,000 x g) for 30 seconds at 4°C. The supernatant which captains the cytosolic fraction was carefully pipetted out without disturbing the pellet in the tube and stored at -80°C. Finally, nuclear pellets were resuspended by vortex in ice-cold complete nuclear extraction buffer and centrifuged (14,000 x g) for 30 seconds at 4°C, saving the supernatant (nuclear cell extract). Protein concentration was measured using the Bio-Rad Protein Assay Dye Reagent.

Nuclear p53 DNA binding activity

Nuclear p53 DNA binding activity was determined using Cayman's p53 Transcription Factor Assay (600020), following the manufacturer's protocol. The assay kit is a DNA-binding enzyme-linked immunosorbent assay (ELISA). Specific double-stranded DNA (dsDNA) sequence containing a p53 response element (RE) is bound onto each well of a 96-well plate. Equal amounts of nuclear cell extracts and controls were added to each well and incubated for an hour at room temperature without agitation. After incubation, wells were washed with assay wash buffer.

Transcription factor p53 primary antibody (Cayman, 600023) was added to each well, excluding blank control well and incubated for another one hour at room temperature without agitation. Again, wells were washed and incubated with diluted transcription factor goat anti-mouse HRP conjugate except for blank control. After one-hour incubation at room temperature, wells were washed and incubated with transcription factor developing solution for 15-45 minutes at room temperature with gentle agitation and protected from light. Finally, stop solution was added in each well and measured absorbance at 450 nm.

TP53 knockdown by small interfering ribonucleic acid (siRNA)

The TP53 Flexitube siRNAs Hs_TP53 siRNA8 (SI02623754) and siRNA13 (SI04384079) were purchased from Qiagen. U2OS cells were seeded in 10-cm culture plates (4.0×10^5 cells per plate) or in 6-well culture plates (3.0×10^4 cells per well). After 24 hours incubation, cells were transfected with siRNAs (two independent sequences per target gene) targeting TP53 using Oligofectamine (Invitrogen, 12252011) for 48 h. Briefly, a 1 to 10 dilution of Oligofectamine into OptiMEM Reduced Serum media (Thermo, 31985070) was incubated for 5 min at room temperature. After 5 minutes, Oligofectamine solution was combined with Human TP53 siRNA8 (25nM) and TP53 siRNA13 (25nM) and incubated for 20 min at room temperature. Fresh McCoy's media with 10% FBS was added to cells. After the 20 min incubation, the transfection complex solution was added to the cells. Media was changed after 24 hours. AllStars Negative Control siRNA (Qiagen, SI03650318) was used as a siRNA control.

p53 target gene expression

Following siRNAs and HDM2 inhibitor treatments, total RNA was extracted from U2OS cells using the RNeasy Mini Kit (Qiagen, 74104) and Qiashredder kit (Qiagen, 79654), following the manufacturer's protocol. The RNA concentration was determined with Thermo NanoDrop 2000 UV-Vis spectrophotometer. cDNA was synthesized from 0.1 µg RNA sample using the iScript Select cDNA Synthesis Kit (Bio-Rad, 170-8896). Reverse transcription was performed in Eppendorf Mastercycler-Pro System and diluted in Tris-EDTA (TE) buffer. Then synthesized cDNA samples were mixed with Applied Biosystems Fast SYBR Green Master Mix (Thermo, 4385612). Quantitative Real-Time Polymerase Chain Reaction (qRT-PCR) was completed using Applied Biosystems ViiA7 Real-Time PCR Systems and analyzed using Quant Studio RT-PCR Software. Primers for human *TP53* (fwd: CCTCAGCATCTT ATCCGAGTGG, rev: TGGATGGTGGTACAGTCAGAGC), *CDKN1A* (fwd: AGGTGGACCTGGAGACTCTCAG, rev: TCCTCTTGGAGAAGATCAGCCG), *DRAM1* (fwd: CGGATGGTCATCTCTGCCGTTT, rev: CTGTCCATTCACAGATCGCACTC), *SESN2* (fwd: AGATGGAGAGCCGCTTTGAGCT, rev: CCGAGTGAAGTCCTCATATCCG), *FOXO3A* (fwd: TCTACGAGTGGATGGTGCGTTG, rev: CTCTTGCCAGTTCCCTCATTCTG), *ATG4A* (fwd: CCAAGCCAGAAGTGACAACCAC, rev: GACAGACCTTCAAGTTGAGTTCC), and *ULK1* (fwd: TGAGCCGAGAATGGGGCTTC, rev: CTGCTTCACAGTGGACGACA) were used to measure p53-target autophagy-related genes in response to HDM2 inhibition. Human *HPRT1* (fwd: ATGGACAGGACTGAACGTCTTGCT, rev: GCTTTGATGTAATCCAGCAGGTCAGC) was used as a reference gene.

Fluorescent microscopy and vesicle quantification

Monoclonal U2OS cell line was generated and displayed a moderate expression of ptfLC3B plasmid, a gift from Tamotsu Yoshimori (Addgene plasmid #21074) (Kimura et al., 2007). Twenty thousand U2OS-ptfLC3B cells were added on autoclaved round 8 mm diameter, 1.5 thickness coverslip (Electron Microscopy Science, 72296-08) placed into each well of 24-well tissue culture plate and allowed to settle for 24 hours. Cells were transfected with siRNA target genes and non-targeting siRNA control. Twenty-four hours post-transfection, media was changed with fresh McCoy's 5A with 10% FBS. Then transfected cells were treated with MK-8242 for 24 hours or rapamycin for 2 hours adding BafA1 for the last 1.5 hours of treatment. Equal concentration of DMSO was used for vehicle control. After treatments, U2OS-ptfLC3B cells were fixed in 4% formaldehyde (Pierce/Thermo, 28908), washed with 1X DPBS (Thermo, 14190250),), and stained with Hoechst nuclear stain (Invitrogen, H1399). Cells were imaged using a 60X oil objective, in FITC and DAPI channels, on a Nikon Ti Eclipse fluorescent microscope. U2OS-ptfLC3B images were deconvolved, top-hat transformation (peak identification), and threshold (intensity) using NIS Elements Software to quantify EGFP-LC3-positive puncta per cell (Martin et al., 2013).

Microscopy-based human kinase screen

U2OS-ptfLC3B cells (4.5 x 10^3 cells per well) were seeded in 96-well glass bottom plates. After 24-hour incubation, cells were transfected with siRNA pool (four independent sequences per target gene) and non-targeting control siRNA. Total of 755 gene targets, including positive controls (*ATG5/12* and *ATG9A/B* siRNA), were screened in sixteen 96-well plates. Twenty hours post-transfection, cells were treated with MK-8242 for another 24 hours adding BafA1 for the last

hour. After treatments, cells were washed with PBS and permeabilized with 0.02% digitonin (Sigma-Aldrich, D141) for 10 minutes. Then cells were washed with PBS and fixed with 2% formaldehyde. Cell nuclei were stained using Hoechst and mounted using Fluoro-Gel (Electron Microscopy Sciences, #17985-10). Finally, cells were imaged using 20X objective, in 403 and 488 nm excitation lasers, on Nikon A1 confocal microscope. Five z-planes with 4uM interval were captured in two adjacent fields of view. Z-planes were combined into a maximum intensity projection. Autophagy was quantified by calculating the object intensity per cell (the measured total fluorescence intensity of GFP-LC3 divided by the number of nuclei within a field of view).

CHAPTER 3.

REGULATION OF AUTOPHAGY BY p53 AND KRAS SIGNALING IN NSCLC

ABSTRACT

Cancer cells can utilize autophagy as a survival mechanism in response to nutrient-deprived or hypoxic microenvironments. However, the function of autophagy in cancer is complex and depends on tumor types and stages and activity of several oncogenes and tumor suppressors. In the molecular level, autophagy is highly conserved catabolic pathway regulated by mTORC1. Here, I assessed the relationship of p53- and RAS-signaling with autophagy in KRAS-driven NSCLC by using two compounds targeting each signaling pathway. Following HDM2 inhibition, stabilized p53 induced autophagy in mutant KRAS NSCLC lines harboring wild-type p53 status. Furthermore, selective mutant $KRAS^{G12C}$ inhibitor suppressed $KRAS^{G12C}$/MAPK/ERK signaling pathway which triggered autophagy in $KRAS^{G12C}$ mutant NSCLC. These data indicate that activation of p53 signaling and suppression of RAS signaling, both upstream regulator of mTORC1 activity, drives autophagy in KRAS-driven NSCLC cell lines. This study also provides evidence that target agents can effectively inhibit their target protein and promote autophagy in cancer cells.

INTRODUCTION

Normal cells require autophagy to degrade their intracellular components, including proteins and organelles, to maintain cellular homeostasis. For cancer cells, the role of autophagy can depend on many biological factors, including tumor subtypes, activation of specific oncogenes, or tumor suppressor loss. For instance, defective autophagy (*beclin1*$^{+/-}$ and *atg5*$^{-/-}$) leads to excess oxidative stress and increased DNA damage and genomic instability which cause tumorigenesis in liver (Mathew et al., 2009) and breast (Karantza-Wadsworth et al., 2007). Mechanistically, both oncoproteins and tumor suppressor proteins that regulate mTORC1 activity could modulate autophagy. The White group demonstrated that oncoprotein AKT activation inhibits autophagy survival pathway in defective apoptosis tumor cells (Degenhardt et al., 2006). On the other hand, prostate cancer model with phosphatase and tensin homolog (*Pten*) loss promotes autophagy and tumor growth (Santanam et al., 2016).

The protein p53 is another tumor suppressor associated with autophagy. Historically, p53 is known as "the guardian of the genome" because of its ability to halt cellular proliferation in cells with a damaged genome (Kastenhuber and Lowe, 2017; Lane, 1992). p53 is frequently mutated or deleted in human cancer. However, almost two-thirds (63%) of all cancer do not have a mutation in p53, and thus are wild-type for p53. In lung adenocarcinoma, 51% of cases are mutant for p53, and 49% of cases wild-type for p53 (Sanchez-Vega et al., 2018). The function of p53 in autophagy is complex and dependent on its subcellular localization. The Kroemer group observed the negative effect of cytosolic p53 to autophagy both *in vitro* and *in vivo* (Tasdemir et al., 2008). The nuclear function of p53 in autophagy was observed using *Myc/p53ER*^{TAM} lymphoma mouse model, which tumors were resistant to apoptosis due to lack of nuclear p53 (Amaravadi et al., 2007). When

the Thompson group administered tamoxifen to these mice, nuclear p53 was restored which was associated with tumor cell death. However, they also detected autophagy in surviving tumor cells (Amaravadi et al., 2007). Therefore, this model suggests that nuclear p53 promotes autophagy to favor tumor cell survival.

Aside from p53, autophagy also has a unique relationship with the Ras oncogenes. Indeed, Ras mutations correlate with high levels of basal autophagy that is necessary for tumor maintenance (Guo et al., 2011). The relationship between Ras and autophagy was further tested using a GEMM of lung cancer driven by oncogenic mutant *Kras* (*Kras*^{G12D}) with simultaneous deletion of essential autophagy genes, such as *Atg7* and *Atg5*. This autophagy-deficient *Kras*^{G12D} GEMM showed a dramatic reduction of tumor cell proliferation and lung tumor burden compared to mice with tumors containing intact autophagy (Guo et al., 2013a; Rao et al., 2014). Notably, Atg7-deficient lung tumors showed an accumulation of defective mitochondria and progression of carcinoma to benign oncocytomas (Guo et al., 2013a). These findings strengthen the importance of autophagy for tumorigenic growth of Ras-driven cancer cells.

In lung adenocarcinoma, 49% of cases are wild-type p53, and 35% of cases are mutant KRAS (Huynh and Campbell, 2016; Sanchez-Vega et al., 2018). As the above genetic experiments highlighted a therapeutic opportunity to target autophagy in cancer; I wanted to improve our understanding of the relationship of these two proteins with autophagy. Therefore, I hypothesized that using HDM2 inhibitors to stabilize active wild-type p53 and therapeutically inhibiting oncogenic mutant KRAS will promote autophagy in NSCLC cell lines. I will test my hypothesis using two small compounds, each selectively targeting HDM2, the E3 ligase for p53, and mutant KRAS^{G12C}.

Under unstress condition, low level of p53 is tightly maintained to avoid excessive p53 accumulation and activation of its regulated pathways. In order to do this, E3 ubiquitin-protein ligase HDM2 binds to the amino-terminal domain of p53 and ubiquitinate p53 for proteasome degradation (Kussie et al., 1996). Interestingly, p53 also regulates the expression HDM2 creating an autoregulatory feedback loop between the two proteins resulting to even balance of the p53 and HDM2 protein level (Tisato et al., 2017; Wu et al., 1993). However, HDM2 gene is amplified or overexpressed in some tumor cells (Sanchez-Vega et al., 2018). Therefore, disrupting the HDM2-p53 interaction has been a therapeutic target in cancer. This includes the discovery of cis-imidazoline analogs named nutlins (Vassilev et al., 2004). Nutlin binds to the p53 binding site on HDM2 which blocks the HDM2-p53 interaction, stabilize p53 and actives p53 signaling pathway. Today, additional small molecule HDM2 inhibitors have been developed, showing promising preclinical data setting clinical studies for further therapeutic evaluation (Ravandi et al., 2016; Tisato et al., 2017; Wagner et al., 2017).

Despite failed attempts, ongoing effort to target Ras for cancer treatment continues. In fact, the National Cancer Institute (NCI) formed the RAS Initiative to expand strategies targeting RAS and to generate effective treatment approaches against RAS-driven cancers. KRAS is the most frequently mutated isoform of RAS genes. Furthermore, KRAS G12C is a hotspot mutation that accounts for about 12% of all codon G12 mutations across all cancer types. KRAS G12C mutations are found in 40% of KRAS mutant NSCLC, providing the rationale for others to develop G12C selective small molecules (Huynh and Campbell, 2016). Kevan Shokat led the first group to exploit the thiol group of KRAS G12C and used fragment-based screening to identify compounds that inhibit $KRAS^{G12C}$ (Ostrem et al., 2013). With subsequent improvements, Yi Lui and colleagues developed two small molecules: ARS-853 (Lito et al., 2016; Patricelli et al., 2016) and ARS-1620

(Janes et al., 2018). Both small molecules selectively target mutant $KRAS^{G12C}$ by forming a covalent bond with the inactive guanosine diphosphate (GDP)-bound state of $KRAS^{G12C}$.

In this study, I investigated whether treatment with an HDM2 selective inhibitor nutlin-3a or a $KRAS^{G12C}$ selective inhibitor ARS-853 affected autophagy. I showed that HDM2 inhibition leads to wild-type p53 stabilization and increased autophagy as measured by LC3B-II levels. Consistent with my previous observation (**Chapter 2**), blocking the HDM2-p53 interaction by with an HDM2 inhibitor stabilized and activated wild-type p53 leading autophagy induction in wild-type p53 NSCLC cell lines. I also observed a similar phenotype in $KRAS^{G12C}$ mutant lung lines by inhibiting $KRAS^{G12C}$ activity. Together, my findings illustrate that nutlin-3a and ARS-853 promote autophagy.

RESULTS

Wild-type p53 induces autophagy in KRAS-driven NSCLC response to HDM2 inhibition

I wanted to test if inhibiting HDM2 induces autophagy in mutant KRAS NSCLC cell lines harboring wild-type p53. One of the most common small molecules to target HDM2 is the cis-imidazoline analogs, nutlins. Here, I used nutlin-3a to block HDM2 interaction with wild-type p53. First, I validated the inhibitory effect of nutlin-3a to HDM2 by measuring the protein level of p53 and $p21^{Cip1/Waf1}$ (hereafter referred to as p21). I treated four NSCLC lines which carry either wild-type (SW1573 and A549), mutant (H2030), and deleted (H358) *TP53* with 10 μM nutlin-3a for 24 hours. As shown in **Figure 3**, p21 and p53 protein level increased in wild-type p53 NSCLC SW1573 (**Figure 3.1A**) and A549 (**Figure 3.1B**) after 24 hours nutlin-3a treatment compared to mutant (H2030) and deleted (H358) *TP53* cells. H2030 cells carry mutant $p53^{G262V}$ which occurs in the DNA-binding domain and inhibits the transactivation of p53 target genes, including *CDKN1A* (p21). As expected, the protein expression of p53 and p21 on this cell line was unaffected by nutlin-3a (**Figure 3.1C**). Furthermore, H358 cells with a p53 deletion failed to show p21 protein expression after nutlin-3a treatment (**Figure 3.1D**).

A growing body of work suggests that p53 could also regulate "non-canonical" programs, including autophagy (Kastenhuber and Lowe, 2017). To test whether HDM2 inhibition and stabilization of p53 induce autophagy, I looked at well-known autophagy marker LC3B-II using immunoblotting. Again, the four mutant KRAS NSCLC lines described above were treated with 10 μM nutlin-3a for 24 hours adding 100 nM BafA1 at the last 1.5 hours to inhibit lysosomal degradation stage of autophagy. Measuring the level of LC3B-II protein level post-treatment, I found increased accumulation BafA1-induced LC3B-II level in nutlin-3a treated SW1573

(TP53^{WT}) (**Figure 3.1A**) and A549 (TP53^{WT}) (**Figure 3.1B**) compared to H2030 (TP53^{G262V}) (**Figure 3.1C**) and H358 (TP53^{DEL}) (**Figure 3.1D**). My results suggest that accumulation of active p53 due to HDM2 inhibition triggers autophagy in oncogenic mutant KRAS, wild-type p53 NSCLC lines.

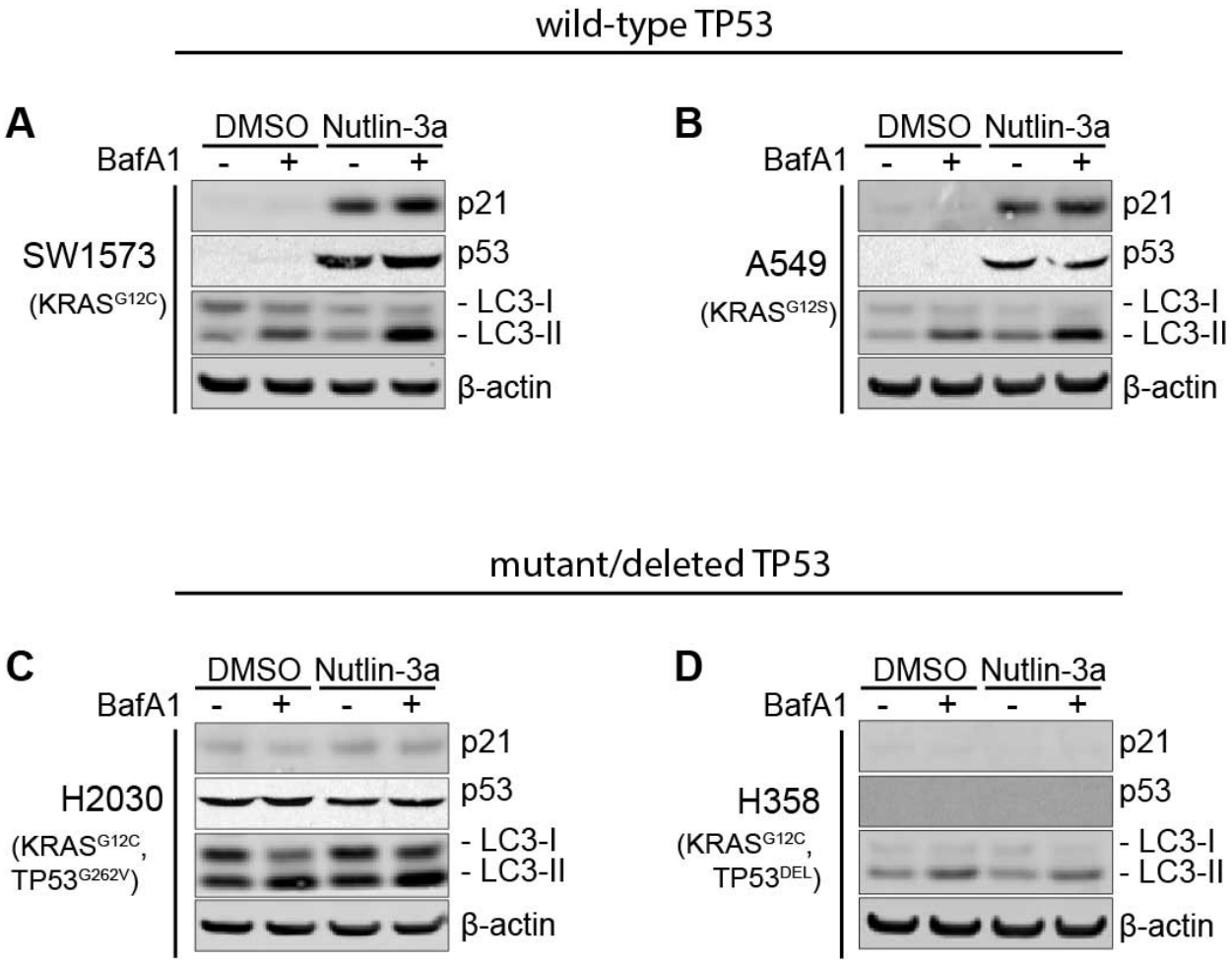

Figure 3.1. Nutlin-3a induces autophagy in wild-type p53 KRAS-driven NSCLC.

KRAS-driven NSCLC lines harboring wild-type *TP53* **(A)** SW1573 and **(B)** A549, mutant *TP53* **(C)** H2030, and deleted *TP53* **(D)** H358 treated with 10 μM nutlin-3a for 24 hours with (+) or without (-) BafA1 (100 nM) for the final 1.5 hours of treatment (n=3 biological replicate).

Inhibition of KRAS^{G12C} signaling promotes autophagy in KRAS^{G12C} NSCLC

Attempts to develop compounds targeting oncogenic KRAS resulted in switch II loop region (S-IIP) KRAS^{G12C} specific inhibitors. ARS-853 is one of the first S-IIP inhibitors developed (Lito et al., 2016; Ostrem and Shokat, 2016; Patricelli et al., 2016). To validate the cellular effect of ARS-853 on KRAS signaling, specifically MAPK/ERK pathway, I treated a group of NSCLC lines with either KRAS *p.G12C* (H2030, H358, and H23) or KRAS wild-type alleles (H226 and H1437). Consistent with previous reports, 10 μM ARS-853 inhibited downstream pathway components p44/42 MAPK (ERK1/2) phosphorylation (p-ERK1/2) in KRAS^{G12C} NSCLC (**Figure 3.2A**) and not in KRAS^{WT} NSCLC (**Figure 3.2B**). Interestingly, I observed a dramatic suppression of p-ERK1/2 after 3 hours ARS-853 (10 μM) treatment contrast to the previous report that showed maximal inhibition in 6 hours (Lito et al., 2016). Aside from p-ERK1/2, I also looked at the effect of ARS-853 on the downstream activity of mTORC1. I also used AZD8055, an ATP-competitive mTOR inhibitor, as a positive control. After 3 hours of treatment, I found that ARS-853 decreased the phosphorylation mTOR substrate p70 S6 kinase in KRAS^{G12C} NSCLC, while AZD8055 (100 nM) showed complete inhibition (**Figure 3.2A**). These findings suggest that ARS-853 suppresses KRAS^{G12C} signaling and further downstream mTORC1 activity in KRAS^{G12C} NSCLC. It was noteworthy that I did not observe any pronounced effect with BafA1 treatment.

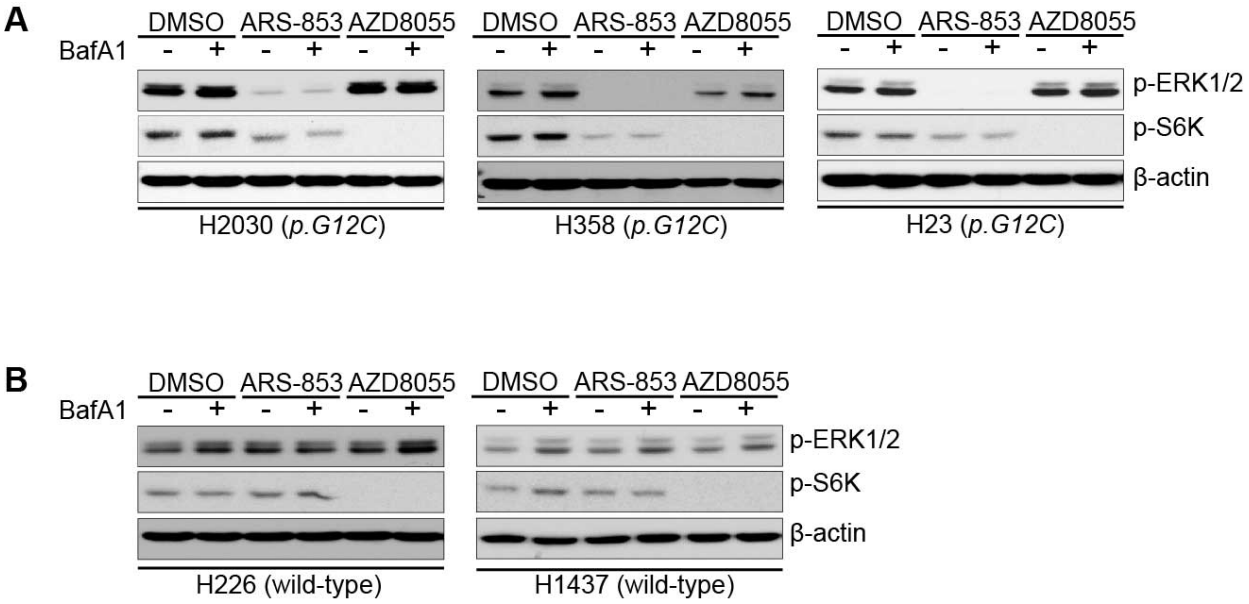

Figure 3.2. KRAS^{G12C} inhibitor ARS-853 suppresses KRAS^{G12C}/RAF/ERK signaling and mTORC1 activity.

(A) Mutant KRAS^{G12C} (H2030, H358, and H23) and **(B)** Wild-type KRAS (H226 and H1437) NSCLC lines treated with ARS-853 (10 μM) or AZD8055 (100 nM) for 3 hours, with (+) or without (-) BafA1 (100 nM) for the final hour of treatment.

mTOR is a master regulator of cellular metabolism which is a key determinant for cell growth. Deregulation of mTOR complex signaling (mTORC1 and mTORC2) has been implicated in many human diseases, including cancer. Thus, it is not a surprise mTOR is an appealing pharmacological target. Although not a direct inhibition, my ARS-853 results suggest suppression mTORC1 activity in $KRAS^{G12C}$ NSCLC. Since mTORC1 is also a master regulator of autophagy, I wanted to examine if $KRAS^{G12C}$ inhibitor ARS-853 induces autophagy. Furthermore, I predicted that the mutant $KRAS^{G12C}$ inhibitor ARS-853 would induce autophagy in mutant $KRAS^{G12C}$ NSCLC cell lines. To test my prediction, I first determined the effective dose of ARS-853 in the mutant $KRAS^{G12C}$ H358 (**Figure 3.3A**), using $KRAS^{WT}$ H226 (**Figure 3.3B**) as negative control. Both NSCLC cell lines were treated with increasing concentration of ARS-853 for 3 hours adding BafA1 on the final hour. I found that 5.0 μM ARS-853 effectively blocked the phosphorylation of ERK1/2 in H358 cells but not in H226 cells. Analyzing the effect of ARS-853 on autophagy in $KRAS^{G12C}$ NSCLC, I also found that 5.0 μM with BafA1 was sufficient to increase LC3B-II protein level in H358 (**Figure 3.3A**).

I then treated two more mutant $KRAS^{G12C}$ NSCLC cell lines (H2030 and SW1573) with 5.0 μM ARS-853 to confirm my observed LC3B-II phenotype in H358 cells. As shown in **Figure 3.4**, ARS-853 treated H2030 (**Figure 3.4B**), and SW1573 (**Figure 3.4C**) showed decreased p-ERK1/2 and increased the accumulation of BafA1-induced LC3B-II when compared to control $KRAS^{G12S}$ NSCLC line, A549 (**Figure 3.4D**). These findings agreed with my hypothesis that treating $KRAS^{G12C}$ mutant cell lines with ARS-853 inhibits both ERK signaling and mTOR signaling, leading to autophagy induction.

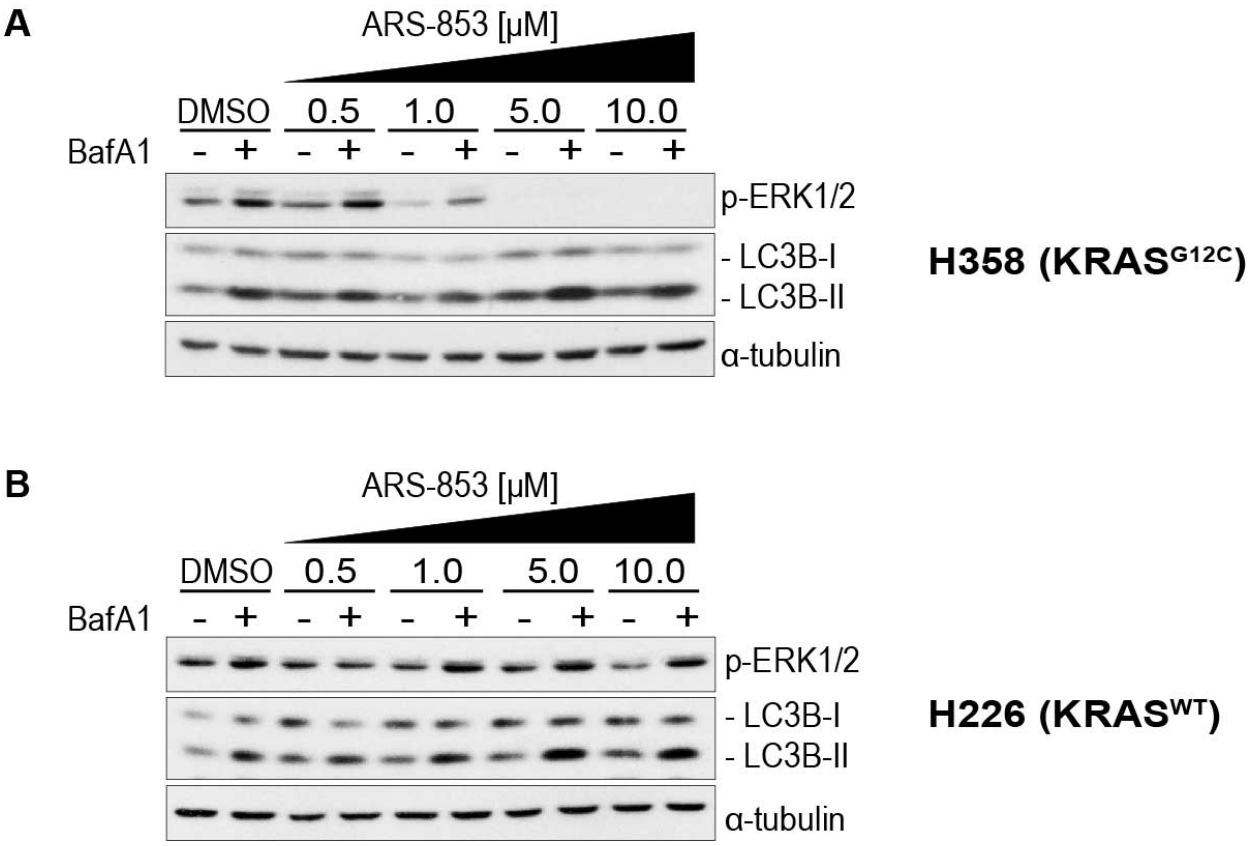

Figure 3.3. ARS-853 efficiently promotes autophagy by suppressing KRAS^{G12C}/RAF/ERK pathway.

(A) Mutant KRAS^{G12C} (H358) and **(B)** wild-type (WT) KRAS (H226) NSCLC lines treated with increasing concentration of ARS-853 for 3 hours, with (+) or without (-) BafA1 (100 nM) for the final hour of treatment (n=2 biological replicate).

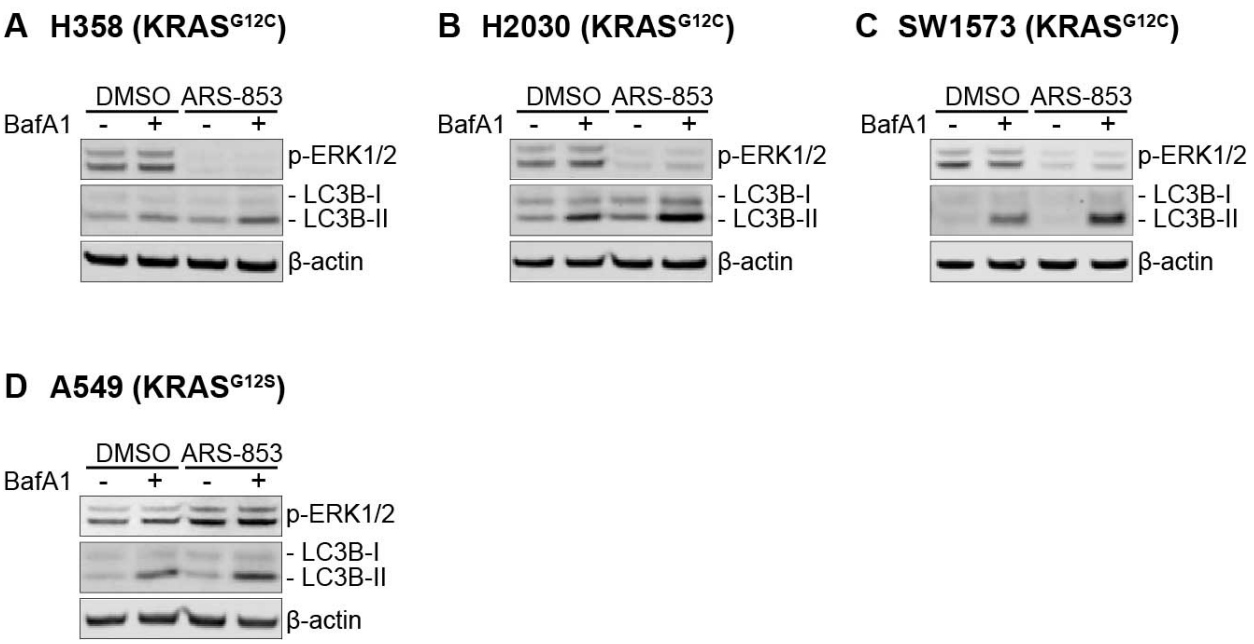

Figure 3.4. KRAS^{G12C} mutant NSCLC lines activate autophagy in response to ARS-853. Mutant KRAS^{G12C} **(A)** H358, **(B)** H2030, and **(C)** SW1573 and non-mutant KRAS^{G12C} **(D)** A549 cells treated with 5.0 μM ARS-853 for 3 hours with (+) or without (-) BafA1 (100nM) for the final 1.5 hours of treatment (n=3 biological replicate).

DISCUSSION

The role of autophagy in cancer is complex and context dependent. Mechanistically, autophagy is a highly conserved catabolic process that is controlled by mTOR signaling, specifically mTORC1. Therefore, small molecules designed to target the mTOR signaling pathway often stimulate autophagy and can provide a cell survival advantage and potentially drug resistance (Kim and Guan, 2015; Rebecca and Amaravadi, 2016). In this study, I investigated the effect of two compounds on autophagy in wild-type p53 and mutant $KRAS^{G12C}$ NSCLC cell lines. Nutlin-3a selectively targets HDM2 and blocks the HDM2-p53 interaction to stabilize nuclear p53. Whereas, ARS-853 selectively targets mutant $KRAS^{G12C}$ and locks KRAS into its GDP inactive form.

The tumor suppressor p53 is believed to have a dual function in autophagy, which depends on its subcellular localization. Cytosolic p53 is reported to inhibit autophagy (Morselli et al., 2008; Tasdemir et al., 2008) while nuclear p53 promotes autophagy by transactivating p53-target autophagy-related genes. Accordingly, in **Chapter 2**, I demonstrated that inhibiting HDM2-p53 interaction using an HDM2 inhibitor stabilizes and activates nuclear p53 leading to autophagy induction. Here, I used nutlin-3a, the first selective preclinical small molecule HDM2 inhibitor to further investigate the effects on autophagy in mutant KRAS NSCLC cell lines. After a 24-hour treatment, I found that nutlin-3a increased the accumulation of LC3B-II protein level in mutant KRAS NSCLC harboring wild-type p53 status compared to cells carrying mutant or deleted p53 (**Figure 3.1**). These results agree with our prior study of another HDM2 inhibitor, MK-8242. Collectively, my observations suggest that HDM2 inhibitors are capable of inducing p53-dependent autophagy by stabilizing p53 in mutant KRAS NSCLC.

To evaluate the effect of selective $KRAS^{G12C}$ inhibitor, ARS-853, on autophagy in NSCLC, I used a group of NSCLC cell lines, harboring either G12C or non-G12C mutant KRAS with either wild-type, mutant or deleted *TP53* (**Table 3.1**). After a 3-hour treatment, I found that ARS-853 inhibited the MAPK/ERK signaling pathway (phosphorylation of ERK1/2) in mutant $KRAS^{G12C}$ NSCLC lines. In addition, ARS-853 effectively reduced the mTORC1 activity, examined through phosphorylation of mTOR substrate p70 S6 kinase, in mutant $KRAS^{G12C}$ cells (**Figure 3.2**). Consequently, ARS-853 increased the accumulation of LC3B-II in the presence of BafA1 in mutant G12C KRAS NSCLC lines compared to non-mutant G12C cells (**Figure 3.4**). These results indicate that suppression of RAS/RAF/MEK/ERK signaling pathway and mTOC1 activity by ARS-853 can trigger autophagy response in NSCLC cell lines that carry $KRAS^{G12C}$ mutation.

Many studies have shown that autophagy can promote survival during therapeutic stress (chemotherapy, radiotherapy, and targeted agents) and potentially mediate therapeutic resistance (Amaravadi et al., 2007; Carew et al., 2007; Degtyarev et al., 2008; Zhang et al., 2012). For example, Rebecca et al. demonstrated that AKT inhibitor MK-2206 alone or in combination with chemotherapy drug paclitaxel/carboplatin enhanced the number of autophagosome and accumulation of LC3B-II in treated BRAF and NRAS wild-type melanoma cell lines. This suggest that autophagy can promote adaptive resistance to AKT inhibitor. Indeed, the Smalley group showed that autophagy defect, genetically and chloroquine treatment, in combination with MK-2206 and chemotherapy drugs treated melanoma tumor cells were unable to induce autophagy and instead exhibited increased cell death (Rebecca et al., 2014). Here, I showed that small compounds nutlin-3a and ARS-853 effectively inhibit their respected target protein and capable of inducing autophagy in cancer cells. However, since LC3B-II is just one of the markers for autophagy I proposed additional work to analyze other biomarkers for autophagy, such as ULK1. The

serine/threonine kinase ULK1 is known for its prominent role in autophagy induction and directly inhibited by mTORC1. As the two inhibitors, nutlin-3a and ARS-853, target the mTOR signaling pathway, it is critical to know how each inhibitor affects ULK1 and autophagy induction. Furthermore, ULK1 is considered to be a promising target for autophagy inhibition which led to the development of small molecules directly targeting ULK1 kinase. I would predict that the addition of ULK1 inhibitor may be one strategy to block the autophagy induction and potential onset resistance triggered by HDM2 inhibitor and selective $KRAS^{G12C}$.

Table 3.1. *KRAS* and *TP53* Status of Non-Small Cell Lung Cancer Lines.

Sample Name	*KRAS* Status	*TP53* Status
A549	Missense (*p.G12S*)	Wild Type
H1437	Wild Type	Missense (*p.R267P*)
H2030	Missense (*p.G12C*)	Missense (*p.G262V*)
H226*	Wild Type	
H23	Missense (*p.G12C*)	Missense (*p.M246I*)
H358	Missense (*p.G12C*)	Deleted[1,2]
LU99A	Missense (*p.G12C*)	Wild Type
SW1573	Missense (*p.G12C*)	Wild Type

KRAS and TP53 status are determined and reported from the Broad Institute Cancer Cell Line Encyclopedia, cancer.sanger.ac.uk

*No reported mutation and contained wild-type TP53 function.

[1](Takahashi et al., 1992)

[2](Hata et al., 2017)

MATERIALS AND METHODS

Mammalian cell cultures and reagents

The human non-small cell lung cancer lines (NSCLC) H226 (CRL-5826), H1437 (CRL-5872), H2030 (CRL-5914), H358 (CRL-5807), SW1573 (CRL-2170), and A549 (CCL-185) were purchased from the American Type Culture Collection (ATCC). The human NSCLC line LU-99A (JRCB0044) was obtained from the Japanese Collection of Research Bioresources Cell Bank (JRCB). All NSCLC lines were cultured in RPMI-1640 medium (Gibco, 11875-093) supplemented with 10% fetal bovine serum (FBS). Cells were maintained at 37°C in a humidified atmosphere containing 5% CO_2.

Cells treatments

H226 (2.0 x 10^5 cells/well), H1473 (2.0 x 10^5 cells/well), H2030 (3.0 x 10^5 cells/well), H358 (3.0 x 10^5 cells/well), SW1573 (3.0 x 10^5 cells/well), and LU99A (5.0 x 10^5 cells/well) was cultured in 6-well culture plates 18-24 hours before the start of treatments. The next day, media was changed using fresh RPMI-1640 plus 10% FBS. Cells were treated with selective covalent $KRAS^{G12C}$ inhibitor ARS-853 (MedChemExpress, HY-19706) or ATP-competitive mTOR inhibitor AZD8055 (Selleckchem, S1555) for three hours adding vacuole H+-ATPase inhibitor BafA1 on the last hour or 1.5 hours of treatment. NSCLC cell lines were also treated with selective HDM2 inhibitor nutlin-3a (Selleckchem, S1061) for 24 hours adding BafA1 on the last 1.5 hours of treatment. Equal concentration of DMSO was used for the vehicle control treatment.

Western blot analysis

After the end of treatments, whole cell lysates were prepared using the freshly prepared ice-cold lysis buffer. Lysate samples were then incubated in the ice bath for 10 min and clarified by centrifugation for 10 min at 13,000 rpm and 4°C. The total protein concentration was measured using Bio-Rad Protein Assay Dye Reagent. Next, a sample solution containing fresh 10% beta-mercaptoethanol was added to each sample lysate and boiled for 5 min. Proteins were resolved by SDS-polyacrylamide gel or pre-cast Invitrogen 4-12% BOLT Bis-Tris Plus gel and electrotransferred onto either nitrocellulose or polyvinylidene difluoride membrane. Membranes was blocked with 5% nonfat dry milk in 1X Tris-buffered solution and 0.1% Tween-20 (0.1% T-TBS) or Thermo Scientific StartingBlock (TBS) Blocking Buffer. Primary antibody diluted in 5% BSA, 0.1% T-TBS solution or Thermo Scientific StartingBlock T20 (TBS) was added to the membrane and incubated overnight at 4°C. The next day, the membrane was washed three 5-minute 0.1% T-TBS washes. Afterwards, the membrane was incubated in secondary antibody diluted in 5% milk/BSA, 0.1% T-TBS buffer or StartingBlock T20 (TBS) Blocking Buffer for 1 hour at room temperature. Protein bands were detected by enhanced chemiluminescence, West Femto Maximum Sensitivity Substrate (Thermo, 34095), or imaged using LI-COR Odyssey Infrared Imaging System and quantified with LI-COR Image Studio Software. Following antibodies were used: LC3B (1:1000), p21 Waf1/Cip1 (1:1000; CST, 2947), p53 (1:1000; CST, 2527), phospho-p44/42 MAPK (Erk1/2) (Thr202/Tyr204) (1:1000; CST, 9101), phospho-p70 S6 kinase (Thr389) (1:1000; CST, 9205), and β-actin (1:5000; CST, 3700). One to ten thousand dilution of secondary antibody GE Healthcare HRP-conjugated or LI-COR IRDye infrared fluorescent 800CW/680RD was used. Finally, protein bands were detected by enhanced

chemiluminescence, West Femto Maximum Sensitivity Substrate or imaged using LI-COR Odyssey Infrared Imaging System and quantified with LI-COR Image Studio Software.

CHAPTER 4.

ULK1 INHIBITION SENSITIZE ONCOGENIC KRAS^{G12C} MUTANT NSCLC TO KRAS^{G12C} INHIBITOR ARS-853

ABSTRACT

The serine/threonine kinase unc-51-like autophagy initiating kinase 1 (ULK1) governs the initiation of autophagy. ULK1 activation is regulated by nutrient-sensing mTORC1 and energy-sensing AMPK. Through the years, ULK1 becomes a popular target for autophagy inhibition. Currently, there are nine reported small compound ULK1 inhibitors. Here, I investigated the efficacy of newly established ULK1 inhibitor, ULK-101, in KRAS mutant NSCLC cell lines. Previous reports showed that Ras-transformed cells rely more on autophagy for survival. Also, autophagy is activated in tumor cells treated with therapeutic drugs. To address this issue, I treated a group of KRAS mutant NSCLC lines with ULK-101 or in combination with selective $KRAS^{G12C}$ inhibitor, ARS-853. My recent study showed that ARS-853 could drive autophagy in $KRAS^{G12C}$ NSCLC. Following ULK1 inhibition, autophagy is inhibited in $KRAS^{G12C}$ mutant NSCLC cell lines. ULK-101 also suppressed cell viability of KRAS mutant NSCLC lines in nutrient-restricted condition. Moreover, inhibition of ULK1 with ULK-101 enhanced the ability of $KRAS^{G12C}$ inhibitor ARS-853 to impair cell viability of $KRAS^{G12C}$ mutant NSCLC lines. Taken together, these data show that autophagy inhibition by targeting ULK1 enhance the sensitivity of $KRAS^{G12C}$ NSCLC to ARS-853. Furthermore, my findings highlight the opportunity to design future investigations of autophagy inhibitors as potential anticancer agents.

INTRODUCTION

Autophagy is a cellular recycling mechanism that degrades intracellular proteins and organelles. The conserved process maintains cellular homeostasis and induces cell survival in response to different forms of stress, including nutrient deprivation and cytotoxic insults. Autophagy starts with the formation of autophagy-related proteins complex and nucleation of isolation membranes which leads to the formation of double-membraned autophagosome sequestering intracellular components. The matured autophagosome then fuses to lysosome forming autolysosome where acidic hydrolases degrade the engulfed autophagosome and sequestered cargo into new macromolecules for cells to reuse (Dikic and Elazar, 2018; Klionsky et al., 2016).

Yoshinori Ohsumi's brilliant experiments in *S. cerevisiae* was a notable turning point in the autophagy research. By challenging his yeast model in nutrient starvation, Ohsumi discovered fifteen autophagy genes, most of which ultimately identified in mammalian cells (Tsukada and Ohsumi, 1993). One of these fifteen genes was *ATG1*, which later characterized as a serine/threonine protein kinase homologous to *Caenorhabditis elegans* unc-51 protein kinase (Matsuura et al., 1997). In mammalian cells, the Tooze group identified unc-51-like autophagy initiating kinase 1 (ULK1), one of the four mammalian orthologs of yeast Atg1, as an essential modulator of autophagy (Chan et al., 2007). Upstream signaling complexes that recognize the cellular levels of nutrient or amino acids (mTORC1) and energy (AMPK) (Alers et al., 2012; Roach, 2011) controls ULK1 kinase activity. Once activated, ULK1 forms a ULK complex (Chan et al., 2009; Ganley et al., 2009) and initiates autophagy by phosphorylating the components of PIK3C3, particularly Beclin-1 (Russell et al., 2013).

As ULK1 represent the initial biochemical step of autophagy, ULK1 becomes an attractive target for autophagy inhibition. Indeed, there are currently nine reported small compound ULK1 inhibitors, most coming from published works in 2015. The first reported ULK1 inhibitor, Compound 1, was established by Kevan Shokat and colleagues. The Shokat group provided the first crystal-structure ULK1 kinase bound to a series of potent inhibitors, with Compound 1 being the top hit (Lazarus et al., 2015) and later, Compound 3 (Lazarus and Shokat, 2015). Other labs, like the Ganley group used *in vitro* screening of known kinase inhibitors which lead them to identify two TANK-binding protein 1 (TKB1) inhibitors, MRT67307 and MRT68921, both targets ULK1 with high potency (Petherick et al., 2015). Reuben Shaw and his team developed SBI-0206965 from focal adhesion kinase (FAK) inhibitor. They screened promising pyrimidine analogs for ULK1 inhibition of VPS34 phosphorylation. Further analyses using structure-activity relationship led to the first reported potent ULK1/2 inhibitor SBI-0206965 (Egan et al., 2015). Moreover, SBI-0206965 treated NSCLC cell lines showed impaired cell viability and increased sensitivity to chemotherapy agent cisplatin (Tang et al., 2017).

In 2017, the Roush group used *in silico* high-throughput screen leading to the discovery of two indazole ULK1 inhibitors SR-17398 and SR-20295 (Wood et al., 2017). Recently, the MacKeigan group identified two new small molecule ULK1 inhibitors, ULK-100 and ULK-101. Each showing better potency blocking ULK1 kinase activity, both *in vitro* and cell-based assays, when compared to small compound SBI-0206965. They also demonstrated that ULK-101 is a highly selective ULK1 inhibitor compared to ULK-100 and SBI-0206965 (Martin et al., 2018).

From the Shokat group first crystal-structure ULK1 kinase to MacKeigan's recent developed ULK1 inhibitor ULK-101, these investigators helped the field uncover the vital role of ULK1 in autophagy. Importantly, each study provided a proof-of-concept that targeting ULK1

could block autophagy. However, there is still much to learn from the discovery of these ULK1 inhibitors and function of ULK1 kinase. We still need to investigate the effects of ULK1 inhibitors in human diseases, specifically cancer. In 2018, MacKeigan and his team demonstrated that ULK-101 effectively suppress the viability of KRAS-driven NSCLC lines cultured in starvation media (Martin et al., 2018). Established Optistarve media used in the study induce autophagy without compromising the viability of the cells. In this study, I further evaluated the efficacy of ULK1 inhibitor ULK-101 on KRAS mutant NSCLC cell lines. Using the LC3B-II immunoblot assay, I observed suppressed autophagy in ULK-101 treated $KRAS^{G12C}$ NSCLC cell lines. Also, I examined the therapeutic potential of ULK-101 by evaluating its effect on inhibiting cell viability of KRAS mutant NSCLC cell lines, alone and in combination with selective mutant $KRAS^{G12C}$ inhibitor, ARS-853. In **Chapter 3**, I observed that $KRAS^{G12C}$ inhibitor ARS-853 promotes autophagy in $KRAS^{G12C}$ NSCLC lines. Therefore, I hypothesized that blocking autophagy by targeting ULK1 would enhance the sensitivity of $KRAS^{G12C}$ NSCLC to ARS-853. My data showed that in starvation media, ULK1 inhibition in combination with selective $KRAS^{G12C}$ inhibitor showed a more than the additive effect in cell viability of $KRAS^{G12C}$ NSCLC.

Interestingly, ULK-101 and ARS-853 combination also decreased the cell viability of A549, which harbor $KRAS^{G12S}$ mutation, when cultured in starvation media. Together, my current study provided evidence that KRAS mutant NSCLC, particularly $KRAS^{G12C}$ NSCLC, could use autophagy to evade target therapy. Furthermore, my preliminary data provided a rationale for further examinations of small molecules targeting autophagy core proteins as promising anticancer agents.

RESULTS

ULK1 kinase induces autophagy

For autophagy to commence, inactive mTORC1 releases ULK1 to form ULK complex required to initiate autophagosome formation (Alers et al., 2012; Kim et al., 2011). To confirm this essential function of ULK1 in autophagy, I used allosteric mTOR inhibitor rapamycin and HDM2 inhibitor MK-8242. As described in **Chapter 2**, MK-8242 interferes with HDM2-p53 interaction which leads to stabilization of p53, a mTORC1 negative regulator (Saxton and Sabatini, 2017). I also added BafA1 (100nM) on the last part of each treatment to disrupt the lysosomal function and inhibit the degradation stage of autophagy. BafA1 treatment allows me to measure the LC3B-II protein level associated with the overall rate of autophagy. As expected, both rapamycin (100nM) and MK-8242 (1.0 μM) enhanced the BafA1-induced LC3B-II protein level compared to BafA1 only treatment (**Figure 4.1A**).

I also confirmed the involvement of ULK1 in autophagy by genetically inhibiting ULK1 using siRNA system. I transfected U2OS cells with siRNAs targeting ULK1 and treated with either rapamycin or MK-8242. As shown in **Figure 4.1A**, ULK1 knockdown reduced the BafA1-induced LC3B-II accumulation in response to rapamycin treatment. I also observed similar LC3B-II phenotype in ULK1 knockdown cells treated with HDM2 inhibitor MK-8242 (**Figure 4.1A**). Taken together, my results validated the importance of ULK1 kinase in autophagy induction.

ULK1 inhibitor ULK-101 suppresses autophagy in NSCLC cell lines

Given that autophagy is considered to promote cell survival in advanced cancer, many laboratories started screening for potential small molecule inhibitors that specifically target the

autophagy core proteins. Since ULK1 represent the initial molecular player of the complex that induces autophagy, ULK1 become an attractive target for autophagy inhibition. Therefore, many researchers focused on developing small molecule inhibitors against ULK1 and autophagy induction. Recently, a new small molecule, ULK-101, demonstrated effective inhibition of ULK1 kinase and suppressed the initiation stage of autophagy. ULK-101 also exhibited a more potent and selective inhibitor for ULK1 compared to SBI-0206965 (Egan et al., 2011; Martin et al., 2018).

In this study, I tested if ULK-101 could effectively inhibit autophagy in KRAS-driven NSCLC lines. I used two oncogenic KRAS-driven NSCLC, H358 (mutant $KRAS^{G12C}$) and H226 (wild-type KRAS) cells. I first treated H358 and H226 with gradient concentrations of ULK-101 (0.63-10 μM) for 3 hours adding BafA1 (100nM) at the final hour of treatment. To determine the effect of the small molecule ULK-101 on the autophagy of each cell line, I measured the accumulation of LC3B-II protein using immunoblot assay. As shown in **Figure 4.1**, I found that the highest dose (10 μM) of ULK-101 effectively reduced the BafA1-induced LC3B-II protein accumulation compared with BafA1 only treatment control, both in H358 (**Figure 4.1B**) and H226 (**Figure 4.1C**) cells.

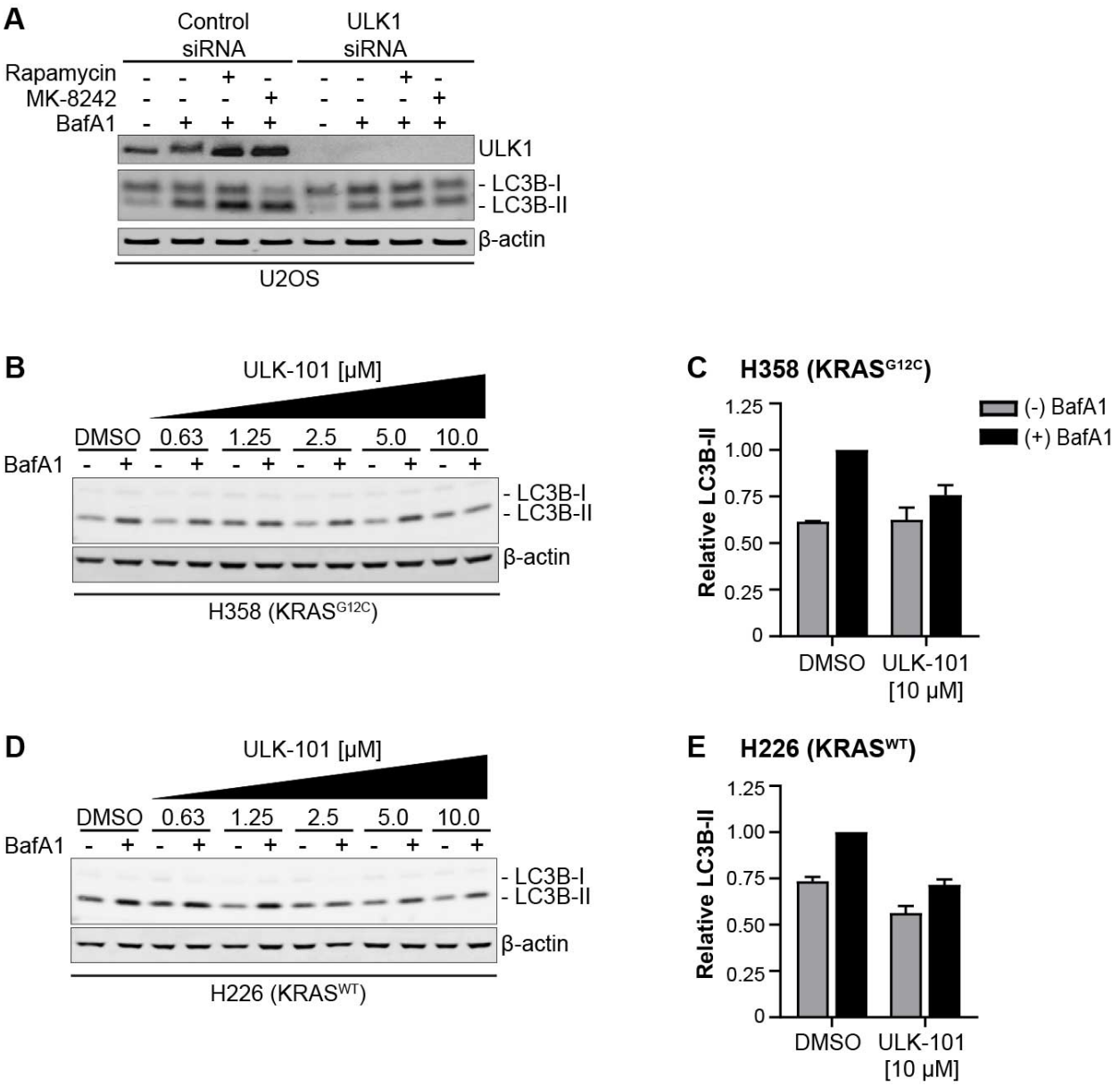

Figure 4.1. ULK1 kinase plays an essential role in autophagy.

(A) Control siRNA and ULK1 siRNA U2OS cells treated with 1.0 μM MK-8242 for 24 hours or 100 nM Rapamycin for 3 hours, with (+) or without (-) 100 nM BafA1 for the final 1.5 hours of treatment (n=2 biological replicate). NSCLC **(B)** H358 (mutant $KRAS^{G12C}$) and **(D)** H226 (wild-type (WT) KRAS) treated with increasing concentration of ULK-101 (0.63-10 μM) for 3 hours, with (+) or without (-) 100 nM BafA1 for the final hour of treatment. **(C and E)** Bar graphs

Figure 4.1 (cont'd)

represented quantification of LC3B-II protein band divided by corresponding β-actin loading control and normalized to 1.0 for the BafA1 only control treatment (n=2 biological replicates; mean and SEM).

ULK1-101 does not suppress autophagy in A549 KRAS^{G12S} NSCLC

Next, I wanted to extend my evaluation of ULK-101 autophagy inhibition to other KRAS mutant NSCLC lines, particularly mutant KRAS^{G12C} NSCLC. G12 mutations account for about 80% of all KRAS mutation. In addition, G12C mutation is a hotspot mutation frequently observed in KRAS isoform. In lung adenocarcinoma, KRAS G12C mutation accounts for 40% of all KRAS mutation (Huynh and Campbell, 2016). Since KRAS-driven NSCLC showed autophagy-dependent cell survival (Guo et al., 2013b), I wanted to determine if ULK-101 demonstrate a common negative effect on autophagy in other mutant KRAS NSCLC cell lines.

I used two NSCLC cell lines with KRAS^{G12C} (H2030 and SW1573) and one NSCLC cell line with KRAS^{G12S} NSCLC (A549). All three cells were treated with 10 μM of ULK-101 for 3 hours adding BafA1 for the last 1.5 hours of the treatment. Interestingly, ULK-101 treated H2030 (**Figure 4.2A**), and SW1573 (**Figure 4.2B**) cells showed reduced accumulation of BafA1-induced LCB3-II protein. However, I failed to observe decreased accumulation of BafA1-induced LC3B-II in ULK-101 treated A549 cells (**Figure 4.2C**). Thus, my results suggest that KRAS^{G12C} NSCLC cell lines showed favorable sensitivity to ULK1 inhibitor ULK-101.

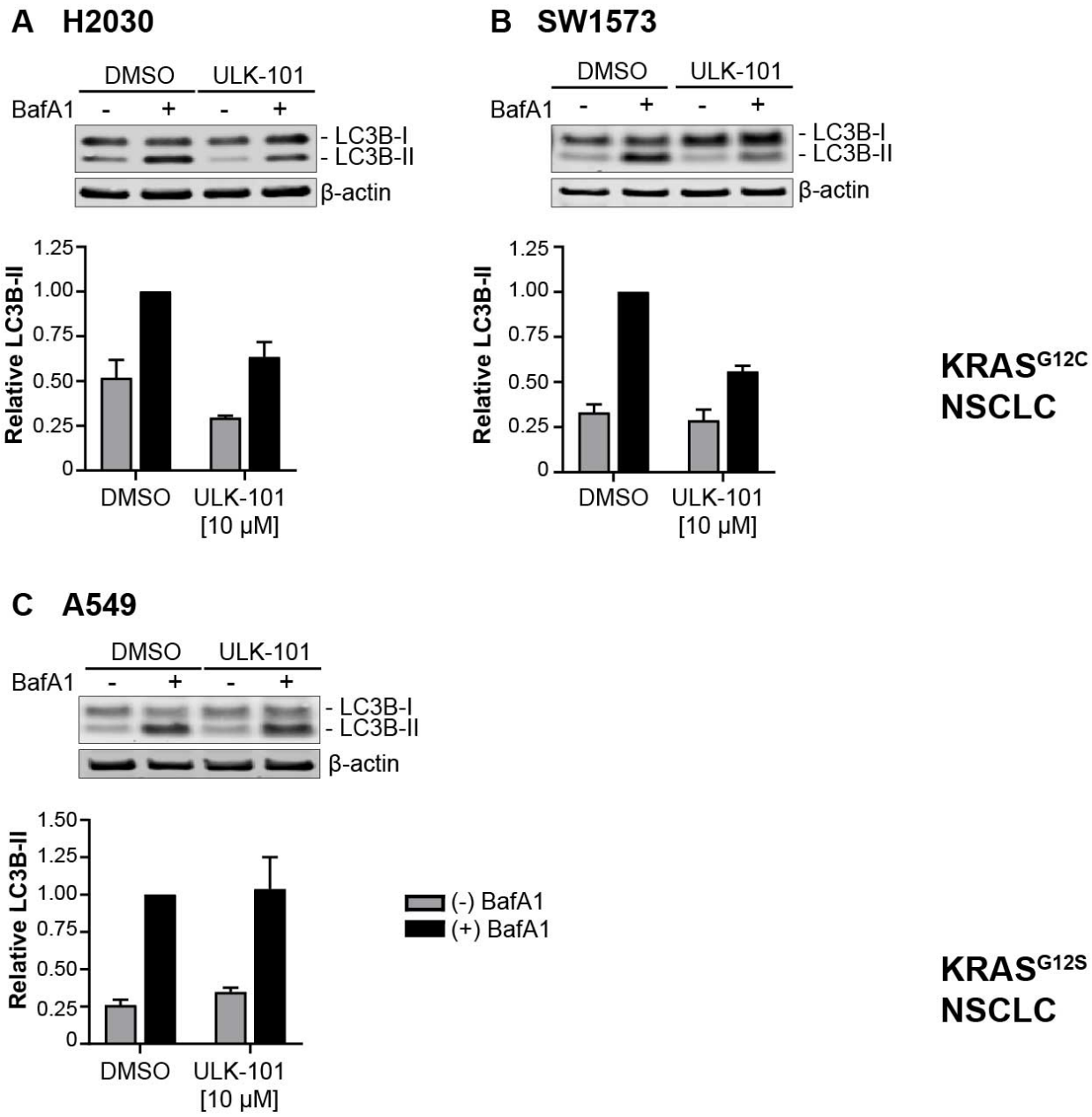

Figure 4.2. ULK1 inhibition suppresses autophagy in KRAS^{G12C} mutant NSCLC cell lines.

KRAS^{G12C} **(A)** H2030 and **(B)** SW1573, and KRAS^{G12S} **(C)** A549 NSCLC treated with 10 μM ULK-101 for 3 hours with (+) or without (-) 100 nM BafA1 for the final 1.5 hours of treatment. Bar graphs represented quantification of LC3B-II protein band divided by corresponding β-actin

Figure 4.2 (cont'd)

loading control and normalized to 1.0 for the BafA1 only control treatment (n=2 to 3 biological replicates; mean and SEM)

ULK-101 sensitizes of KRAS^{G12C} NSCLC in nutrient-restricted conditions

The MacKeigan group found that ULK-101 exert a more favorable inhibitory effect on the viability osteosarcoma and oncogenic KRAS-driven NSCLC lines when cultured in a starvation media (labeled as Optistarve media). Optistarve media contain a minimal level of serum, amino acids, and vitamins compared to an RPMI-1640 culture media (full growth media) (see above Material and Methods; (Martin et al., 2018)). Autophagy is a survival mechanism cancer cells utilize in response to stress, including nutrient deprivation and hypoxic condition. Indeed, Optistarve media provided the nutrient stressor to cancer cell lines to trigger autophagy.

As mentioned above, KRAS-driven NSCLC are reported to depend on autophagy for survival. Therefore, I wanted to assess the sensitivity of KRAS^{G12C} mutant NSCLC cell lines to the small molecule, ULK-101. Furthermore, I observed a declined accumulation of LC3B-II in ULK-101 treated KRAS^{G12C} NSCLC lines (**Figure 4.1B, 4.2A, and 4.2B**). Based on my findings, I hypothesized that ULK-101 would restrain autophagic survival mechanism on KRAS^{G12C} NSCLC lines when cultured in nutrient restricted media. To test my hypothesis, I used three KRAS^{G12C} NSCLC lines (H2030, SW1573, and LU99A). I cultured the cells in either full growth (FM) and Optistarve (OS) media and treated with increasing concentration of ULK-101 (0.10-100 μM). After 48 hours of treatment, I aspirated the media from each well, washed with 1X DPBS, and replaced with fresh FM. I incubated the cells for another five days to recover. Using the CellTiter-Glo Luminescent Viability Assay, I measured the amount of ATP on each well (treated and non-treated), which is proportional to the number of live cells present in the culture. I used the data collected from the assay to generate a relative cell viability curve for each cell line. Agreeable with my hypothesis, I found that ULK-101 modestly reduced the cell viability curve of H2030 (**Figure 4.3B**) and LU99A (**Figure 4.3C**) when cultured in OS. However, I did not see any change

difference in the viability curve of SW1573 (**Figure 4.3D**) treated with ULK-101 cultured in OS versus FM. I also found that three $KRAS^{G12C}$ NSCLC sensitivity to ULK-101 did not show any correlation with their *TP53* status (**Figure 4.3; Table 4.1**).

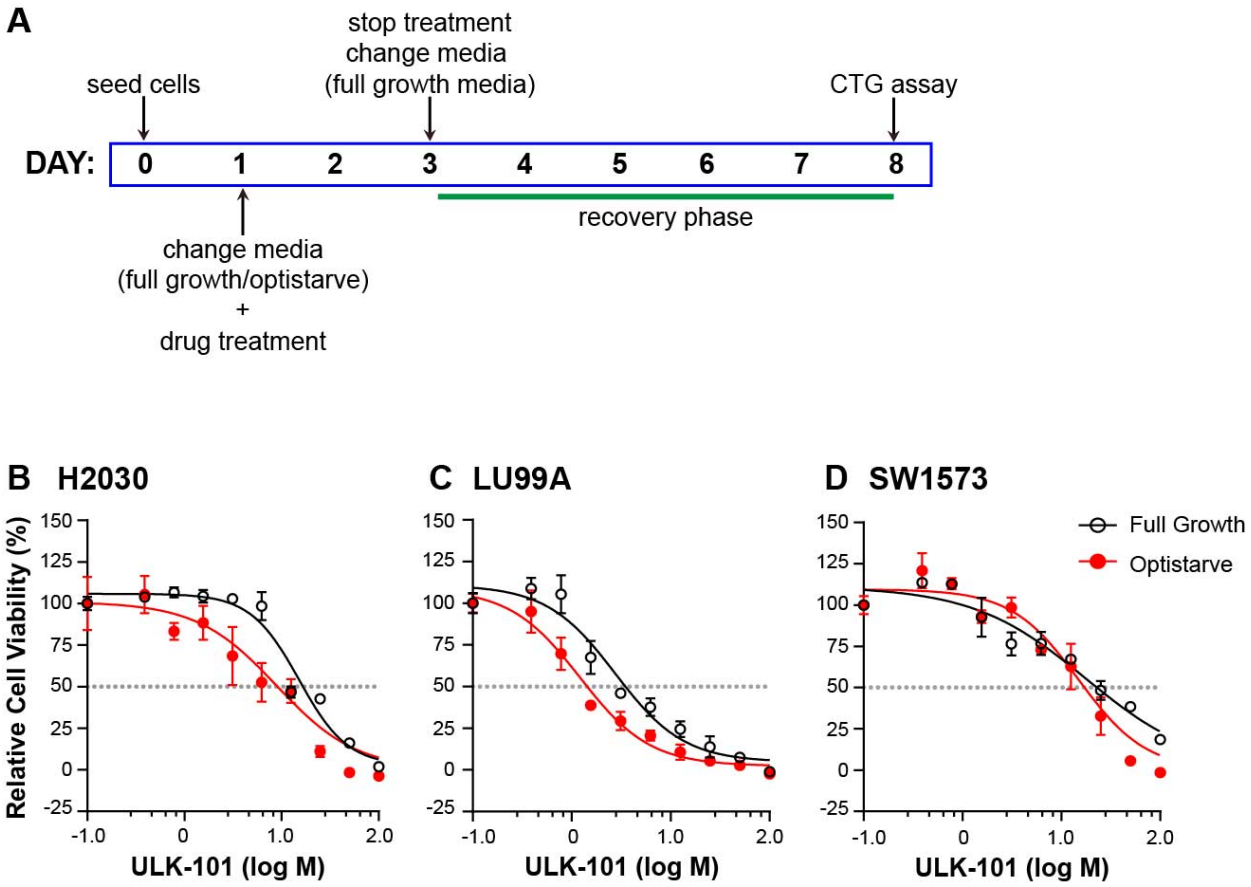

Figure 4.3. ULK-101 sensitize KRAS^{G12C} mutant NSCLC lines.

(A) Experimental design of the clonogenic survival experiment. KRAS^{G12C} NSCLC lines seeded and incubated for 18-24 hours before a 2-day treatment with increasing concentration of ULK-101 (0.10, 0.39, 0.78, 1.56, 3.13, 6.25, 12.5, 25, 50, and 100 μM) in either full growth or Optistarve media. After 48-hour treatment, media washed and replaced with fresh drug-free full growth media. Cell viability measured after a 5-day recovery phase. Relative cell viability curve of ULK-101 treated **(B)** H2030, **(C)** LU99A and **(D)** SW1573 NSCLC cell lines determined by CellTiter-Glo luminescent assay (n=3 technical replicate; mean and SEM).

Table 4.1. ULK-101 sensitivity in KRAS mutant NSCLC.

Cell Line	KRAS Mutation	p53 Status	Full Growth (FM)	Optistarve (OS)	Fold Change (FM/OS)
H2030	*p.G12C*	*p.G262V*	15.1	8.9	1.7
LU99A	*p.G12C*	Wild Type	2.8	1.2	2.3
SW1573	*p.G12C*	Wild Type	17.6	15.0	1.2

Combination of ULK-101 and ARS-853 reduces cell viability in nutrient-restricted conditions

In the previous chapter, I observed increased accumulation of LC3B-II in ARS-853 treated $KRAS^{G12C}$ NSCLC cell lines suggesting that selective $KRAS^{G12C}$ inhibitor promotes autophagy (**Chapter 3, Figure 3.4**). Moreover, my above findings (**Figure 4.3**) and our laboratory recently published data showed that several KRAS-driven NSCLC lines, including $KRAS^{G12C}$ NSCLC, showed sensitivity to ULK-101 when cultured in OS (Martin et al., 2018). With that, I hypothesized that combining ULK-101 with ARS-853 will further abolish the cell viability of mutant $KRAS^{G12C}$ NSCLC.

I first measured the cell viability curve of $KRAS^{G12C}$ mutant NSCLC lines (H2030, SW1573, and LU99A) to selective $KRAS^{G12C}$ inhibitor ARS-853. I used $KRAS^{G12S}$ NSCLC A549 as non-G12C mutant control for ARS-853 treatment. Again, I used our lab's established clonogenic assay (**Figure 4.3A**) to measure the viability curve of each KRAS mutant NSCLC cell line to ARS-853 cultured in FM and OS media. I found that the $KRAS^{G12C}$ NSCLC lines showed a nearly two-fold increase in ARS-853 sensitivity when cultured in nutrient-restricted media (OS) compared to full growth media (FM) (**Figure 4.4A-C; Table 4.2**). Interestingly, $KRAS^{G12S}$ A549 cells (**Figure 4.4D**) also showed sensitivity to high dose treatments, starting from 10μM concentration, of ARS-853 cultured in OS media.

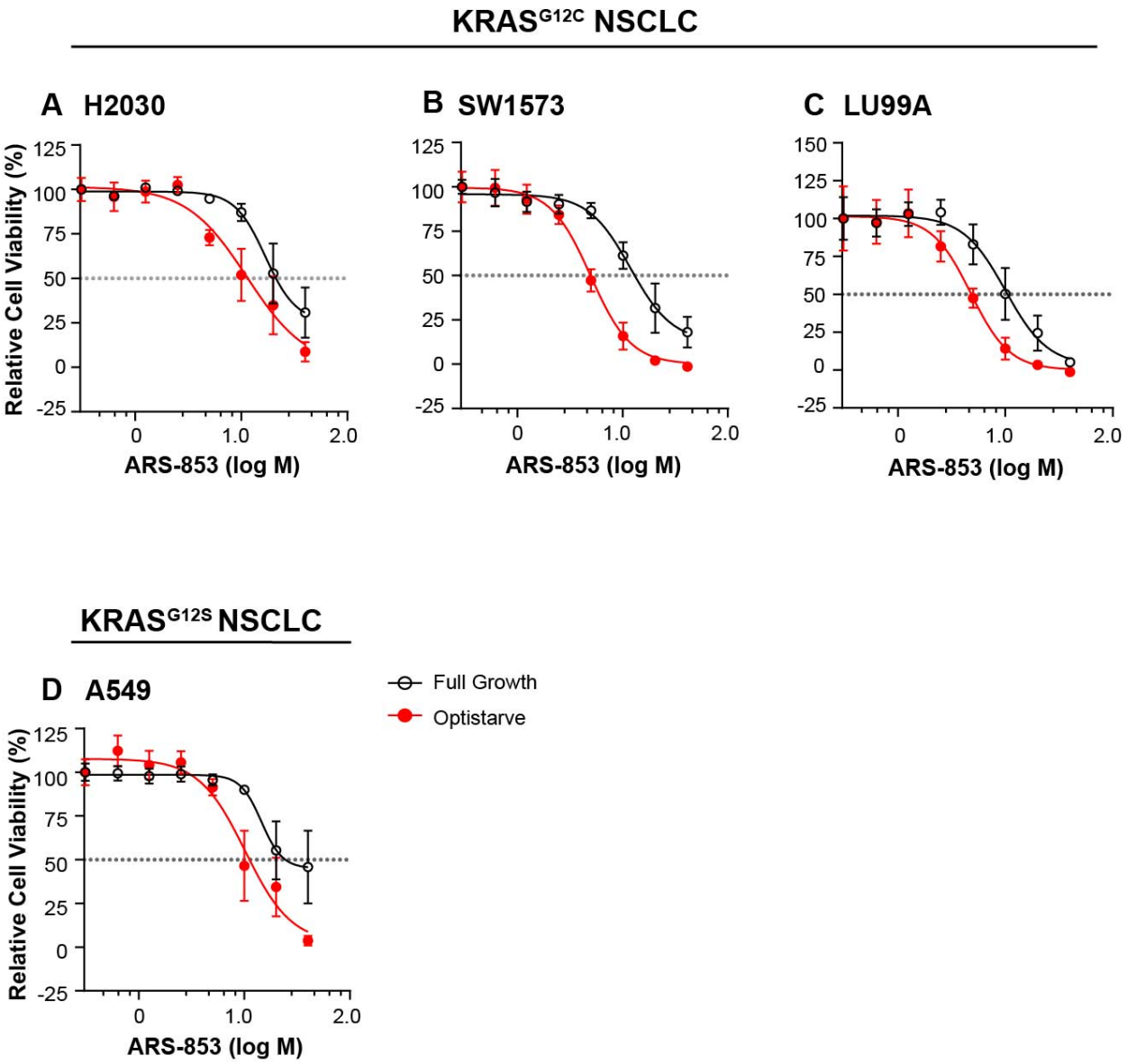

Figure 4.4. ARS-853 shows favorable efficacy on KRAS mutant NSCLC in nutrient-restricted conditions.

Mutant KRAS^{G12C} (H2030, SW1573, and LU99A) and KRAS^{G12S} (A549) NSCLC lines were treated with increasing concentration of ARS-853 (0.31, 0.63, 1.25, 2.5, 5.0, 10, 20, and 40 μM) in either full growth or Optistarve media for 48 hours. Treatment media washed and replaced with fresh full growth media. After 5-day recovery phase, relative cell viability curve of ARS-853 treated **(A)** H2030, **(B)** SW1573, **(C)** LU99A, and **(D)** A549 cells determined by CellTiter-Glo

Figure 4.4 (cont'd)

luminescent assay (n = 2 biological repeat, with three technical replicates per data point; mean and SEM).

Table 4.2. ARS-853 sensitivity in KRAS mutant NSCLC.

Cell Line	KRAS Mutation	p53 Status	Full Growth (FM)	Optistarve (OS)	Fold Change (FM/OS)
H2030	*p.G12C*	*p.G262V*	16.8	11.3	1.5
SW1573	*p.G12C*	Wild Type	11.7	5.0	2.4
LU99A	*p.G12C*	Wild Type	10.0	4.8	2.1
A549	*p.G12S*	Wild Type	-	10.2	

Next, I used the Bliss Independence model to evaluate the efficacy of ULK-101 and ARS-853 combination in $KRAS^{G12C}$ mutant NSCLC. The Bliss Independence model (BLISS, 1939) is used to assess combined effects of a drug with the assumption that each drug act independently (i.e. different sites of action) but contributes to a common result (Foucquier and Guedj, 2015). I chose three different concentration of ARS-853 based on the reported selectivity (Patricelli et al., 2016) and my observed inhibitory efficacy of ARS-853 (**Chapter 3, Figure 3.3A**). For ULK-101 treatment, I used 10 μM concentration which showed effective autophagy inhibition (**Figure 4.1B and 4.1C; Figure 4.2A and 4.2B**). Following our lab clonogenic assay, I treated $KRAS^{G12C}$ NSCLC H2030 and SW1573, and $KRAS^{G12S}$ NSCLC A549 with ARS-853 (5.0, 2.5 and 1.25μM), ULK-101 (10 μM), or combination cultured in FM and OS media. After 48 hours, I aspirated treatment media, washed with DPBS, and replaced with fresh FM. I then incubated the cells for another 5 days to recover. Finally, I used the CellTiter-Glo viability assay to measure the effect of each treatment (single-agent and combination) to each cell line.

Agreeable to my hypothesis, I found that $KRAS^{G12C}$ H2030 and SW1573 showed more sensitivity to ARS-853 and ULK-101 combination when cultured in OS compared to FM media (**Figure 4.5A-4.5D** and **Table 4.3 and 4.4**). Based on Bliss Independence model, ARS-853 (2.5 μM) and ULK-101 (10 μM) combination reduced H2030 cell viability by 91%, greater than expected inhibition value of 59% cultured in OS media (**Table 4.3**). Moreover, ARS-853 (2.5 μM) and ULK-101 (10 μM) combination treatment reduced SW1573 cell viability by 79% which is also higher than expected (46%) (**Table 4.3**). Strikingly, I also observed a more than the additive effect of 2.5 μM ARS-853 and 10 μM ULK-101 combination in $KRAS^{G12S}$ A549 cell viability when cultured in OS media (**Table 4.3**).

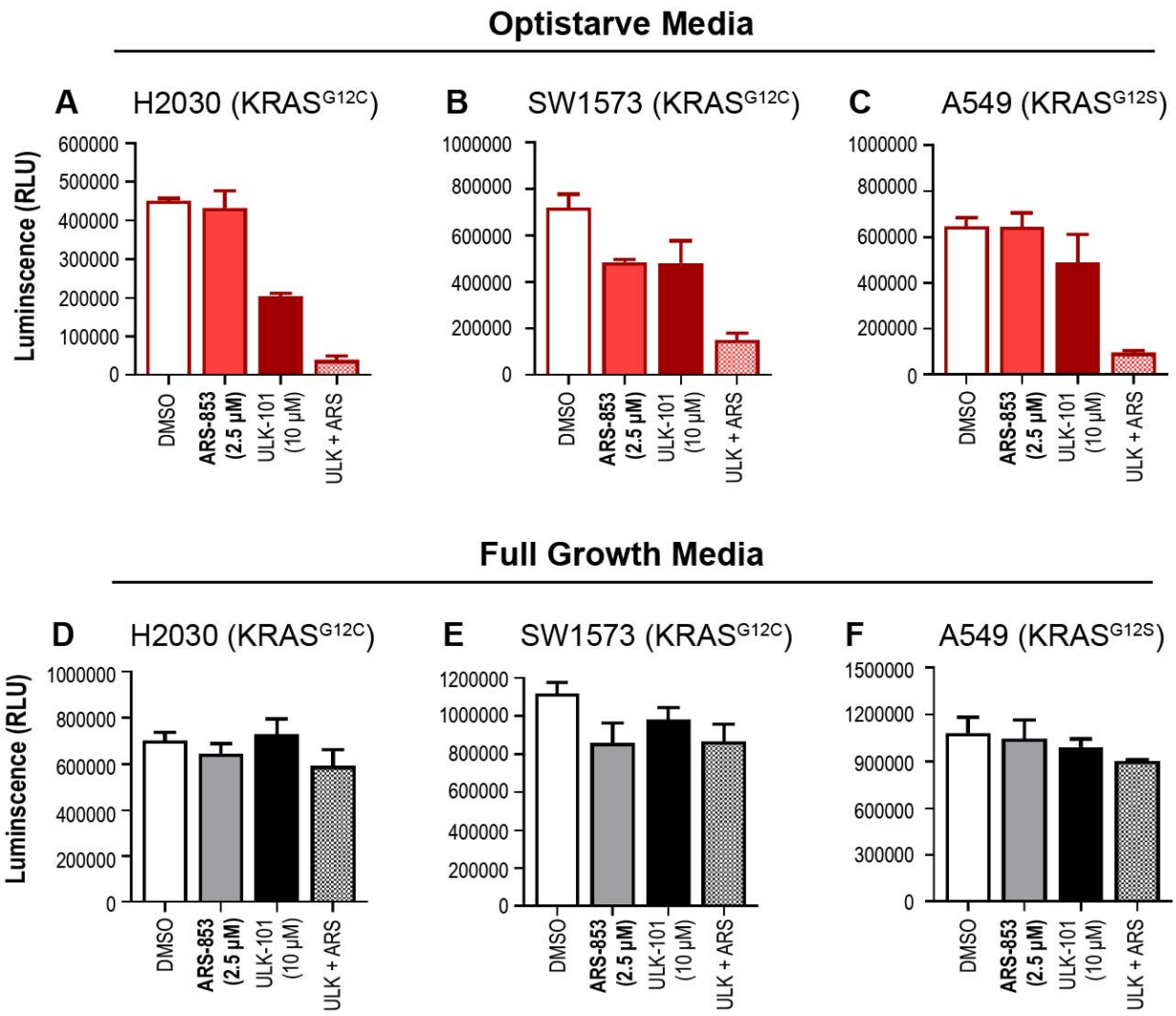

Figure 4.5. ULK-101 reduces KRAS mutant NSCLC viability in combination with ARS-853 in nutrient-restricted conditions.

H2030, SW1573, and A549 NSCLC lines treated with ARS-853 (2.5 µM), ULK-101 (10 µM), and in combination in either **(A-C)** Optistarve or **(D-F)** full growth media for 48 hours. Treated media washed, replaced by fresh full growth media, and incubated for 5 days. Bar graphs represented luminescence reading of CellTiter-Glo luminescent viability assay (n=3 technical replicates per data point; mean and SEM).

Table 4.3. Bliss Independence model calculations of additivity for ULK-101 with ARS-853 in Optistarve media.

Optistarve Media		Single Compound		ARS-853 + ULK-101	
NSCLC Line	**KRAS Mutation**	**Relative Growth Inhibition (ARS-853 (μM))**	**Relative Growth Inhibition (ULK-101 (10 μM))**	**Expected Additive Inhibition Value**	**Experiment Growth Inhibition**
H2030	*p.G12C*	0.40 **(5.0)**	0.55	0.73	0.91
		0.1 (2.5)	**0.55**	**0.59**	**0.91**
		0.33 **(1.25)**	0.68	0.79	0.59
SW1573	*p.G12C*	0.71 **(5.0)**	0.33	0.81	0.92
		0.19 (2.5)	**0.33**	**0.46**	**0.79**
		0 **(1.25)**	0.18	0.18	0.20
A549	*p.G12S*	0.26 **(5.0)**	0.32	0.50	0.89
		0 (2.5)	**0.32**	**0.33**	**0.87**
		0 **(1.25)**	0.50	0.48	0.65

Table 4.4. Bliss Independence model calculations of additivity for ULK-101 with ARS-853 in full growth media.

Full Growth Media		Single Compound		ARS-853 + ULK-101	
NSCLC Line	**KRAS Mutation**	**Relative Growth Inhibition (ARS-853 (μM))**	**Relative Growth Inhibition (ULK-101 (10 μM))**	**Expected Additive Inhibition Value**	**Experiment Growth Inhibition**
H2030	*p.G12C*	0.10 **(5.0)**	0	0.10	0.24
		0.03 (2.5)	**0**	**0.03**	**0.16**
		0.12 **(1.25)**	0.09	0.19	0.03
SW1573	*p.G12C*	0.31 **(5.0)**	0.12	0.40	0.29
		0.22 (2.5)	**0.12**	**0.32**	**0.22**
		0.05 **(1.25)**	0	0.05	0
A549	*p.G12S*	0.09 **(5.0)**	0.08	0.16	0.20
		0.03 (2.5)	**0.08**	**0.11**	**0.20**
		0.09 **(1.25)**	0.10	0.19	0.31

DISCUSSION

Transformed cells rely more on autophagy. This is likely due to multiple stressors highly proliferative tumor cells faced, including hypoxia (Degenhardt et al., 2006) and increased metabolic demands (Guo et al., 2011; Lock et al., 2011). Furthermore, *in vivo* studies showed that deletion of essential autophagy genes such as *Atg7* (Guo et al., 2013a) and *Atg5* (Rao et al., 2014) dramatically inhibited tumor progression of lung adenocarcinoma driven by oncogenic *Kras*. In this study, I wanted to understand how autophagy provides an adaptive mechanism that contributes to the survival and potential therapeutic resistance of $KRAS^{G12C}$ NSCLC cell lines.

Previous assessments of small molecule ULK1 inhibitors demonstrated the importance of ULK1 in the autophagy induction. The Shaw group showed that deactivation of ULK1 by SBI-0206965 effectively inhibited the phosphorylation of ULK1 substrates VPS34 (Ser249) and Beclin-1 (Ser15) (Egan et al., 2015). Likewise, the MacKeigan group observed a reduction of Beclin-1 Ser15 phosphorylation in response to ULK1 inhibitor ULK-101 which also showed better potency and selectivity to ULK1 compared to SBI-0206965 (Martin et al., 2018). Here, I assessed the inhibitory effect of ULK-101 on autophagy in KRAS mutant NSCLC lines. I found that acute treatment of ULK-101 (10μM) effectively reduced the BafA1-induced LC3B-II protein accumulation of $KRAS^{G12C}$ NSCLC lines but showed no effect on the autophagic activity of $KRAS^{G12S}$ A549 cells. This indicates that ULK-101 demonstrates a more favorable blockage of autophagy in $KRAS^{G12C}$ NSCLC lines. Also, my findings suggest $KRAS^{G12C}$ mutation as a potential biomarker for NSCLC that could benefit to autophagy inhibition.

Next, I investigated the effect of ULK-101 on the cell viability of KRAS mutant NSCLC lines, particularly $KRAS^{G12C}$ NSCLC. Prior to my study, other investigators used ULK1 inhibitors

to suppress the cell viability of NSCLC cell lines. Conghua Xie and colleagues reported that ULK1 overexpression promotes cell proliferation of NSCLC lines. By combining SBI-0206965 with cisplatin, they observed impaired viability of NSCLC lines (Tang et al., 2017). Following Tang et al. observation, the MacKeigan group evaluated the effect of ULK-101 in a group of KRAS-driven NSCLC cell lines. They treated NSCLC with a concentration gradient of ULK-101 and cultured the cells in either full growth (FM) or Optistarve (OS) media for 48 hours. After an additional 5-day recovery period, ULK-101 treated and nutrient-stressed KRAS-driven NSCLC lines revealed suppressed cell viability (Martin et al., 2018). Here, I predicted that $KRAS^{G12C}$ NSCLC lines cultured in OS media would also reveal vulnerability to ULK-101. I used the MacKeigan lab established cell survival assay illustrated in **Figure 4.3A**. Although not a noticeable effect, I observed reduced cellular viability of $KRAS^{G12C}$ NSCLC (H2030 and LU99A) due to ULK1 inhibition. In summary, my current data together with the two independent studies (Martin et al., 2018; Tang et al., 2017) provided additional evidence that autophagy promotes survival mechanism on KRAS-driven NSCLC.

Many cancer therapies upregulate autophagy, a counterproductive result as autophagy can induce tumor cell survival. In lung cancer model, epidermal growth factor receptor tyrosine kinase inhibitors (EGFR-TKI) gefitinib and erlotinib showed activation of autophagy in NSCLC cell lines. Autophagy inhibition with either CQ or with siRNA targeting *ATG5* and *ATG7* treatment greater the cytotoxic effect of EGFR-TKIs on NSCLC cell lines (Han et al., 2011). Notably, the utility of ULK1 inhibitor SBI-0206965 also revealed increased sensitivity of NSCLC cell lines to mTOR inhibitor rapamycin (Egan et al., 2015) and a cytotoxic agent, cisplatin (Tang et al., 2017). Collectively, these studies demonstrated the value of autophagy inhibitors in future regimens of cancer treatment.

In **Chapter 3**, I observed increased accumulation of BafA1-induced LC3B-II level in $KRAS^{G12C}$ NSCLC treated with selective $KRAS^{G12C}$ inhibitor ARS-853. ARS-853 selectively inhibit $KRASG^{12C}$/MAPK/ERK signaling by covalently binding to inactive GDP-$KRAS^{G12C}$ and interfere KRAS interaction with guanine nucleotide exchange factors. Modulation of $KRAS^{G12C}$/MAPK/ERK signaling by ARS-853 promote suppression of cell proliferation of $KRAS^{G12C}$ NSCLC lines (Lito et al., 2016; Patricelli et al., 2016). Since oncogenic Ras-driven tumors showed dependence to autophagy for survival, I hypothesized that autophagy inhibition would further enhance the cytostatic effect of ARS-853 in $KRAS^{G12C}$ NSCLC cell lines. Mechanistically, inhibiting $KRAS^{G12C}$/MAPK/ERK signaling suppressed the activation of mTORC1, the master regulator of autophagy. In order to test my hypothesis, I again used the clonogenic assay to determine the cell viability curve of KRAS mutant NSCLC to ARS-853. I found that all three $KRAS^{G12C}$ NSCLC lines showed about two-fold increase sensitivity to ARS-853 when cultured in OS compared to FM. Notably, $KRAS^{G12S}$ A549 revealed sensitivity to high doses of ARS-853 in OS condition.

Next, I treated $KRAS^{G12C}$ H2030 and SW1573 along with $KRAS^{G12S}$ A549 cells with ULK-101 (10 μM), ARS-853 (5.0, 2.5 and 1.25 μM), or combination cultured in FM and OS media. Reports demonstrated that ARS-853 revealed IC_{50} of 2.5 μM target and cell proliferation inhibition (Lito et al., 2016). Furthermore, targeted cysteine selectivity profiling screen showed that ARS-853 start to covalently bind to other targets at doses higher than 3.0 μM (Patricelli et al., 2016). Therefore, I focused my investigation in KRAS mutant NSCLC lines treated with ULK-101 (10 μM), ARS-853 (2.5 μM), or combination cultured in OS. I found that cotreatment of ULK-101 with ARS-853 enhanced the cytostatic effect of $KRAS^{G12C}$ inhibition.

Strikingly, the combination of ULK-101 and ARS-853 also showed additivity on $KRAS^{G12S}$ A549 cells when cultured in OS media. It is possible that the observed data was due to the additional stressor from OS media. The OS media contained limited nutrients necessary to induce upstream signaling inputs to the RAS/RAF/ERK pathway. In addition, RAS mutants showed various degree of nucleotide exchange kinetics *in vitro* (Hunter et al., 2015) which could create additional susceptibility to the KRAS mutant cells in OS condition. To test my hypothesis, I treated A549 cells with ULK-101 (10 μM), ARS-853 (2.5 μM), or combination culture in OS for 48 hours and measured p-ERK1/2. Indeed, my initial investigation revealed a reduction in ERK1/2 phosphorylation in A549 cells cultured in OS compared to FM media with or without ARS-853 (**Figure 4.6**). ERK1/2 regulate a large number of cytoplasmic and nuclear substrates that modulate cellular proliferation, survival, and motility (Roskoski, 2012). Thus, suppression of ERK1/2 phosphorylation caused by nutrient starvation could lead to adverse effects that increased the cytostatic effect of ULK-101 and ARS-853 combination treatment in A549 cells. The unexpected results I found in A549 cells suggest future studies to better understand autophagy in the spectrum of oncogenic RAS mutation. Further studies would provide a careful and rational selection of combination therapies for KRAS mutant NSCLC.

In summary, my present study provided encouraging data for further assessment of combination regiments including autophagy inhibition and target agents to enhance therapy on NSCLC, particularly $KRAS^{G12C}$ mutant NSCLC. In addition, I found that ULK-101 revealed effective inhibition of autophagy and suppression of cell viability as a single agent. Thus, my findings suggest future development of selective autophagy inhibitors, such as ULK-101, may be of clinical benefit for adjuvant treatment for NSCLC.

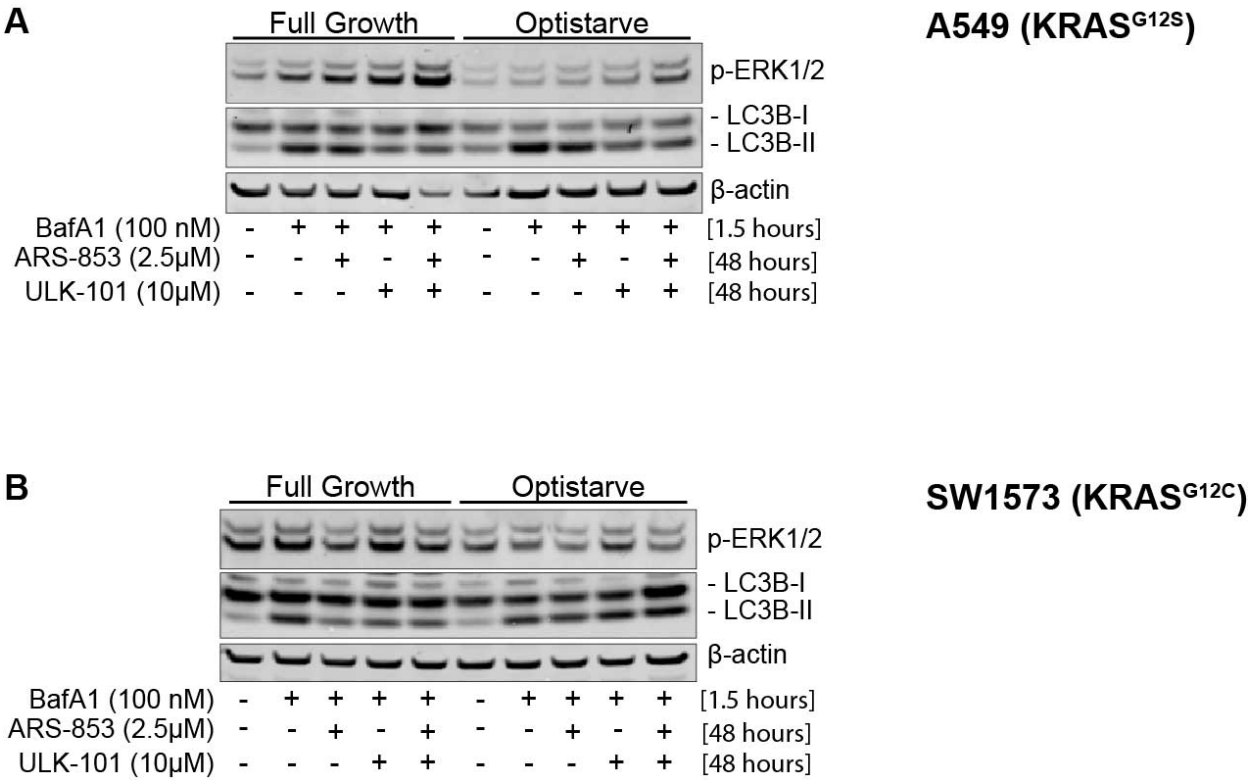

Figure 4.6. KRAS^{G12S} A549 NSCLC shows decreased phosphorylation of ERK1/2 in nutrient-restricted conditions.

(A) A549 (KRAS^{G12S}) and **(B)** SW1573 (KRAS^{G12C}) NSCLC treated with ARS-853 (2.5 μM), ULK-101 (10 μM), and in combination cultured in full growth and Optistarve media for 48 hours. BafA1 is added for the final 1.5 hours of treatment.

MATERIALS AND METHODS

Mammalian cell cultures, reagents, and antibodies

The human osteosarcoma U2OS, and NSCLC H226, A549, H2030, SW1573, and LU99A were cultured in RPMI-1640 supplemented with 10% FBS. All cells were maintained in a humidified atmosphere containing 5% CO_2 at 37°C and seeded 18-24 hours before the start of treatments or assays. Cells were treated with either mTOR inhibitor rapamycin, HDM2 inhibitor MK-8242, $KRAS^{G12C}$ inhibitor ARS-853, or ULK1 inhibitor ULK-101 (Merck & Co., Inc). Vacuole H+-ATPase inhibitor Bafilomycin A1 was added on the final 1.5 hours of treatment to block lysosomal function. All inhibitor stock solutions were prepared in Dimethyl Sulfoxide (DMSO) (Sigma-Aldrich, D2650), aliquoted, and stored at -80°C freezer. Equal concentration of DMSO was used for control treatments. Rabbit polyclonal antibody LC3B, rabbit polyclonal antibodies phospho-p44/42 MAPK (Thr202/Tyr204), rabbit monoclonal antibody ULK1 (CST, 8054) were used for Western blot analysis. Mouse monoclonal antibody β-actin was used as a loading control. Horseradish peroxide (HRP)-conjugated and IRDye infrared fluorescent 800CW/680RD were used as secondary antibodies for western blotting.

Western blot analysis

Cell lysates were prepared in ice-cold lysis buffer [10mM potassium phosphate, 1 mM ethylenediaminetetraaceticacid (EDTA), 10 mM magnesium chloride, 5 mM ethylene-bis(oxyethylenenitrilo)tetraacetic acid (EGTA), 50 mM bis-glycerophosphate, 0.5% Nonidet P-40 (NP-40), 0.1% Brij35, 0.1% sodium deoxycholate, 2 mM dithiothreitol, 1 mM sodium orthovanadate, 5 mM sodium fluoride, and protease inhibitor cocktail]. Lysate samples were

incubated in an ice bath for 10 min and clarified by centrifugation for 10 min at 13,000 rpm and 4°C. Supernatant was collected and stored in -80°C freezer until further used. Total protein concentration was determined using Protein Assay Dye Reagent Concentrate (Bio-Rad, 5000006). Sample solution [25mM Tris-HCl, 10% SDS, 38% glycerol, and bromophenol blue] containing fresh 10% beta-mercaptoethanol was added to lysates and boiled for 5 min. Proteins were resolved by sodium dodecyl sulfate-polyacrylamide gel or Invitrogen pre-cast 4-12% BOLT Bis-Tris Plus gel and electrotransferred onto either nitrocellulose or polyvinylidene difluoride membranes. Membranes were blocked with 5% nonfat dry milk in 1X Tris-buffered solution and 0.1% Tween-20 (0.1% T-TBS) or Thermo StartingBlock (TBS) Blocking Buffer followed by overnight incubation of primary antibodies diluted in 5% BSA, 0.1% T-TBS solution or Thermo StartingBlock T20 (TBS) Blocking Buffer at 4°C. After three 5-minute 0.1% T-TBS washes, membranes were incubated in secondary antibodies diluted in 5% milk/BSA, 0.1% T-TBS buffer or StartingBlock T20 (TBS) Blocking Buffer for 1 hour at room temperature. Protein bands were detected by enhanced chemiluminescence, Thermo West Femto Maximum Sensitivity Substrate, or imaged using LI-COR Odyssey Infrared Imaging System and quantified with LI-COR Image Studio Software.

ULK1 knockdown by small interfering ribonucleic acid (siRNA)

Flexitube siRNA Hs_ULK1 siRNA5 (SI02223270) and siRNA6 (SI02223277) were obtained from Qiagen, reconstituted in UltraPure DNase/RNase-Free Distilled Water (Invitrogen, 10977-015) to obtain 20uM solution stock, aliquoted, and stored in -80C freezer. U2OS cells (4.0 x 10^5 cells per plate) seeded on 10-cm culture plates before the start of the assay. Cells were transfected with a combination of ULK1 siRNA5 and siRNA6 using Oligofectamine (Invitrogen,

12252011) for 48 hours. Qiagen AllStars Negative Control siRNA included as a control siRNA. In summary, 1:10 dilution of Oligofectamine into OptiMEM Reduced Serum media (Thermo, 31985070) was incubated for 5 min at room temperature. After 5 minutes, Oligofectamine solution was combined with human *ULK1* siRNA5 and siRNA6 (25nM each) and incubated for 20 min at room temperature. Fresh RPMI-1640 with 10% FBS was added to cells. After the 20 min incubation, Oligofectamine-siRNAs transfection complex solution was added to the cells. Media was changed with fresh RPMI-1640 with 10% FBS after 24 hours.

Clonogenic survival assay

KRAS mutant NSCLC H2030 (1.0 X 10^3 cells/well), SW1573 (2.5 x 10^3 cells/well), LU99A (2.0 x 10^3 cells/well), and A549 (1.0 x 10^3 cells/well) were seeded on 96-well white wall, clear bottom cultured microplate (Greiner-Bio, 655098) in RPMI-1640 media supplemented with 10% FBS. After 18-24 hours, media was aspirated and wells rinsed with 1X DPBS without calcium and magnesium (Gibco, 14190144). Full growth (RPMI-1640 + 10% FBS) or Optistarve media (1X HBSS with 0.1% FBS,1 mM L-Glutamine (Gibco, 25030), 2 g/L D-glucose, 12.5% RPMI 1640 Amino Acid Solution (Sigma-Aldrich, R7131), and 25% RPMI 1640 Vitamin Solution (Sigma-Aldrich, R7256) was then added to each well. NSCLC lines were treated with increasing concentration of ULK-101 (final concentration of 0.10, 0.39, 0.78, 1.56, 3.13, 6.25, 12.5, 25, 50, and 100 μM) or ARS-853 (final concentration of 0.31, 0.63, 1.25, 2.5, 5.0, 10, 20, and 40 μM) for 48 hours. An equal concentration of DMSO used as vehicle control and media only as a negative control. After the 2-day treatment, media were aspirated, wells rinsed with 1X DPBS, and replaced with fresh full growth media. Cell viability was determined after a 5-day recovery phase.

Cell viability was measured with the CellTiter-Glo Luminescent Cell Viability Assay (Promega, G7570) following the manufacturer's protocol with minor modification. Briefly, CellTiter-Glo (CTG) reagent was diluted in 1X DPBS (1:1). Media from 96-well microplate was dumped, wells rinsed with 1X DPBS, and dried by gently tapping the inverted microplate on paper towel. One hundred microliters of CTG: DPBS mixture was added to each treated well and gently rocked for 5 minutes. The amount of ATP on each well which is proportional to the number of live cells present was measured using Molecular Devices SpectraMax i3x Multi-Mode Microplate Luminescent Reader. Luminescent readings (RLU) for each treatment was calculated and analyzed using GraphPad Prism 8.

Drug combination evaluation

$KRAS^{G12C}$ (H2030 and SW1573) and $KRAS^{G12S}$ (A549) NSCLC lines were seeded into 96-well white wall, clear bottom cultured microplate. After 18-24 hours, cells were cultured in full growth or Optistarve media with 10 μM ULK-101, increasing concentration of ARS-853 (0.31, 0.63, 1.25, 2.5, 5.0, 10, 20, and 40 μM), or combination for 48 hours. Equal concentration of DMSO was used as vehicle control and media only as negative control. After two days, treatment was stopped and replenished with full growth media. Cells were incubated and allowed to recover for another five days. Cell viability was measured with CellTiter-Glo Luminescent Cell Viability Assay.

Additivity of ULK-101 and ARS-853 was determined using Bliss Independence model ($\mathbf{E_{AB} = E_A + E_B - E_AE_B}$) (BLISS, 1939; Foucquier and Guedj, 2015); where E_A the effect of drug A, E_B the effect of drug B, and E_{AB} the combined effect of drug A and B.

CHAPTER 5.

OVERALL DISCUSSION

Overall Conclusion

A conserved catabolic cellular pathway, autophagy sequesters and degrades intracellular components in lysosomes to recycle macromolecules to maintain cellular homeostasis. For cancer cells, the role of autophagy is dynamic and depends on many factors including tumor types, tumor stages, and activation of several tumor suppressors and oncogenes. In fact, reports showed that autophagy suppresses the initiation of tumorigenesis in normal tissue and later becomes a supporting system for advanced cancer (Guo et al., 2013b; Santana-Codina et al., 2017; White, 2012, 2015). My thesis focused on the unique relationship of autophagy with tumor suppressor p53 and oncoprotein KRAS in cancer cells, particularly in NSCLC. The results discussed in this study illustrated that HDM2 inhibitor (MK-8242 and nutlin-3a)-induced stabilization of wild-type p53 activates autophagy through regulation of many autophagy modulators (*DRAM*, *FOXO3A*, *SESN2*, and *MRCKα*) and autophagy core genes (*ATG4A*, and *ULK1*). I also learned that pharmacologic inhibition (ARS-853) of mutant $KRAS^{G12C}$ could trigger autophagy in $KRAS^{G12C}$ mutant NSCLC cell lines. At the molecular level, my data showed ARS-853 indirectly promotes autophagy through inhibition of $KRAS^{G12C}$/MAPK/ERK signaling which regulate mTORC1, the major inhibitor of autophagy.

Although it is possible that not all tumors would benefit to autophagy inhibition, some investigators showed positive outcome when combining autophagy inhibitor (i.e., CQ) with other therapeutic drugs (Amaravadi et al., 2007; Han et al., 2011; Rebecca and Amaravadi, 2016; Rebecca et al., 2014). With that, I took the opportunity to design a combination study using a novel ULK1 inhibitor (ULK-101) with ARS-853 in NSCLC. I found that selectively inhibiting ULK1 dramatically enhanced the ability of selective $KRAS^{G12C}$ inhibitor to impair the viability of $KRAS^{G12C}$ NSCLC cell lines. Together, my study provided evidence that autophagy serves as a

survival pathway in tumor cells and that further assessment of small molecule that modulates autophagy pathway may be potential cancer therapeutic option in wild-type p53 and mutant $KRAS^{G12C}$ NSCLC.

Wild-type p53 induces autophagy in tumor cells in response to HDM2 inhibitor

The role of p53 in autophagy depends on its subcellular localization. Indeed, the function of p53 in autophagy remained to be controversial. A group of researchers believed that cytoplasmic p53 inhibits autophagy. The Kroemer group demonstrated that silencing p53, either by pifithrin-α or siRNA treatment, could activate autophagy (Tasdemir et al., 2008). In addition, cytoplasmic p53 and mutant p53, specifically p53 mutation that consistently localized the protein in the cytosol, could efficiently inhibit autophagy (Morselli et al., 2008). Contrary, other groups showed that activation of nuclear p53 in response to cellular stress transactivated autophagy-related genes, such as *SESN2* (Budanov and Karin, 2008), *DRAM* (Crighton et al., 2006), and autophagy core genes *ATG4*, *ATG7*, and *ULK1* (Kenzelmann Broz et al., 2013) required for autophagy.

In **Chapter 2 and 3**, I sought to uncover the underlying mechanism of wild-type p53 in autophagy. I used two HDM2 inhibitors (MK-8242 and nutlin-3a) to stabilize the p53 protein and investigate autophagy induction in the context of wild-type p53 in osteosarcoma and NSCLC cells. Using LC3B-II immunoblotting, I found that stable and active p53 caused by MK-8242 or nutlin-3a treatment dramatically induced autophagy in U2OS osteosarcoma cell line and KRAS-driven NSCLC cell lines harboring wild-type p53 (**Figure 2.1C and 3.1A, B**).

Completing kinome siRNA screening and qRT-PCR of MK-8242 treated U2OS cells helped me identified and clarified mediators of p53-regulated autophagy, including ULK1 and MRCKα (**Figure 2.3**). The identification of ULK1 kinase was self-explanatory as ULK1 is a well-

known regulator of autophagy induction. However, identification of MRCKα kinase was intriguing as there is no current reported association of MRCKα to autophagy. MRCKα is characterized as CDC42 effector protein kinase and regulates actin-myosin cytoskeleton through phosphorylation of MLC2, MYPT1, and LIMK1/2.

Although identification of MRCKα was unexpected, actin cytoskeleton was already associated with autophagy (Aplin et al., 1992; Kast and Dominguez, 2017; Kruppa et al., 2016). Indeed, actin cytoskeleton, particularly actin regulatory proteins Arp2/3, NPFs, and myosins, were linked to various stages of autophagy. For example, in starvation-induced autophagy, JMY showed a mechanical role during autophagosome formation, as JMY colocalized with actin and LC3 at autophagosome and depletion of JMY by siRNA reduced the number of autophagosomes (Coutts and La Thangue, 2015).

Also, myosin, such as MYO2, along with actin cytoskeleton could provide transports for autophagy proteins during autophagosome biogenesis and formation (Kruppa et al., 2016). In fact, the Chen group reported that ULK1 could mediate the activation of non-muscle myosin II (MYO2) during ATG9 trafficking and formation of autophagosomes (Tang et al., 2011). Here, MRCKα knockdown suppressed the MK-8242 induced level of EGFP-LC3B puncta representing the autophagosome formation (**Figure 2.4C and 2.4D**). Thus, suggesting a critical role of MRCKα during autophagosome elongation/maturation during p53-dependent autophagy. Since MRCKα regulates the activity of MYO2 through direct phosphorylation of MLC2 (Serine 19) our novel insight supports the importance of actin-myosin cytoskeleton during autophagosome biogenesis and formation in p53 context.

Inhibition of KRAS^{G12C} signaling drives autophagy in NSCLC

Aside from evaluating the connection of wild-type p53 and autophagy, I also sought to investigate the relationship between mutant KRAS^{G12C} and autophagy in NSCLC. Many researchers showed that autophagy promotes survival to highly proliferative tumor cells, particularly Ras-transformed cells, during the stress of nutrient deprivation (Guo et al., 2011; Lock et al., 2011; Yang et al., 2011). Autophagy could also mediate survival to therapies including cytotoxic chemotherapies (Amaravadi and Thompson, 2007; Zhang et al., 2012) and target agents (Carew et al., 2007; Rebecca et al., 2014) used for cancer. Here, using the recently developed selective KRAS^{G12C} inhibitor ARS-853, I evaluated autophagy response in KRAS^{G12C} mutant NSCLC cell lines. ARS-853 was established to trap KRAS^{G12C} on its non-functional state (GDP-bound state) and prevent from activating downstream pathway including RAF/MEK/ERK signaling pathway (Lito et al., 2016; Patricelli et al., 2016). Mechanistically, mTORC1 is a downstream effector of the RAS/RAF/ERK signaling pathway. Active mTORC1 plays a central role in regulating various cellular processes contributing to cell growth, such as protein and lipid synthesis and autophagy (Saxton and Sabatini, 2017). Therefore, I predicted that modulating KRAS^{G12C} signaling pathway will induce autophagy in KRAS^{G12C} NSCLC lines.

Here, I treated four KRAS^{G12C} NSCLC cell lines (H23, H358, H2030, and SW1573) with ARS-853. I also used non-G12C KRAS mutant NSCLC cell lines (H226, H1437, and A549) as controls (**Table 3.1**). Consistent with previous reports, I found that ARS-853 suppressed the KRAS^{G12C}/RAF/MEK/ERK signaling exclusively in KRAS^{G12C} NSCLC lines (**Figure 3.2**). Notably, I found that inhibiting the upstream KRAS^{G12C} signaling showed a various degree of autophagy induction in each KRAS^{G12C} NSCLC cell lines (**Figure 3.4A-C**). This could be due to additional genetic alterations of each tumor cell, such as p53 status. Together, my results support

my prediction that selective $KRAS^{G12C}$ inhibitor could trigger autophagy response in NSCLC cell lines carrying $KRAS^{G12C}$ mutation.

Evaluation of ULK1 inhibitor in KRAS mutant NSCLC cell lines

In **Chapter 4**, I wanted to understand the value of autophagy inhibition in cancer cells, particularly in mutant KRAS NSCLC. Based on previous preclinical studies, autophagy inhibitions showed positive output when combined with ineffective treatment against cancer cells. The Thompson group saw this effect when they inhibited autophagy in lymphoma tumor cells, by CQ treatment or *Atg5* knockdown. They showed that CQ treatment enhanced the cytotoxicity effect of alkylating agent to tumor cells (Amaravadi and Thompson, 2007). Most recently, two independent groups demonstrated that inhibiting autophagy regulator ULK1 increased the sensitivity of NSCLC to mTOR inhibitor rapamycin (Egan et al., 2015) and cytotoxic drug cisplatin (Tang et al., 2017).

These impressive results prompted me to hypothesize that ULK1 inhibition would sensitize $KRAS^{G12C}$ NSCLC when challenged in starvation condition and enhance tumor vulnerability to $KRAS^{G12C}$ target inhibitor. In order to test my hypothesis, I first investigated the effect the newly reported selective ULK1 inhibitor, ULK-101, in KRAS mutant NSCLC cell lines. I treated three $KRAS^{G12C}$ NSCLC cell lines (H358, H2030, and SW1573) with ULK-101 for three hours. I found that 10 μM concentration of ULK-101 effectively suppressed autophagy in $KRAS^{G12C}$ NSCLC H358 (**Figure 4.1B and 4.1C**), H2030 (**Figure 4.2A**), and SW1573 (**Figure 4.2B**).

It is important to note that from the beginning of my thesis study, I have measured autophagy in KRAS-driven NSCLC cell lines cultured in full growth media which represent the nutrient-rich condition. Fundamentally, tumor cells showed autophagy upregulation when exposed

to stress such as hypoxia and nutrient depleted condition (Degenhardt et al., 2006). In order to properly measure the level of autophagy in tumor cells, I started to use the MacKeigan lab starvation media Optistarve (OS) (Martin et al., 2018). The OS media contain a restricted amount of nutrients compared to full growth media (RPMI-1640 with 10% FBS) we used to maintain our NSCLC lines. OS media would, therefore, provide similar physiological stressor on cancer cells to induce autophagy. From this time forward, I investigated the efficacy of ULK1 and $KRAS^{G12C}$ selective inhibitor in KRAS mutant NSCLC cell lines cultured in OS condition.

Recently, our lab also demonstrated that oncogenic KRAS-driven NSCLC cell lines, including $KRAS^{G12C}$ H2030 and $KRAS^{G12S}$ A549 cells, cultured in OS condition were highly susceptible to ULK1 inhibitor ULK-101 compared to treated cells in FM (Martin et al., 2018). Following the same assay, I examined the vulnerability of $KRAS^{G12C}$ mutant NSCLC to ULK-101 cultured in nutrient-restricted media (**Figure 4.3**). Although my results did not present a dramatic impaired cellular viability, I found that $KRAS^{G12C}$ NSCLC, particularly H2030 and LU99A, cultured in OS media showed more sensitivity to ULK-101. Thus, my data suggest that inhibiting the integral kinase ULK1 is enough to repress the autophagy survival mechanism in $KRAS^{G12C}$ NSCLC in nutrient-deprived condition.

Before I continued to evaluate the therapeutic efficacy of ULK-101 and ARS-853 combination in KRAS mutant NSCLC lines ($KRAS^{G12C}$ and $KRAS^{G12S}$), I also measured the viability curve of these cells to ARS-853 by clonogenic assay. All three $KRAS^{G12C}$ showed nearly two-fold increase sensitivity to ARS-853 when cultured in OS compared to FM. Strikingly, $KRAS^{G12S}$ A549 NSCLC line also showed sensitivity to the highest doses of ARS-853. This could be due to an off-target effect of ARS-853. The Liu group reported that ARS-853 started to interact

with other surface-exposed reactive cysteines in a concentration greater than 3.0 μM (Patricelli et al., 2016).

Based on my cell viability curve measurement, $KRAS^{G12C}$ NSCLC lines showed susceptibility to both target inhibitors, ULK-101 (**Figure 4.3, Table 4.1**) and ARS-853 (**Figure 4.4, Table 4.2**). These data suggest that single-agent treatment of ULK-101 and ARS-853 could effectively suppress the viability of $KRAS^{G12C}$ NSCLC lines. However, my observed increased BafA1-induced accumulation of LC3B-II in ARS-853 treated $KRAS^{G12C}$ NSCLC (**Figure 3.4**) also indicate a possibility of autophagy adaptive response allowing these cells to survive the insult of ARS-853. To test this assumption, I designed a ULK-101 and ARS-853 combination treatment and measured $KRAS^{G12C}$ NSCLC viability by clonogenic assay. Consistent with my hypothesis, I found that inhibiting the activity of ULK1 drastically decreased the viability of H2030 and SW1573 $KRAS^{G12C}$ NSCLC in a combination of a lower dosage of ARS-853 cultured in OS media (**Figure 4.5, Table 4.3**).

Unexpectedly, I also observed high sensitivity of $KRAS^{G12S}$ A549 NSCLC in ULK-101 and ARS-853 treatment cultured in OS condition. This is intriguing as ARS-853 selectively target oncogenic KRAS signaling in $KRAS^{G12C}$ mutant NSCLC (Lito et al., 2016; Patricelli et al., 2016). One possibility for this surprising outcome was that NSCLC lines treated with ULK-101 and ARS-853 were also exposed in nutrient-deprived media. This starvation condition alone could hinder other growth signaling pathway critical in tumor cells. Indeed, my preliminary data showed that decreased phosphorylation of ERK1/2 on A549 cells cultured in OS for 48 hours with or without ULK-101 and ARS-853 (**Figure 4.6**). With this unexpected outcome from A549 cells, it would be necessary to conduct more investigation about the role of autophagy in the spectrum of oncogenic RAS mutation.

Future Directions

A great deal of evidence demonstrates the importance of autophagy as a survival mechanism to cancer cells in response to stresses including starvation and therapeutic insult. Remarkably, some cancer cells show a greater dependence on autophagy than others. Indeed, KRAS-driven tumor cells are more susceptibility to autophagy inhibition. My present study agrees with this notion as I observed the suppressed viability of $KRAS^{G12C}$ NSCLC lines when treated single agent ULK-101 in starvation. Furthermore, by combining ULK-101 with ARS-853, I found dramatically impaired viability on $KRAS^{G12C}$ NSCLC cell lines in starvation.

Notably, I found that $KRAS^{G12C}$ NSCLC H2030, harboring mutant $p53^{G262V}$, showed higher sensitivity to ULK-101 alone and in combination compared to $KRAS^{G12C}$ NSCLC SW1573 ($p53^{WT}$). I found this intriguing since p53 showed a dual function in autophagy. Also, it is still unclear whether p53 function could dictate the sensitivity of tumor cells to autophagy inhibitions. For instance, in KRAS-driven PDAC model, p53 alteration showed no correlation to the degree of sensitivity of pancreatic cancer cells to autophagy inhibition (Yang et al., 2014). In lung cancer *in vivo* model, autophagy deficiency could activate p53 which lead to suppression of tumor growth, but it could also be due to p53-independent mechanisms (Guo et al., 2013b; White, 2016). Therefore, determining the mechanism by which autophagy could modulate the activity of p53 and vice versa is very important.

As the autophagy research started the effort to develop small molecules targeting autophagy core proteins, it is important to note that pharmacologic inhibition of autophagy is not likely irreversible. Previous mouse models used to unveil the role of autophagy in advanced cancer were extreme and irreversible experiments. Therefore, a parallel experiment that genetically inhibits autophagy (i.e., siRNA and CRISPR) is required when evaluating target agents against

autophagy proteins. These combined experiments could improve our understanding of the function of autophagy in advanced cancers.

REFERENCES

REFERENCES

Aguilera, M.O., Beron, W., and Colombo, M.I. (2012). The actin cytoskeleton participates in the early events of autophagosome formation upon starvation induced autophagy. Autophagy *8*, 1590-1603.

Aita, V.M., Liang, X.H., Murty, V.V., Pincus, D.L., Yu, W., Cayanis, E., Kalachikov, S., Gilliam, T.C., and Levine, B. (1999). Cloning and genomic organization of beclin 1, a candidate tumor suppressor gene on chromosome 17q21. Genomics *59*, 59-65.

Akin, D., Wang, S.K., Habibzadegah-Tari, P., Law, B., Ostrov, D., Li, M., Yin, X.M., Kim, J.S., Horenstein, N., and Dunn, W.A., Jr. (2014). A novel ATG4B antagonist inhibits autophagy and has a negative impact on osteosarcoma tumors. Autophagy *10*, 2021-2035.

Alers, S., Loffler, A.S., Wesselborg, S., and Stork, B. (2012). Role of AMPK-mTOR-Ulk1/2 in the regulation of autophagy: cross talk, shortcuts, and feedbacks. Mol Cell Biol *32*, 2-11.

Amaravadi, R.K., Lippincott-Schwartz, J., Yin, X.M., Weiss, W.A., Takebe, N., Timmer, W., DiPaola, R.S., Lotze, M.T., and White, E. (2011). Principles and current strategies for targeting autophagy for cancer treatment. Clinical cancer research : an official journal of the American Association for Cancer Research *17*, 654-666.

Amaravadi, R.K., and Thompson, C.B. (2007). The roles of therapy-induced autophagy and necrosis in cancer treatment. Clinical cancer research : an official journal of the American Association for Cancer Research *13*, 7271-7279.

Amaravadi, R.K., and Winkler, J.D. (2012). Lys05: a new lysosomal autophagy inhibitor. Autophagy *8*, 1383-1384.

Amaravadi, R.K., Yu, D., Lum, J.J., Bui, T., Christophorou, M.A., Evan, G.I., Thomas-Tikhonenko, A., and Thompson, C.B. (2007). Autophagy inhibition enhances therapy-induced apoptosis in a Myc-induced model of lymphoma. J Clin Invest *117*, 326-336.

Aplin, A., Jasionowski, T., Tuttle, D.L., Lenk, S.E., and Dunn, W.A., Jr. (1992). Cytoskeletal elements are required for the formation and maturation of autophagic vacuoles. J Cell Physiol *152*, 458-466.

Arstila, A.U., and Trump, B.F. (1968). Studies on cellular autophagocytosis. The formation of autophagic vacuoles in the liver after glucagon administration. Am J Pathol *53*, 687-733.

Bago, R., Malik, N., Munson, M.J., Prescott, A.R., Davies, P., Sommer, E., Shpiro, N., Ward, R., Cross, D., Ganley, I.G*., et al.* (2014). Characterization of VPS34-IN1, a selective inhibitor of Vps34, reveals that the phosphatidylinositol 3-phosphate-binding SGK3 protein kinase is a downstream target of class III phosphoinositide 3-kinase. Biochem J *463*, 413-427.

Bieging, K.T., Mello, S.S., and Attardi, L.D. (2014). Unravelling mechanisms of p53-mediated tumour suppression. Nature reviews. Cancer *14*, 359-370.

Blanchoin, L., Boujemaa-Paterski, R., Sykes, C., and Plastino, J. (2014). Actin dynamics, architecture, and mechanics in cell motility. Physiol Rev *94*, 235-263.

BLISS, C.I. (1939). THE TOXICITY OF POISONS APPLIED JOINTLY1. Annals of Applied Biology *26*, 585-615.

Budanov, A.V., and Karin, M. (2008). p53 target genes sestrin1 and sestrin2 connect genotoxic stress and mTOR signaling. Cell *134*, 451-460.

Carew, J.S., Espitia, C.M., Zhao, W., Han, Y., Visconte, V., Phillips, J., and Nawrocki, S.T. (2017). Disruption of Autophagic Degradation with ROC-325 Antagonizes Renal Cell Carcinoma Pathogenesis. Clinical cancer research : an official journal of the American Association for Cancer Research *23*, 2869-2879.

Carew, J.S., and Nawrocki, S.T. (2017). Drain the lysosome: Development of the novel orally available autophagy inhibitor ROC-325. Autophagy *13*, 765-766.

Carew, J.S., Nawrocki, S.T., Kahue, C.N., Zhang, H., Yang, C., Chung, L., Houghton, J.A., Huang, P., Giles, F.J., and Cleveland, J.L. (2007). Targeting autophagy augments the anticancer activity of the histone deacetylase inhibitor SAHA to overcome Bcr-Abl-mediated drug resistance. Blood *110*, 313-322.

Carlier, M.F., Criquet, P., Pantaloni, D., and Korn, E.D. (1986). Interaction of cytochalasin D with actin filaments in the presence of ADP and ATP. J Biol Chem *261*, 2041-2050.

Chan, E.Y., Kir, S., and Tooze, S.A. (2007). siRNA screening of the kinome identifies ULK1 as a multidomain modulator of autophagy. J Biol Chem *282*, 25464-25474.

Chan, E.Y., Longatti, A., McKnight, N.C., and Tooze, S.A. (2009). Kinase-inactivated ULK proteins inhibit autophagy via their conserved C-terminal domains using an Atg13-independent mechanism. Mol Cell Biol *29*, 157-171.

Chan, E.Y.W., and Olson, M.F. (2016). Regulation of Autophagy by Actin-Associated Signaling Pathways. In Autophagy: Cancer, Other Pathologies, Inflammation, Immunity, Infection, and Aging, pp. 105-122.

Choi, A.M., Ryter, S.W., and Levine, B. (2013). Autophagy in human health and disease. N Engl J Med *368*, 651-662.

Cliby, W., Ritland, S., Hartmann, L., Dodson, M., Halling, K.C., Keeney, G., Podratz, K.C., and Jenkins, R.B. (1993). Human epithelial ovarian cancer allelotype. Cancer Res *53*, 2393-2398.

Coutts, A.S., and La Thangue, N.B. (2015). Actin nucleation by WH2 domains at the autophagosome. Nat Commun *6*, 7888.

Crighton, D., Wilkinson, S., O'Prey, J., Syed, N., Smith, P., Harrison, P.R., Gasco, M., Garrone, O., Crook, T., and Ryan, K.M. (2006). DRAM, a p53-induced modulator of autophagy, is critical for apoptosis. Cell *126*, 121-134.

De Duve, C. (1963). The Lysosome Concept. In Ciba Foundation Symposium - Anterior Pituitary Secretion (Book I of Colloquia on Endocrinology), A.V. De Reuck, and M.P. Cameron, eds.

de Duve, C. (2005). The lysosome turns fifty. Nat Cell Biol *7*, 847-849.

De Duve, C., Pressman, B.C., Gianetto, R., Wattiaux, R., and Appelmans, F. (1955). Tissue fractionation studies. 6. Intracellular distribution patterns of enzymes in rat-liver tissue. Biochem J *60*, 604-617.

Degenhardt, K., Mathew, R., Beaudoin, B., Bray, K., Anderson, D., Chen, G., Mukherjee, C., Shi, Y., Gelinas, C., Fan, Y.*, et al.* (2006). Autophagy promotes tumor cell survival and restricts necrosis, inflammation, and tumorigenesis. Cancer Cell *10*, 51-64.

Degtyarev, M., De Maziere, A., Orr, C., Lin, J., Lee, B.B., Tien, J.Y., Prior, W.W., van Dijk, S., Wu, H., Gray, D.C.*, et al.* (2008). Akt inhibition promotes autophagy and sensitizes PTEN-null tumors to lysosomotropic agents. J Cell Biol *183*, 101-116.

Deter, R.L., Baudhuin, P., and De Duve, C. (1967). Participation of lysosomes in cellular autophagy induced in rat liver by glucagon. J Cell Biol *35*, C11-16.

Diao, J., Liu, R., Rong, Y., Zhao, M., Zhang, J., Lai, Y., Zhou, Q., Wilz, L.M., Li, J., Vivona, S.*, et al.* (2015). ATG14 promotes membrane tethering and fusion of autophagosomes to endolysosomes. Nature *520*, 563-566.

Dikic, I., and Elazar, Z. (2018). Mechanism and medical implications of mammalian autophagy. Nat Rev Mol Cell Biol *19*, 349-364.

Dooley, H.C., Razi, M., Polson, H.E., Girardin, S.E., Wilson, M.I., and Tooze, S.A. (2014). WIPI2 links LC3 conjugation with PI3P, autophagosome formation, and pathogen clearance by recruiting Atg12-5-16L1. Mol Cell *55*, 238-252.

Dowdle, W.E., Nyfeler, B., Nagel, J., Elling, R.A., Liu, S., Triantafellow, E., Menon, S., Wang, Z., Honda, A., Pardee, G.*, et al.* (2014). Selective VPS34 inhibitor blocks autophagy and uncovers a role for NCOA4 in ferritin degradation and iron homeostasis in vivo. Nat Cell Biol *16*, 1069-1079.

Egan, D., Kim, J., Shaw, R.J., and Guan, K.L. (2011). The autophagy initiating kinase ULK1 is regulated via opposing phosphorylation by AMPK and mTOR. Autophagy *7*, 643-644.

Egan, D.F., Chun, M.G., Vamos, M., Zou, H., Rong, J., Miller, C.J., Lou, H.J., Raveendra-Panickar, D., Yang, C.C., Sheffler, D.J.*, et al.* (2015). Small Molecule Inhibition of the Autophagy Kinase ULK1 and Identification of ULK1 Substrates. Mol Cell *59*, 285-297.

el-Deiry, W.S., Tokino, T., Velculescu, V.E., Levy, D.B., Parsons, R., Trent, J.M., Lin, D., Mercer, W.E., Kinzler, K.W., and Vogelstein, B. (1993). WAF1, a potential mediator of p53 tumor suppression. Cell *75*, 817-825.

el-Deiry, W.S., Tokino, T., Waldman, T., Oliner, J.D., Velculescu, V.E., Burrell, M., Hill, D.E., Healy, E., Rees, J.L., Hamilton, S.R.*, et al.* (1995). Topological control of p21WAF1/CIP1 expression in normal and neoplastic tissues. Cancer Res *55*, 2910-2919.

Fakharzadeh, S.S., Rosenblum-Vos, L., Murphy, M., Hoffman, E.K., and George, D.L. (1993). Structure and organization of amplified DNA on double minutes containing the mdm2 oncogene. Genomics *15*, 283-290.

Fakharzadeh, S.S., Trusko, S.P., and George, D.L. (1991). Tumorigenic potential associated with enhanced expression of a gene that is amplified in a mouse tumor cell line. Embo j *10*, 1565-1569.

Feng, Z., Zhang, H., Levine, A.J., and Jin, S. (2005). The coordinate regulation of the p53 and mTOR pathways in cells. Proceedings of the National Academy of Sciences of the United States of America *102*, 8204-8209.

Fitzwalter, B.E., Towers, C.G., Sullivan, K.D., Andrysik, Z., Hoh, M., Ludwig, M., O'Prey, J., Ryan, K.M., Espinosa, J.M., Morgan, M.J.*, et al.* (2018). Autophagy Inhibition Mediates Apoptosis Sensitization in Cancer Therapy by Relieving FOXO3a Turnover. Dev Cell *44*, 555-565 e553.

Foucquier, J., and Guedj, M. (2015). Analysis of drug combinations: current methodological landscape. Pharmacol Res Perspect *3*, e00149.

Ganley, I.G., Lam du, H., Wang, J., Ding, X., Chen, S., and Jiang, X. (2009). ULK1.ATG13.FIP200 complex mediates mTOR signaling and is essential for autophagy. J Biol Chem *284*, 12297-12305.

Gao, X., Zacharek, A., Salkowski, A., Grignon, D.J., Sakr, W., Porter, A.T., and Honn, K.V. (1995). Loss of heterozygosity of the BRCA1 and other loci on chromosome 17q in human prostate cancer. Cancer Res *55*, 1002-1005.

Glaumann, H., and Ahlberg, J. (1987). Comparison of different autophagic vacuoles with regard to ultrastructure, enzymatic composition, and degradation capacity--formation of crinosomes. Experimental and molecular pathology *47*, 346-362.

Goodall, M.L., Wang, T., Martin, K.R., Kortus, M.G., Kauffman, A.L., Trent, J.M., Gately, S., and MacKeigan, J.P. (2014). Development of potent autophagy inhibitors that sensitize oncogenic BRAF V600E mutant melanoma tumor cells to vemurafenib. Autophagy *10*, 1120-1136.

Guo, J.Y., Chen, H.Y., Mathew, R., Fan, J., Strohecker, A.M., Karsli-Uzunbas, G., Kamphorst, J.J., Chen, G., Lemons, J.M., Karantza, V.*, et al.* (2011). Activated Ras requires autophagy to maintain oxidative metabolism and tumorigenesis. Genes Dev *25*, 460-470.

Guo, J.Y., Karsli-Uzunbas, G., Mathew, R., Aisner, S.C., Kamphorst, J.J., Strohecker, A.M., Chen, G., Price, S., Lu, W., Teng, X.*, et al.* (2013a). Autophagy suppresses progression of K-ras-induced lung tumors to oncocytomas and maintains lipid homeostasis. Genes Dev *27*, 1447-1461.

Guo, J.Y., Xia, B., and White, E. (2013b). Autophagy-mediated tumor promotion. Cell *155*, 1216-1219.

Gurkar, A.U., Chu, K., Raj, L., Bouley, R., Lee, S.H., Kim, Y.B., Dunn, S.E., Mandinova, A., and Lee, S.W. (2013). Identification of ROCK1 kinase as a critical regulator of Beclin1-mediated autophagy during metabolic stress. Nat Commun *4*, 2189.

Gurumurthy, S., Xie, S.Z., Alagesan, B., Kim, J., Yusuf, R.Z., Saez, B., Tzatsos, A., Ozsolak, F., Milos, P., Ferrari, F.*, et al.* (2010). The Lkb1 metabolic sensor maintains haematopoietic stem cell survival. Nature *468*, 659-663.

Gutierrez, M.G., Munafo, D.B., Beron, W., and Colombo, M.I. (2004). Rab7 is required for the normal progression of the autophagic pathway in mammalian cells. J Cell Sci *117*, 2687-2697.

Han, W., Pan, H., Chen, Y., Sun, J., Wang, Y., Li, J., Ge, W., Feng, L., Lin, X., Wang, X.*, et al.* (2011). EGFR tyrosine kinase inhibitors activate autophagy as a cytoprotective response in human lung cancer cells. PLoS One *6*, e18691.

Hata, A.N., Rowley, S., Archibald, H.L., Gomez-Caraballo, M., Siddiqui, F.M., Ji, F., Jung, J., Light, M., Lee, J.S., Debussche, L.*, et al.* (2017). Synergistic activity and heterogeneous acquired resistance of combined MDM2 and MEK inhibition in KRAS mutant cancers. Oncogene *36*, 6581-6591.

Holland, P., and Simonsen, A. (2015). Actin shapes the autophagosome. Nat Cell Biol *17*, 1094-1096.

Hunter, J.C., Manandhar, A., Carrasco, M.A., Gurbani, D., Gondi, S., and Westover, K.D. (2015). Biochemical and Structural Analysis of Common Cancer-Associated KRAS Mutations. Mol Cancer Res *13*, 1325-1335.

Huynh, M.V., and Campbell, S.L. (2016). Getting a Handle on RAS-targeted Therapies: Cysteine Directed Inhibitors. Mini reviews in medicinal chemistry *16*, 383-390.

Itakura, E., Kishi-Itakura, C., and Mizushima, N. (2012). The hairpin-type tail-anchored SNARE syntaxin 17 targets to autophagosomes for fusion with endosomes/lysosomes. Cell *151*, 1256-1269.

Jager, S., Bucci, C., Tanida, I., Ueno, T., Kominami, E., Saftig, P., and Eskelinen, E.L. (2004). Role for Rab7 in maturation of late autophagic vacuoles. J Cell Sci *117*, 4837-4848.

Janes, M.R., Zhang, J., Li, L.S., Hansen, R., Peters, U., Guo, X., Chen, Y., Babbar, A., Firdaus, S.J., Darjania, L.*, et al.* (2018). Targeting KRAS Mutant Cancers with a Covalent G12C-Specific Inhibitor. Cell *172*, 578-589.e517.

Jiang, P., and Mizushima, N. (2014). Autophagy and human diseases. Cell Res *24*, 69-79.

Jiang, P., Nishimura, T., Sakamaki, Y., Itakura, E., Hatta, T., Natsume, T., and Mizushima, N. (2014). The HOPS complex mediates autophagosome-lysosome fusion through interaction with syntaxin 17. Mol Biol Cell *25*, 1327-1337.

Joerger, A.C., and Fersht, A.R. (2016). The p53 Pathway: Origins, Inactivation in Cancer, and Emerging Therapeutic Approaches. Annu Rev Biochem *85*, 375-404.

Jung, C.H., Jun, C.B., Ro, S.H., Kim, Y.M., Otto, N.M., Cao, J., Kundu, M., and Kim, D.H. (2009). ULK-Atg13-FIP200 complexes mediate mTOR signaling to the autophagy machinery. Mol Biol Cell *20*, 1992-2003.

Junttila, M.R., and Evan, G.I. (2009). p53--a Jack of all trades but master of none. Nature reviews. Cancer *9*, 821-829.

Kabeya, Y., Mizushima, N., Ueno, T., Yamamoto, A., Kirisako, T., Noda, T., Kominami, E., Ohsumi, Y., and Yoshimori, T. (2000). LC3, a mammalian homologue of yeast Apg8p, is localized in autophagosome membranes after processing. Embo j *19*, 5720-5728.

Kale, V.P., Hengst, J.A., Desai, D.H., Amin, S.G., and Yun, J.K. (2015). The regulatory roles of ROCK and MRCK kinases in the plasticity of cancer cell migration. Cancer Lett *361*, 185-196.

Karantza-Wadsworth, V., Patel, S., Kravchuk, O., Chen, G., Mathew, R., Jin, S., and White, E. (2007). Autophagy mitigates metabolic stress and genome damage in mammary tumorigenesis. Genes Dev *21*, 1621-1635.

Kast, D.J., and Dominguez, R. (2015). WHAMM links actin assembly via the Arp2/3 complex to autophagy. Autophagy *11*, 1702-1704.

Kast, D.J., and Dominguez, R. (2017). The Cytoskeleton-Autophagy Connection. Current biology : CB *27*, R318-r326.

Kast, D.J., Zajac, A.L., Holzbaur, E.L., Ostap, E.M., and Dominguez, R. (2015). WHAMM Directs the Arp2/3 Complex to the ER for Autophagosome Biogenesis through an Actin Comet Tail Mechanism. Current biology : CB *25*, 1791-1797.

Kastenhuber, E.R., and Lowe, S.W. (2017). Putting p53 in Context. Cell *170*, 1062-1078.

Kenzelmann Broz, D., Spano Mello, S., Bieging, K.T., Jiang, D., Dusek, R.L., Brady, C.A., Sidow, A., and Attardi, L.D. (2013). Global genomic profiling reveals an extensive p53-regulated autophagy program contributing to key p53 responses. Genes Dev *27*, 1016-1031.

Kim, J., Kundu, M., Viollet, B., and Guan, K.L. (2011). AMPK and mTOR regulate autophagy through direct phosphorylation of Ulk1. Nat Cell Biol *13*, 132-141.

Kim, Y.C., and Guan, K.L. (2015). mTOR: a pharmacologic target for autophagy regulation. J Clin Invest *125*, 25-32.

Kimura, S., Noda, T., and Yoshimori, T. (2007). Dissection of the autophagosome maturation process by a novel reporter protein, tandem fluorescent-tagged LC3. Autophagy *3*, 452-460.

Klionsky, D.J., Abdelmohsen, K., Abe, A., Abedin, M.J., Abeliovich, H., Acevedo Arozena, A., Adachi, H., Adams, C.M., Adams, P.D., Adeli, K.*, et al.* (2016). Guidelines for the use and interpretation of assays for monitoring autophagy (3rd edition). Autophagy *12*, 1-222.

Kroemer, G., Marino, G., and Levine, B. (2010). Autophagy and the integrated stress response. Mol Cell *40*, 280-293.

Kruiswijk, F., Labuschagne, C.F., and Vousden, K.H. (2015). p53 in survival, death and metabolic health: a lifeguard with a licence to kill. Nat Rev Mol Cell Biol *16*, 393-405.

Kruppa, A.J., Kendrick-Jones, J., and Buss, F. (2016). Myosins, Actin and Autophagy. Traffic *17*, 878-890.

Kurdi, A., Cleenewerck, M., Vangestel, C., Lyssens, S., Declercq, W., Timmermans, J.P., Stroobants, S., Augustyns, K., De Meyer, G.R.Y., Van Der Veken, P.*, et al.* (2017). ATG4B inhibitors with a benzotropolone core structure block autophagy and augment efficiency of chemotherapy in mice. Biochemical pharmacology *138*, 150-162.

Kussie, P.H., Gorina, S., Marechal, V., Elenbaas, B., Moreau, J., Levine, A.J., and Pavletich, N.P. (1996). Structure of the MDM2 oncoprotein bound to the p53 tumor suppressor transactivation domain. Science *274*, 948-953.

Laddha, S.V., Ganesan, S., Chan, C.S., and White, E. (2014). Mutational landscape of the essential autophagy gene BECN1 in human cancers. Mol Cancer Res *12*, 485-490.

Lane, D.P. (1992). Cancer. p53, guardian of the genome. Nature *358*, 15-16.

Lazarus, M.B., Novotny, C.J., and Shokat, K.M. (2015). Structure of the human autophagy initiating kinase ULK1 in complex with potent inhibitors. ACS Chem Biol *10*, 257-261.

Lazarus, M.B., and Shokat, K.M. (2015). Discovery and structure of a new inhibitor scaffold of the autophagy initiating kinase ULK1. Bioorg Med Chem *23*, 5483-5488.

Leung, T., Chen, X.Q., Tan, I., Manser, E., and Lim, L. (1998). Myotonic dystrophy kinase-related Cdc42-binding kinase acts as a Cdc42 effector in promoting cytoskeletal reorganization. Mol Cell Biol *18*, 130-140.

Levine, A.J. (1997). p53, the cellular gatekeeper for growth and division. Cell *88*, 323-331.

Liang, X.H., Jackson, S., Seaman, M., Brown, K., Kempkes, B., Hibshoosh, H., and Levine, B. (1999). Induction of autophagy and inhibition of tumorigenesis by beclin 1. Nature *402*, 672-676.

Limpert, A.S., Lambert, L.J., Bakas, N.A., Bata, N., Brun, S.N., Shaw, R.J., and Cosford, N.D.P. (2018). Autophagy in Cancer: Regulation by Small Molecules. Trends Pharmacol Sci *39*, 1021-1032.

Lito, P., Solomon, M., Li, L.S., Hansen, R., and Rosen, N. (2016). Allele-specific inhibitors inactivate mutant KRAS G12C by a trapping mechanism. Science *351*, 604-608.

Liu, J., and Debnath, J. (2016). The Evolving, Multifaceted Roles of Autophagy in Cancer. Adv Cancer Res *130*, 1-53.

Lock, R., Roy, S., Kenific, C.M., Su, J.S., Salas, E., Ronen, S.M., and Debnath, J. (2011). Autophagy facilitates glycolysis during Ras-mediated oncogenic transformation. Mol Biol Cell *22*, 165-178.

Martin, K.R., Barua, D., Kauffman, A.L., Westrate, L.M., Posner, R.G., Hlavacek, W.S., and Mackeigan, J.P. (2013). Computational model for autophagic vesicle dynamics in single cells. Autophagy *9*, 74-92.

Martin, K.R., Celano, S.L., Solitro, A.R., Gunaydin, H., Scott, M., O'Hagan, R.C., Shumway, S.D., Fuller, P., and MacKeigan, J.P. (2018). A Potent and Selective ULK1 Inhibitor Suppresses Autophagy and Sensitizes Cancer Cells to Nutrient Stress. iScience *8*, 74-84.

Mathew, R., Karp, C.M., Beaudoin, B., Vuong, N., Chen, G., Chen, H.Y., Bray, K., Reddy, A., Bhanot, G., Gelinas, C.*, et al.* (2009). Autophagy suppresses tumorigenesis through elimination of p62. Cell *137*, 1062-1075.

Matsuura, A., Tsukada, M., Wada, Y., and Ohsumi, Y. (1997). Apg1p, a novel protein kinase required for the autophagic process in Saccharomyces cerevisiae. Gene *192*, 245-250.

McAfee, Q., Zhang, Z., Samanta, A., Levi, S.M., Ma, X.H., Piao, S., Lynch, J.P., Uehara, T., Sepulveda, A.R., Davis, L.E.*, et al.* (2012). Autophagy inhibitor Lys05 has single-agent antitumor activity and reproduces the phenotype of a genetic autophagy deficiency. Proceedings of the National Academy of Sciences of the United States of America *109*, 8253-8258.

McEwan, D.G., Popovic, D., Gubas, A., Terawaki, S., Suzuki, H., Stadel, D., Coxon, F.P., Miranda de Stegmann, D., Bhogaraju, S., Maddi, K.*, et al.* (2015). PLEKHM1 regulates autophagosome-lysosome fusion through HOPS complex and LC3/GABARAP proteins. Mol Cell *57*, 39-54.

Mleczak, A., Millar, S., Tooze, S.A., Olson, M.F., and Chan, E.Y. (2013). Regulation of autophagosome formation by Rho kinase. Cellular signalling *25*, 1-11.

Moreau, K., Ghislat, G., Hochfeld, W., Renna, M., Zavodszky, E., Runwal, G., Puri, C., Lee, S., Siddiqi, F., Menzies, F.M.*, et al.* (2015). Transcriptional regulation of Annexin A2 promotes starvation-induced autophagy. Nat Commun *6*, 8045.

Morselli, E., Tasdemir, E., Maiuri, M.C., Galluzzi, L., Kepp, O., Criollo, A., Vicencio, J.M., Soussi, T., and Kroemer, G. (2008). Mutant p53 protein localized in the cytoplasm inhibits autophagy. Cell cycle (Georgetown, Tex.) *7*, 3056-3061.

Mrakovcic, M., and Frohlich, L.F. (2018). p53-Mediated Molecular Control of Autophagy in Tumor Cells. Biomolecules *8*.

Murrow, L., and Debnath, J. (2013). Autophagy as a stress-response and quality-control mechanism: implications for cell injury and human disease. Annu Rev Pathol *8*, 105-137.

Nakamura, S., and Yoshimori, T. (2017). New insights into autophagosome-lysosome fusion. J Cell Sci *130*, 1209-1216.

Novikoff, A.B., Beaufay, H., and De Duve, C. (1956). Electron microscopy of lysosomerich fractions from rat liver. J Biophys Biochem Cytol *2*, 179-184.

Olson, M.F., and Sahai, E. (2009). The actin cytoskeleton in cancer cell motility. Clin Exp Metastasis *26*, 273-287.

Ostrem, J.M., Peters, U., Sos, M.L., Wells, J.A., and Shokat, K.M. (2013). K-Ras(G12C) inhibitors allosterically control GTP affinity and effector interactions. Nature *503*, 548-551.

Ostrem, J.M., and Shokat, K.M. (2016). Direct small-molecule inhibitors of KRAS: from structural insights to mechanism-based design. Nat Rev Drug Discov *15*, 771-785.

Papinski, D., Schuschnig, M., Reiter, W., Wilhelm, L., Barnes, C.A., Maiolica, A., Hansmann, I., Pfaffenwimmer, T., Kijanska, M., Stoffel, I.*, et al.* (2014). Early steps in autophagy depend on direct phosphorylation of Atg9 by the Atg1 kinase. Mol Cell *53*, 471-483.

Patricelli, M.P., Janes, M.R., Li, L.S., Hansen, R., Peters, U., Kessler, L.V., Chen, Y., Kucharski, J.M., Feng, J., Ely, T.*, et al.* (2016). Selective Inhibition of Oncogenic KRAS Output with Small Molecules Targeting the Inactive State. Cancer Discov *6*, 316-329.

Peppard, J.V., Rugg, C., Smicker, M., Dureuil, C., Ronan, B., Flamand, O., Durand, L., and Pasquier, B. (2014). Identifying Small Molecules which Inhibit Autophagy: a Phenotypic Screen Using Image-Based High-Content Cell Analysis. Current chemical genomics and translational medicine *8*, 3-15.

Petherick, K.J., Conway, O.J., Mpamhanga, C., Osborne, S.A., Kamal, A., Saxty, B., and Ganley, I.G. (2015). Pharmacological inhibition of ULK1 kinase blocks mammalian target of rapamycin (mTOR)-dependent autophagy. J Biol Chem *290*, 28726.

Rabinowitz, J.D., and White, E. (2010). Autophagy and metabolism. Science *330*, 1344-1348.

Rao, S., Tortola, L., Perlot, T., Wirnsberger, G., Novatchkova, M., Nitsch, R., Sykacek, P., Frank, L., Schramek, D., Komnenovic, V.*, et al.* (2014). A dual role for autophagy in a murine model of lung cancer. Nat Commun *5*, 3056.

Ravandi, F., Gojo, I., Patnaik, M.M., Minden, M.D., Kantarjian, H., Johnson-Levonas, A.O., Fancourt, C., Lam, R., Jones, M.B., Knox, C.D.*, et al.* (2016). A phase I trial of the human double minute 2 inhibitor (MK-8242) in patients with refractory/recurrent acute myelogenous leukemia (AML). Leuk Res *48*, 92-100.

Rebecca, V.W., and Amaravadi, R.K. (2016). Emerging strategies to effectively target autophagy in cancer. Oncogene *35*, 1-11.

Rebecca, V.W., Massaro, R.R., Fedorenko, I.V., Sondak, V.K., Anderson, A.R., Kim, E., Amaravadi, R.K., Maria-Engler, S.S., Messina, J.L., Gibney, G.T., *et al.* (2014). Inhibition of autophagy enhances the effects of the AKT inhibitor MK-2206 when combined with paclitaxel and carboplatin in BRAF wild-type melanoma. Pigment cell & melanoma research *27*, 465-478.

Roach, P.J. (2011). AMPK -> ULK1 -> autophagy. Mol Cell Biol *31*, 3082-3084.

Romanov, J., Walczak, M., Ibiricu, I., Schuchner, S., Ogris, E., Kraft, C., and Martens, S. (2012). Mechanism and functions of membrane binding by the Atg5-Atg12/Atg16 complex during autophagosome formation. EMBO J *31*, 4304-4317.

Ronan, B., Flamand, O., Vescovi, L., Dureuil, C., Durand, L., Fassy, F., Bachelot, M.F., Lamberton, A., Mathieu, M., Bertrand, T., *et al.* (2014). A highly potent and selective Vps34 inhibitor alters vesicle trafficking and autophagy. Nature chemical biology *10*, 1013-1019.

Rosenfeldt, M.T., O'Prey, J., Morton, J.P., Nixon, C., MacKay, G., Mrowinska, A., Au, A., Rai, T.S., Zheng, L., Ridgway, R., *et al.* (2013). p53 status determines the role of autophagy in pancreatic tumour development. Nature *504*, 296-300.

Roskoski, R., Jr. (2012). ERK1/2 MAP kinases: structure, function, and regulation. Pharmacological research *66*, 105-143.

Russell, R.C., Tian, Y., Yuan, H., Park, H.W., Chang, Y.Y., Kim, J., Kim, H., Neufeld, T.P., Dillin, A., and Guan, K.L. (2013). ULK1 induces autophagy by phosphorylating Beclin-1 and activating VPS34 lipid kinase. Nat Cell Biol *15*, 741-750.

Saito, H., Inazawa, J., Saito, S., Kasumi, F., Koi, S., Sagae, S., Kudo, R., Saito, J., Noda, K., and Nakamura, Y. (1993). Detailed deletion mapping of chromosome 17q in ovarian and breast cancers: 2-cM region on 17q21.3 often and commonly deleted in tumors. Cancer Res *53*, 3382-3385.

Sanchez-Vega, F., Mina, M., Armenia, J., Chatila, W.K., Luna, A., La, K.C., Dimitriadoy, S., Liu, D.L., Kantheti, H.S., Saghafinia, S., *et al.* (2018). Oncogenic Signaling Pathways in The Cancer Genome Atlas. Cell *173*, 321-337.e310.

Santana-Codina, N., Mancias, J.D., and Kimmelman, A.C. (2017). The Role of Autophagy in Cancer. Annual Review of Cancer Biology *1*, 19-39.

Santanam, U., Banach-Petrosky, W., Abate-Shen, C., Shen, M.M., White, E., and DiPaola, R.S. (2016). Atg7 cooperates with Pten loss to drive prostate cancer tumor growth. Genes Dev *30*, 399-407.

Saxton, R.A., and Sabatini, D.M. (2017). mTOR Signaling in Growth, Metabolism, and Disease. Cell *168*, 960-976.

Scott, R.W., and Olson, M.F. (2007). LIM kinases: function, regulation and association with human disease. J Mol Med (Berl) *85*, 555-568.

Shirahama-Noda, K., Kira, S., Yoshimori, T., and Noda, T. (2013). TRAPPIII is responsible for vesicular transport from early endosomes to Golgi, facilitating Atg9 cycling in autophagy. J Cell Sci *126*, 4963-4973.

Spector, I., Shochet, N.R., Blasberger, D., and Kashman, Y. (1989). Latrunculins--novel marine macrolides that disrupt microfilament organization and affect cell growth: I. Comparison with cytochalasin D. Cell Motil Cytoskeleton *13*, 127-144.

Strohecker, A.M., Guo, J.Y., Karsli-Uzunbas, G., Price, S.M., Chen, G.J., Mathew, R., McMahon, M., and White, E. (2013). Autophagy sustains mitochondrial glutamine metabolism and growth of BrafV600E-driven lung tumors. Cancer Discov *3*, 1272-1285.

Sumi, T., Matsumoto, K., Shibuya, A., and Nakamura, T. (2001). Activation of LIM kinases by myotonic dystrophy kinase-related Cdc42-binding kinase alpha. J Biol Chem *276*, 23092-23096.

Takahashi, T., Carbone, D., Takahashi, T., Nau, M.M., Hida, T., Linnoila, I., Ueda, R., and Minna, J.D. (1992). Wild-type but not mutant p53 suppresses the growth of human lung cancer cells bearing multiple genetic lesions. Cancer Res *52*, 2340-2343.

Takeshige, K., Baba, M., Tsuboi, S., Noda, T., and Ohsumi, Y. (1992). Autophagy in yeast demonstrated with proteinase-deficient mutants and conditions for its induction. J Cell Biol *119*, 301-311.

Tan, I., Ng, C.H., Lim, L., and Leung, T. (2001). Phosphorylation of a novel myosin binding subunit of protein phosphatase 1 reveals a conserved mechanism in the regulation of actin cytoskeleton. J Biol Chem *276*, 21209-21216.

Tan, I., Yong, J., Dong, J.M., Lim, L., and Leung, T. (2008). A tripartite complex containing MRCK modulates lamellar actomyosin retrograde flow. Cell *135*, 123-136.

Tang, F., Hu, P., Yang, Z., Xue, C., Gong, J., Sun, S., Shi, L., Zhang, S., Li, Z., Yang, C.*, et al.* (2017). SBI0206965, a novel inhibitor of Ulk1, suppresses non-small cell lung cancer cell growth by modulating both autophagy and apoptosis pathways. Oncology reports *37*, 3449-3458.

Tang, H., Sebti, S., Titone, R., Zhou, Y., Isidoro, C., Ross, T.S., Hibshoosh, H., Xiao, G., Packer, M., Xie, Y.*, et al.* (2015). Decreased BECN1 mRNA Expression in Human Breast Cancer is Associated with Estrogen Receptor-Negative Subtypes and Poor Prognosis. EBioMedicine *2*, 255-263.

Tang, H.W., Wang, Y.B., Wang, S.L., Wu, M.H., Lin, S.Y., and Chen, G.C. (2011). Atg1-mediated myosin II activation regulates autophagosome formation during starvation-induced autophagy. Embo j *30*, 636-651.

Tasdemir, E., Maiuri, M.C., Galluzzi, L., Vitale, I., Djavaheri-Mergny, M., D'Amelio, M., Criollo, A., Morselli, E., Zhu, C., Harper, F.*, et al.* (2008). Regulation of autophagy by cytoplasmic p53. Nat Cell Biol *10*, 676-687.

Tisato, V., Voltan, R., Gonelli, A., Secchiero, P., and Zauli, G. (2017). MDM2/X inhibitors under clinical evaluation: perspectives for the management of hematological malignancies and pediatric cancer. Journal of hematology & oncology *10*, 133.

Tsukada, M., and Ohsumi, Y. (1993). Isolation and characterization of autophagy-defective mutants of Saccharomyces cerevisiae. FEBS Lett *333*, 169-174.

Unbekandt, M., Belshaw, S., Bower, J., Clarke, M., Cordes, J., Crighton, D., Croft, D.R., Drysdale, M.J., Garnett, M.J., Gill, K.*, et al.* (2018). Discovery of Potent and Selective MRCK Inhibitors with Therapeutic Effect on Skin Cancer. Cancer Res *78*, 2096-2114.

Unbekandt, M., and Olson, M.F. (2014). The actin-myosin regulatory MRCK kinases: regulation, biological functions and associations with human cancer. J Mol Med (Berl) *92*, 217-225.

van der Vos, K.E., Eliasson, P., Proikas-Cezanne, T., Vervoort, S.J., van Boxtel, R., Putker, M., van Zutphen, I.J., Mauthe, M., Zellmer, S., Pals, C.*, et al.* (2012). Modulation of glutamine metabolism by the PI(3)K-PKB-FOXO network regulates autophagy. Nat Cell Biol *14*, 829-837.

Vassilev, L.T., Vu, B.T., Graves, B., Carvajal, D., Podlaski, F., Filipovic, Z., Kong, N., Kammlott, U., Lukacs, C., Klein, C.*, et al.* (2004). In vivo activation of the p53 pathway by small-molecule antagonists of MDM2. Science *303*, 844-848.

Vicente-Manzanares, M., Ma, X., Adelstein, R.S., and Horwitz, A.R. (2009). Non-muscle myosin II takes centre stage in cell adhesion and migration. Nat Rev Mol Cell Biol *10*, 778-790.

Wagner, A.J., Banerji, U., Mahipal, A., Somaiah, N., Hirsch, H., Fancourt, C., Johnson-Levonas, A.O., Lam, R., Meister, A.K., Russo, G.*, et al.* (2017). Phase I Trial of the Human Double Minute 2 Inhibitor MK-8242 in Patients With Advanced Solid Tumors. Journal of clinical oncology : official journal of the American Society of Clinical Oncology *35*, 1304-1311.

Wakatsuki, T., Schwab, B., Thompson, N.C., and Elson, E.L. (2001). Effects of cytochalasin D and latrunculin B on mechanical properties of cells. J Cell Sci *114*, 1025-1036.

Walczak, M., and Martens, S. (2013). Dissecting the role of the Atg12-Atg5-Atg16 complex during autophagosome formation. Autophagy *9*, 424-425.

Wang, C., Hu, Q., and Shen, H.M. (2016). Pharmacological inhibitors of autophagy as novel cancer therapeutic agents. Pharmacological research *105*, 164-175.

Wei, H., Wei, S., Gan, B., Peng, X., Zou, W., and Guan, J.L. (2011). Suppression of autophagy by FIP200 deletion inhibits mammary tumorigenesis. Genes Dev *25*, 1510-1527.

White, E. (2012). Deconvoluting the context-dependent role for autophagy in cancer. Nature reviews. Cancer *12*, 401-410.

White, E. (2015). The role for autophagy in cancer. J Clin Invest *125*, 42-46.

White, E. (2016). Autophagy and p53. Cold Spring Harb Perspect Med *6*, a026120.

Wilkinson, S., Paterson, H.F., and Marshall, C.J. (2005). Cdc42-MRCK and Rho-ROCK signalling cooperate in myosin phosphorylation and cell invasion. Nat Cell Biol *7*, 255-261.

Wood, S.D., Grant, W., Adrados, I., Choi, J.Y., Alburger, J.M., Duckett, D.R., and Roush, W.R. (2017). In Silico HTS and Structure Based Optimization of Indazole-Derived ULK1 Inhibitors. ACS Med Chem Lett *8*, 1258-1263.

Wu, X., Bayle, J.H., Olson, D., and Levine, A.J. (1993). The p53-mdm-2 autoregulatory feedback loop. Genes Dev *7*, 1126-1132.

Xia, P., Wang, S., Du, Y., Zhao, Z., Shi, L., Sun, L., Huang, G., Ye, B., Li, C., Dai, Z.*, et al.* (2013). WASH inhibits autophagy through suppression of Beclin 1 ubiquitination. Embo j *32*, 2685-2696.

Xie, X., Koh, J.Y., Price, S., White, E., and Mehnert, J.M. (2015). Atg7 Overcomes Senescence and Promotes Growth of BrafV600E-Driven Melanoma. Cancer Discov *5*, 410-423.

Yamamoto, A., Tagawa, Y., Yoshimori, T., Moriyama, Y., Masaki, R., and Tashiro, Y. (1998). Bafilomycin A1 prevents maturation of autophagic vacuoles by inhibiting fusion between autophagosomes and lysosomes in rat hepatoma cell line, H-4-II-E cells. Cell structure and function *23*, 33-42.

Yang, A., Rajeshkumar, N.V., Wang, X., Yabuuchi, S., Alexander, B.M., Chu, G.C., Von Hoff, D.D., Maitra, A., and Kimmelman, A.C. (2014). Autophagy is critical for pancreatic tumor growth and progression in tumors with p53 alterations. Cancer Discov *4*, 905-913.

Yang, S., Wang, X., Contino, G., Liesa, M., Sahin, E., Ying, H., Bause, A., Li, Y., Stommel, J.M., Dell'antonio, G.*, et al.* (2011). Pancreatic cancers require autophagy for tumor growth. Genes Dev *25*, 717-729.

Yoshimori, T., Yamamoto, A., Moriyama, Y., Futai, M., and Tashiro, Y. (1991). Bafilomycin A1, a specific inhibitor of vacuolar-type H(+)-ATPase, inhibits acidification and protein degradation in lysosomes of cultured cells. J Biol Chem *266*, 17707-17712.

Zavodszky, E., Seaman, M.N., Moreau, K., Jimenez-Sanchez, M., Breusegem, S.Y., Harbour, M.E., and Rubinsztein, D.C. (2014). Mutation in VPS35 associated with Parkinson's disease impairs WASH complex association and inhibits autophagy. Nat Commun *5*, 3828.

Zhang, Y., Cheng, Y., Ren, X., Zhang, L., Yap, K.L., Wu, H., Patel, R., Liu, D., Qin, Z.H., Shih, I.M.*, et al.* (2012). NAC1 modulates sensitivity of ovarian cancer cells to cisplatin by altering the HMGB1-mediated autophagic response. Oncogene *31*, 1055-1064.

Zientara-Rytter, K., and Subramani, S. (2016). Role of actin in shaping autophagosomes. Autophagy *12*, 2512-2515.